Post-transcriptional regulation of α-synuclein and link to Parkinson's disease

Domenica Marchese

TESI DOCTORAL UPF / ANY 2016

DIRECTOR DE LA TESI

Dr. Gian Gaetano Tartaglia

DEPARTAMENT OF BIOINFORMATICS AND GENOMICS
AT CENTRE FOR GENOMIC REGULATION (CRG)

Acknowledgments

The people that I met during this journey and that in one way or another have influenced my life, my person, my way of thinking, are many. First of all, my supervisor Gian. Thank you for choosing me as your first experimental PhD student (!). Thank you for giving me this great chance, for trusting me even when things were going into 'uncertain' directions, and for making me believe that I was mature enough for facing new challenges and managing difficulties. You also showed me the importance of 'thinking outside the box' and keeping an open-minded attitude toward science. I feel that I have grown a lot during the last four years, and this is in great part because of you.

Thank you Davide. You know how precious you became for me during these years. You are a great person, a professional colleague and amazing friend. The calmness, the wisdom and the optimism with which you are naturally gifted helped me many many times. I always felt free to express myself when I was with you because I never felt judged, not a single time! This is something that I've always appreciated a lot from you.

The past and present lab mates who have worked in close contact with me: Silvia, Teresa, Joana and Elias. I don't need to say the obvious. You know that I have learnt a lot from you at the professional level, but not only. Silvia, you are the first one who pushed me to develop my criticism toward science. Teresa, you and Benni are my model of "multitasking wonder women". From the very beginning the professional interaction with you, Teresa, was very smooth, as if we already knew each other! Later, I also discovered a great person with an exquisite sense of humour and I started to enjoy working with you, which is something that is not obvious at all. Joana, you are as authentic as the 'sardinhas assadas no dia de Santo Antonio', you showed me the importance of being faithful to yourself and to avoid making compromises. From you I learnt that to be a good scientist it is fundamental to keep a balance between the rigor of the intellect and the freedom of imagination. Feeding our creativity and keeping a space where we can escape 'common rules' are as important as working with commitment and responsability. Elias, it was a pleasure to share my last steps at CRG with such a good scientist and generous person! You caught me in a moment when I was tired and disoriented but you were anyway able to inject me with your dose of enthusiasm and confidence, thank you!

Thank you Benni! You are the one who better know about my journey through the PhD and I really have to thank you for all the precious advices along the years. Your enthusiasm for science is contagious, so thank you for reminding me the "bright side" of being a scientist also in those moments when my motivation was touching the ground ☺.

I am very grateful also to all the other members of the Tartaglia lab for all the hilarious moments. Federico, Nieves, Riccardo, Carmen, Stefanie, Fernando, Alex, Alessandro, Natalia, Iona, Petr, Marta, Laura and Irene, life in the lab was much more enjoyable with all of you (especially with Fernando and his amazing stories)!

And then Sergio, you have always been a sweet friend to me. Thank you for sharing "tears and joy" of the PhD. The funny games in the lab and the long 'confessions' on the way home after long and tiring working days have warmed my heart and filled it with joy. Thanks also to the "Aire de Barcelona" and future "Camino de Santiago" team, Silvina and Alessandra, for all the good times, the complicity, the nice dinners and chats with a glass of wine (chicas the best is yet to come!).

Francis, sono felice di aver trovato una nuova amica arrivando a Barcellona. Dal giorno in cui siamo arrivate in questa favolosa cittá e ci siamo conosciute cercando casa sotto la pioggia battente, ne é passata di acqua sotto i ponti! Non dimenticheró mai tutti i momenti felici, le risate, gli episodi tragicomici, le ansie e gli entusiasmi condivisi! Ti ringrazio per essere stata una parte importante di questa tappa della mia vita e ci auguro di continuare a coltivare questa amicizia (visto che hai finalmente guadagnato la sezione "amicizie" e non sei piú in quella dei "coinquilini"? ahahah).

Alessietta! Sei una delle persone con piú risorse ed energie che io conosca. Non sai quanto ammiri il tuo inesauribile entusiasmo e quanto ti sia grata per avermi sempre spronato ad essere coraggiosa e a seguire il mio istinto! Alessandra, in te ho trovato una persona autentica e dall'intelletto raffinato. Ascoltare le tue storie e parlare con te é sempre stato molto piacevole e stimolante. Grazie anche per le sbronze improvvisate al mercoledí sera nella Barceloneta! Vale, mi conosci da piú di metá della mia vita, sono felice che il destino ci abbia fatto rincontrare qui e ti sono grata per la voglia di fare, viaggiare ed esplorare che mi trasmetti ogni volta che mi parli.

A lo largo de mi vida en Barcelona, he tenido también la suerte de compartir mi tiempo y espacio con maravillosos compañeros de piso: Azahara, Davide, Paolo, Michele, Paola y Hans. Cada uno con

sus peculiaridades, sus pequeñas obsesiones, su lado divertido. Aquel día que me vaya de Barcelona me llevare' recuerdos muy lindos de cada uno de vosotros. Azahara y Davide, sois una bomba de energía y entusiasmo, gracias por transmitírmelo! Paolo, eres una persona muy buena y generosa. Michele y Paola, gracias por darme la bienvenida en casa y por haber sido tan amables durante estos últimos meses de escritura loca ofreciéndome comida y suporte moral! Hans, has sido el vecino de habitación mas guay que podría haber esperado tener. Sentirse libre de hablar sola o de cantar porque tu inquilino al lado también lo hace, no es algo muy común! Y gracias por las risas, los frutos secos, el rocódromo, y todos los pequeños gestos de generosidad.

Gracias Barcelona, gracias por tu lado mas espectacular hecho de luces, colores, maravillosos edificios, parques, fiestas y gente de todas partes. Y gracias también por tu lado mas oscuro y enigmático que siempre me ha llamado la atención. Es curioso cómo sentí estar como en casa tras solo un mes viviendo aquí. Eres una cuidad hermosa y encantadora donde parece que siempre puede pasar cualquier cosa!

Ed eccoci qui, famiglia! So che in questi anni avete un pó sofferto le mie lunghissime assenze e improvvise sparizioni. Nonostante ció, avete sempre pazientemente atteso che io riapparissi e non mi avete mai negato la vostra comprensione e generositá. Potrei scrivere qui per ore di quanto siete speciali per me e di quanto senza il vostro supporto e i vostri insegnamenti non avrei mai potuto raggiungere questo traguardo, ma qualsiasi parola non sará mai sufficiente ad esprimere tutta la mia gratitudine. Grazie per avermi donato le ali ed un nido a cui fare ritorno.

Abstract

The role of RNA processing in the pathogenesis of neurodegenerative diseases is still poorly understood. α-synuclein (*SNCA*) is a presynaptic neuronal protein known as the major component of Lewy bodies, the pathological hallmark of Parkinson's disease (PD). Recent evidence suggests a link between the pathogenesis of PD and the expression of *SNCA* mRNA isoforms with 3' untranslated region (3'UTR) of different lengths. The purpose of my doctoral studies was the discovery of RNA-binding proteins (RBPs) regulating *SNCA* at the post-transcriptional level by binding its 3'UTR. Using computational and experimental approaches, I identified a number of *trans*-acting elements that physically interact with *SNCA* and potentially control its metabolism. I especially focused on the characterization of two RBPs, ELAVL1 and TIAR, and showed their implication in *SNCA* mRNA stability and translation efficiency. These two factors might play important roles in the maintenance of α-synuclein level and functionality in physiological and pathological conditions.

Resum

Se sap ben poc sobre el paper del processament del RNA en la patogènesi de les malalties neurodegeneratives. L'α-sinucleïna (*SNCA*) és una proteïna neuronal presinàptica i el principal component dels cossos de Lewy, que al seu torn són la troballa patològica característica en la malaltia de Parkinson (MP). Recentment s'ha suggerit un lligam entre la patogènesi de la MP i l'expressió d'isoformes del mRNA de *SNCA* amb diferents longituds de les regions de 3' no traduïdes (en anglès conegudes com a *untranslated regions* UTRs). El propòsit dels meus estudis de doctorat és descobrir les proteïnes que uneixen el RNA de *SNCA* i el regulen a nivell posttranscripcional. Gràcies a una combinació d'estratègies computacionals i experimentals he identificat elements que interaccionen físicament amb *SNCA* i potencialment en regulen el metabolisme actuant en *trans*. M'he centrat en la caracterització de dues proteïnes que uneixen RNA, ELAVL1 i TIAR, i mostro la seva implicació en la regulació de l'estabilitat del mRNA i l'eficiència en la seva traducció. Aquestes dues proteïnes podrien tenir un paper clau en el manteniment dels nivells de α-sinucleïna i la seva funció en condicions fisiològiques i patològiques.

Preface

Neurodegenerative diseases are a group of largely untreatable disorders with strong socioeconomic impact. They are traditionally regarded as proteinopathies caused by aberrant accumulation and aggregation of proteins in the nervous system. However, over the past decade, several lines of evidence highlighted a link between RNA biology and neurodegeneration. In a number of cases, aggregation-prone proteins are also RNA-binding, as for example TAR DNA-binding 43 (TDP-43) and Fused in Ewing's sarcoma (FUS) that are associated with Amyotrophic Lateral Sclerosis (ALS). Also toxic RNAs containing expanded nucleotide repeats can facilitate protein aggregation, as in the case of Myotonic dystrophy or Fragile X-associated tremor/ataxia syndrome.

Parkinson's disease is a movement disorder characterized by abnormal accumulation and aggregation of α-synuclein protein in dopaminergic neurons. Although most of the efforts have been so far addressed to the investigation of the biochemical properties of α-synuclein, recent studies suggest the implication of post-transcriptional regulation of α-synuclein in the development of the disease. In particular, alterations of specific *SNCA* 3'UTR transcript isoforms levels were observed in patients affected by PD.

The purpose of my studies was the discovery of RNA-binding proteins (RBPs) targeting the UTRs of α-synuclein mRNA and the investigation of their regulatory mechanisms. Indeed, the post-transcriptional control exerted by RBPs and microRNAs is fundamental for tuning α-synuclein expression in response to environmental *stimuli*. As the protein reach critical concentrations at the synaptical terminals in pathological condition, the cell keeps tight control of α-synuclein expression to prevent aggregation.

In Chapter I of Results, I describe a large-scale screening of human proteins for the identification of α-synuclein mRNA interactors. Combining *in vitro* experiments with computational methods and literature search, I identified two candidate proteins for detailed investigation: ELAVL1 and TIAR. I also explored differences in the expression level and activity of *SNCA* transcript isoforms carrying 3'UTRs of different length, generated by a mechanism of alternative polyadenylation.

In Chapter II of Results, I focused on the functional roles of ELAVL1 and TIAR in the regulation of α-synuclein expression. By means of knockdown and overexpression experiments in HeLa cells, I demonstrated that they regulate α-synuclein. I addressed the hypothesis that the two RBPs might influence *SNCA* mRNA stability and translation efficiency with the concomitant participation of miRNAs that could compete with the two RBPs. I also investigated α-synuclein, ELAVL1 and TIAR expression in *post-mortem* brain samples of patients affected by PD and Multiple System Atrophy (MSA) to assess their implication in disease.

Chapter III is dedicated to the presentation of experimental and computational methods for predictions of protein-RNA interactions. The article entitled "Advances in characterization of RNA-binding proteins", illustrates some of the techniques that I have used to characterise RBPs interacting with *SNCA*.

In Chapter IV, I present a computational study on protein interactions with cognate mRNAs. This work introduces the hypothesis that a negative feedback loop between mRNAs and RBPs (examples include TDP43 and Fragile Mental Retardation Protein FMRP) control gene expression reducing the aggregation potential of proteins. The article was published with the title "Principles of self-organization in biological pathways: a hypothesis on the autogenous association of alpha-synuclein". The work highlights the importance of the post-transcriptional regulation of α-synuclein, and more generally of dosage-sensitive genes associated with disease. The experimental validation of the predictions is ongoing in the lab.

Index

INTRODUCTION

1. Neurodegenerative diseases

Neurodegenerative diseases are characterized by selective neuronal or glial vulnerability with degeneration in specific brain regions, and deposits of abnormal proteins intracellularly, in neurons and other cells, or in the extracellular compartment. Neurodegenerative diseases are increasingly being realized to share common cellular and molecular mechanisms including protein aggregation and inclusion body formation (Taylor et al., 2002).

Protein misfolding often leads to aggregation. The initiation of misfolding in a particular cell may be a stochastic event, but the likelihood of aggregation increases with protein concentration (Ciryam et al., 2013; Clarke et al., 2000; Tartaglia et al., 2007). The hallmark of neurodegenerative diseases is the 'amyloid fibril' (Dobson, 1999), but several kinds of other aggregates may form, including disordered or 'amorphous' species. In addition, post-translational modifications of proteins, such as oxidation, nitration, phosphorylation, ubiquitination and sumoylation may enhance aggregation (Beyer and Ariza, 2013).

1.1 Parkinson's disease

Parkinson's disease (PD) is the second most common neurodegenerative disorder of the human brain, after Alzheimer disease. It affects ~1% of the population above the age of 60 (Tanner, 1992).

PD initiates in the central nervous system (CNS) and spreads to the peripheral nervous system (PNS) and the enteric nervous system. The most important feature in the brains of PD patients is the selective loss of dopaminergic pigmented neurons within the substantia nigra (SN) and, to a lesser extent, neurons residing in the ventral tegmental and retrorubral areas. Neurodegeneration affects other neurotransmitter systems including the serotonergic (dorsal raphe), the noradrenergic (locus coeruleus), the cholinergic system (nucleus basalis of Meynert) and the dorsal motor nucleus of the vagus nerve leading to the development of motor and nonmotor symptoms (Dauer and Przedborski, 2003).

Typically PD patients present rigidity, resting tremor, bradykinesia and postural instability, but nonmotor symptoms such as hallucinations, depression, and sleep disorders can precede motor symptoms by many years in the so called 'premotor phase' (Iranzo et al., 2013; Schapira and Tolosa, 2010; Wolters, 2009).
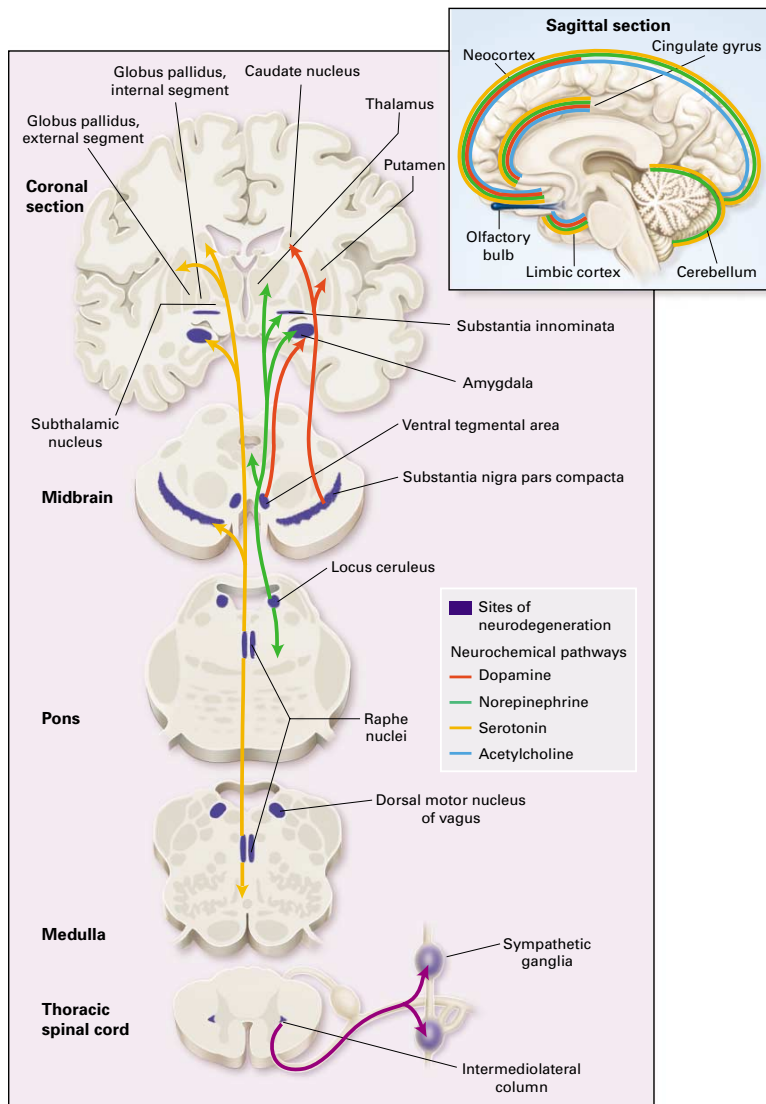
Figure 1. **The Sites of Neurodegeneration and Neurochemical Pathways Involved in Parkinson's Disease**. Brain regions characterized by pathological changes in Parkinson's disease are colored with dark blue. Neurochemical pathways affected are indicated by colored arrows. The link between pathways is indicated on

The neuropathological hallmark of the disease is the presence of eosinophilic inclusions in the soma of neurons known as Lewy bodies (LBs), as well as in the neurites where the inclusions are called Lewy neurites. LBs are composed of a mixture of lipids, neuromelanin and up to several hundred individual proteins, including ubiquitin, Heat-shock proteins, complement proteins, DJ-1, SOD1 and 2, Synphilin-1, Tau, tyrosine hydroxylase, and many others, but the key component is α-synuclein, a small protein enriched at the presynaptic terminals (Spillantini et al., 1997). The inclusions are more than 15 μm in diameter and electron microscopy reveals a dense hyaline core surrounded by a ring of radiating fibrils (Pappolla, 1986) (Fig.2).

Figure 2. Immunohistochemical labeling of Lewy bodies in SNpc dopaminergic neurons with an antibody against α-synuclein (left) and an antibody against ubiquitin (right) [adapted from (Dauer and Przedborski, 2003)]

Following formation and spreading of α-synuclein inclusions it is possible to distinguish six stages of the disease [Braak staging, (Braak et al., 2003)]:

- α-synuclein-positive structures occur in the olfactory bulb and/or the dorsal motor nucleus of the glossopharyngeal and vagal nerves (stage 1)
- Lewy bodies develop in the medulla oblongata and the pontine tegmentum (stage 2)
- Pathology reaches the amygdala and the substantia nigra. At this stage usually motor symptoms begin to appear (stage 3)
- α-synuclein inclusions reach the temporal cortex and the pathology worsen (stage 4)

- Lewy bodies and Lewy neurites appear in the neocortex causing many of the cognitive problems associated with advanced PD (stages 5 and 6)
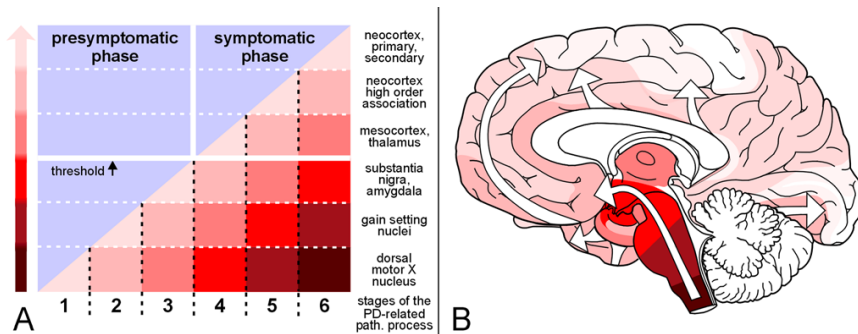
Figure 3. Progression (Braak stages) of Parkinson's disease [from (Braak et al., 2004)]

The diagnosis of PD is based on clinical manifestations, but definite diagnosis requires the identification of LBs and SN dopaminergic neuronal loss. However, LBs are not specific for PD since they are also found in other synucleinopathies, such as "dementia with LBs disease" (Gibb and Lees, 1988).

Treatment with dopaminergic drugs, as levodopa (L-dopa), in order to restore dopamine levels, greatly improves motor symptoms, although nonmotor symptoms are largely refractory to dopaminergic drugs probably due to the different pathological basis (Poewe, 2009).

1.2   Molecular pathogenesis of Parkinson's disease

Parkinson's disease is a multifactorial disease in which different factors such as ageing, genetic susceptibility and environmental insult converge to cause neurodegeneration. Idiopathic PD represents over 90% of PD cases, while genetic PD, caused by mutations in one or more of the PD-associated loci, constitutes 10% of the cases (de Lau and Breteler, 2006).

The environmental causes underlying the pathogenesis of PD are still unclear. Intoxication with 1-methyl-4-phenyl-1,2,3,6-tetrahydropyridine (MPTP), a chemical intermediate used in industry, and viral encephalitis are environmental factors that cause neuronal

degeneration in the SN dopaminergic neurons (Langston et al., 1983). Nevertheless they fail to fully reproduce clinical and pathological features of PD. Paraquat, an herbicide structurally similar to 1-methyl-4-phenylpyridinium (MPP+), the active metabolite of MPTP, and rotenone, a mitochondrial inhibitor used as an insecticide, are present in the environment. Despite human epidemiological studies that have related exposure to herbicides and pesticides in rural environment with elevated risk of a number of chronic diseases, including cancer (Alavanja et al., 2003), diabetes (Cox et al., 2007), respiratory diseases (Boers et al., 2008), skin diseases (Melkonian et al., 2011), fetal diseases, genetic disorders and neurological diseases such as PD (Tanner, 1992), there is no convincing data that proves these toxins to be causative of PD. MPP+, for instance, cannot cross the blood-brain barrier, and rotenone is unstable in solution and only lasts a few days in the lakes (Hisata J., 2002).

Genetic risk factors have emerged as important determinants of sporadic forms of PD. In the past 30 years significant advances have been made in the understanding of the molecular pathogenesis thanks to the identification of genes responsible for the disease with a clear 'mendelian', autosomal dominant or autosomal recessive pattern of inheritance (see Table 1).

Table 1. Genes associated to Parkinson's disease.

Symbol	Locus	Gene name	Inheritance	Phenotype
PARK1/4	4q21-22	SNCA	AD	EOPD
PARK2	6q25.2-q27	Parkin	AR	EOPD
PARK3	2p13	Unknown	AD	Classical PD
PARK5	4p13	UCHL1	AD	Classical PD
PARK6	1p35-p36	DJ-1	AR	EOPD
PARK7	1p36	PINK1	AR	EOPD
PARK8	12q12	LRRK2	AD	Classical PD

PARK9	1p36	ATP13A2	AR	Kufor-Rakeb syndrome; atypical PD with dementia, spasticity and supranuclear gaze palsy
PARK10	1p32	Unknown	Risk factor	Classical PD
PARK11	2q36-37	GIGYF2	AD	LOPD
PARK12	Xq21-q25	Unknown	Risk factor	Classical PD
PARK13	2p12	OMI/HTRA2	AD or risk factor	Classical PD
PARK14	22q13.1	PLA2G6	AR	EO dystonia-parkinsonism
PARK15	22q12-q13	FBX07	AR	EO dystonia-parkinsonism
PARK16	1q32	Unknown	Risk factor	Classical PD
PARK17	16q11.2	VPS35	AD	Classical PD
PARK18	3q27.1	EIF4G1	AD	Classical PD
PARK19	1p31.3	DNAJC6	AR	Juvenile onset, atypical PD
PARK20	21q22.11	SYNJ1	AR	Juvenile onset, atypical PD
PARK21	3q22.1	DNAJC13	AD	LOPD

Abbreviations: AD, autosomal dominant; AR, autosomal recessive; EOPD, early-onset Parkinson's disease, LOPD, late-onset Parkinson's disease; SNCA, α-synuclein; UCHL1, ubiquitin C-terminal hydrolase L1; DJ-1, oncogene DJ-1; PINK1, PTEN-induced putative kinase 1;

LRRK2, leucine-rich repeat kinase 2; ATP13A2, ATPase, type 13A2; GIGYF2, GBR10-interacting GYF protein 2; OMI/HTRA2, HTRA serine peptidase 2; PLA2G6, phospholipase A2 group VI; FBX07, F-box only protein 7; VPS35, VPS35 retromer complex component; EIF4G1, eukaryotic translation initiation factor 4 γ 1; DNAJC6, DnaJ heat shock protein family (Hsp40) member C6; SYNJ1, synaptojanin 1; DNAJC13, DnaJ heat shock protein family (Hsp40) member C13.

An emerging view is that specific genes disrupt cellular homeostasis and lead to neurotoxicity by interacting with environmental factors through common pathways. Mitochondrial dysfunction and oxidative stress, as well as abnormal protein degradation due to alteration in the ubiquitin-proteasome system or in chaperone-mediated autophagy, represent convergent mechanisms contributing to neuronal degeneration. As a matter of fact, many of the proteins encoded by PD-associated genes play important roles in these pathways. **Parkin,** or **E3 ubiquitin ligase,** for instance, is a component of the ubiquitin–proteasome system (UPS). Although Parkin does not interact with native α-synuclein, but with the O-linked glycosylated form and with α-synuclein interacting protein synphilin-1, it rescues neurons from proteasomal dysfunction induced by α-synuclein (Petrucelli et al., 2002). Moreover, mutants of Parkin lead to the accumulation of oxidatively damaged mitochondrial proteins (Palacino et al., 2004). **DJ1** functions as a redox sensitive molecular chaperone. It quenches ROS and protects cells against stress-induced death (Canet-Avilés et al., 2004; Yokota et al., 2003). Importantly, DJ1 is capable of preventing the aggregation of α-synuclein (Shendelman et al., 2004). **PINK1** is a ubiquitously expressed mitochondrial protein with a serine/threonine kinase domain. Loss of PINK1 function affects mitochondrial function by significantly reducing mitochondrial membrane potential and increases level of cell death (Valente et al., 2004). Finally, **LRRK2** is a complex multi-domain protein with kinase activity and capable of autophosphorylation. It might be associated with the outer mitochondrial membrane (OMM) and can bind parkin. Significantly, three PD-associated mutations increase LRRK2 autophosphorylation, hinting at a dominant gain-of-function mechanism (Gloeckner et al., 2006; West et al., 2005).

1.3 Why are substantia nigra dopaminergic neurons especially vulnerable?

Substantia nigra dopaminergic (DA) neurons represent a uniquely susceptible population of cells where all the above-mentioned factors converge.

First, **dopamine metabolism** produces highly reactive oxidative species that in turn oxidize lipids and other cellular components and impair mitochondrial function. Therefore, impairment in the sequestration of dopamine into synaptic vesicles where the pH is lower and dopamine cannot auto-oxidize, may expose dopaminergic neurons to damage (Guzman et al., 2010; Sulzer and Surmeier, 2013; Surmeier et al., 2011).

Second, the **high frequency of autonomous firing** of DA neurons involves a high amount of calcium entry into the cells for release of synaptic vesicles. Differently from ventral tegmental area (VTA) neurons and other populations that express calcium-binding proteins (e.g., calbindin), substantia nigra neurons show a scarcity of these buffering molecules (Chan et al., 2007).

The bioenergetic demands of DA neurons are additionally pushed by the need to maintain elaborate and high **density of connections** with target neurons. This implies that DA neurons are also more exposed to α-synuclein pathological transmission at synapses of poorly myelinated axons and consequent seeding of aggregation. Indeed, over 90% of α-synuclein inclusions are present as Lewy neurites rather than Lewy bodies (Bolam and Pissadaki, 2012; Matsuda et al., 2009).

2. α-synuclein: protein features, aggregation and physiopathological characteristics

2.1. protein domains and structure

α-synuclein is a 140-aminoacid protein enriched at the presynaptic terminals in the central nervous system. The protein has been implicated not only in the pathogenesis of Parkinson's disease, but also Alzheimer's disease (AD), Dementia with Lewy bodies (DLB) and Multiple System Atrophy (MSA) (Baba et al., 1998; Gai et al., 1998; Uéda et al., 1993).

The protein is a member of the synuclein family that includes ß-synuclein and γ-synuclein. α-synuclein consists of three distinct domains: the N-terminal amphipatic region (residues 1-61), the central hydrophobic NAC region (residues 62-95) and the C-terminal acidic region (residues 96-140) (Clayton and George, 1998) (Fig.4).
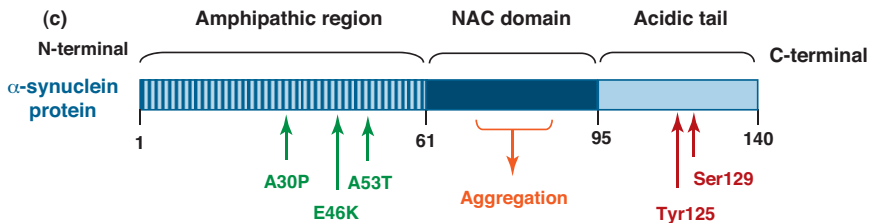
Figure 4. Schematic representation of α-synuclein protein domains with PD-associated mutations and PTM [adapted from (Venda et al., 2010)].

The N-terminal half of protein contains seven imperfect 11-mer repeats with a highly conserved hexamer motif KTKEGV, four of which are located in the N-terminal region and three in the hydrophobic NAC region (Davidson et al., 1998; George et al., 1995). α-synuclein binds to phospholipid vesicles through a conserved apolipoprotein-like class-A2 helix that is made up of the seven 11-mer repeats. Upon binding to membranes, α-synuclein undergoes a shift in secondary structure, from around 3% to over 70% α-helix. This shift is though to be important for the normal function of the protein (Perrin et al., 2000).

The central hydrophobic NAC region of α-synuclein was initially

found in AD brains and defined as the non-Aß component of AD amyloid (NACP). *In vitro* aggregation studies indicate the NAC region is essential for the aggregation and toxicity of α-synuclein (Giasson et al., 2001; Rivers et al., 2008).

The C-terminal domain is less conserved among members of the synuclein family. This region is rich in acidic amino acids and could be important for Ca^{2+} binding (Nielsen et al., 2001). In addition, the C-terminal domain seems to have a chaperone activity that prevents aggregation, and anti-oxidant activity, which protects cells from oxidative damage (Kim et al., 2002). Post-translational modification of the C-term, such as oxidation, nitration and phosphorylation, modulate α-synuclein *in vivo* aggregation propensity. In particular, phosphorylation of serine 129 and tyrosine 125 have opposite effects, the former increases α-synuclein fibrillation while the latter prevents aggregation (Fujiwara et al., 2002).

2.2. α-synuclein physiological functions

a. Synaptic vesicle recycling

Although α-synuclein is distributed to almost all cellular compartments, it is highly enriched at the presynaptic terminals where it weakly binds to neurotransmitter vesicles. Extensive studies indicate that α-synuclein is involved in almost every step of synaptic vesicles trafficking, from docking and fusion to exocytosis and recycling. More specifically, it is believed to play as an activity-dependent negative regulator of transmitter release that restricts the traffic of synaptic vesicles from the reserve pool to the release sites. For example, α-synuclein knockdown in cultured neurons reduced the distal reserve pool of synaptic vesicles (Murphy et al., 2000) and α-synuclein knockout mice exhibited an increase in synaptic paired-pulse facilitation (Abeliovich et al., 2000; Cabin et al., 2002).

Several potential mechanisms have been proposed:

- SNAREs are protein complex consisting of synaptobrevin, syntaxin, and SNAP-25 which play a role in vesicle priming, transferring of docked vesicles into an exocytosis-competent state, and vesicle fusion to the membrane. Repeated release of neurotransmitter vesicles requires cycles of SNARE–complex

assembly and disassembly, with continuous generation of reactive SNARE-protein intermediates. It has been shown that α-synuclein directly binds to the SNARE-protein synaptobrevin-2/vesicle-associated membrane protein 2 (VAMP2) and promote SNARE-complex assembly (Burré et al., 2010);

- In addition, α-synuclein is able to directly bind and inhibit the activity of phospholipase D2 (PLD2), a plasma membrane localized protein that participate in the regulation of vesicle trafficking (Ahn et al., 2002);
- Another possible contribution to vesicles trafficking might be represented by the regulation of actin polymerization, depending on the intracellular Ca^{2+} at the presynaptical terminals, with consequent effect on vesicles transition from the reserve pool to the active zone (Bellani et al., 2010). According to Bellani and co-workers, at basal Ca^{2+} levels (100 nM) α-synuclein reduces the pool of polymerized actin by binding and sequestering actin monomers. Viceversa, at high Ca^{2+} levels (up to 100 uM) reached upon stimulation, α-synuclein loses its affinity for actin monomers and shifts the equilibrium towards the formation of actin filaments, which in turn help vesicles docking and fusion.

b. Dopamine synthesis, vesicular storage and release

A-synuclein regulates production of dopamine by inhibiting the expression and activity of tyrosine hydroxylase (TH), the rate-limiting enzyme responsible for converting tyrosine to L-3,4-dihydroxyphenylalanine (L-DOPA) in the dopamine synthesis pathway. Indeed, overexpression of α-synuclein causes a downregulation of TH mRNA and protein level by reducing TH promoter activity (Baptista et al., 2003; Gao et al., 2007; Yu et al., 2004). Additionally, α-synuclein inhibits TH activity by preventing its phosphorylation and promoting protein phosphatase 2A (PP2A) activity (Peng et al., 2005).

Using a yeast-two-hybrid assay, Dean et al. (2007) demonstrated that α-synuclein also interacts with the vesicular monoamine transporter 2 (VMAT2), responsible for mediating the entry of dopamine neurotransmitter into vesicles after being synthesized. Overexpression of A53T mutant α-synuclein causes a downregulation of VMAT2 with consequent impairment in vesicular DA storage and accumulation of DA in the cytosol, where it undergoes oxidation (Lotharius et al.,

2002).

The results of α-synuclein gene null and overexpression experiments indicate that the protein is an essential presynaptic activity-dependent negative regulator of DA neurotransmission, probably through the aforementioned control of the transport of synaptic vesicles from the reserve pool to the active sites of release (Abeliovich et al., 2000; Cabin et al., 2002).

c. DAT mediated uptake of dopamine and other functions

Several *in vitro* studies show that α-synuclein also regulates the activity of dopamine active transporter (DAT), responsible for the re-uptake of the neurotransmitter into the presynaptic neuron, by controlling its availability at the plasma membrane (Lee et al., 2001; Wersinger and Sidhu, 2003).

Thanks to its low molecular weight, below the nuclear pore complex cut off, α-synuclein is potentially capable of diffusing from the cytosol to the nucleus without a prototypical nuclear localization signal. Indeed, the protein has been suggested to affect nuclear proteins function (Goers et al., 2003; Kontopoulos et al., 2006).

A-synuclein seems to be involved also in mitochondrial maintenance, in agreement with the observation that the protein binds to mitochondria and alterations of its expression levels can impair mitochondrial function (Ellis et al., 2007; Li et al., 2007; Martin et al., 2006).

2.3   α-synuclein and pathology

a. Aggregation

Based on the biophysical characterization of the bacterially expressed and purified protein, α-synuclein physiological form was originally reported to be monomeric and largely unstructured ("natively unfolded") (Weinreb et al., 1996). Today we know that α-synuclein can assume different conformations, from monomeric to fibrillar, from unfolded in solution to α-helical in the presence of lipid containing vesicles, to a ß-pleated sheet or amyloid structure in the fibrils that compose Lewy bodies (Fig.5).

The aggregation pathway of α-synuclein became a subject of intense study when the fibrillar form of the protein was discovered to be the main component of Lewy bodies. Electron microscopy revealed that LBs are made of unbranched α-synclein filaments with a length of 200-600 nm and a width of 5-10 nm. As other amyloid fibrils, these filaments have a cross-ß-structure, and the core comprises five ß-strands (Spillantini et al., 1998).

In addition to the typical amyloid fibrils found in LB, α-synuclein has been reported to form short fibril-like intermediates, the so-called 'protofibrils', and spherical or annular oligomers containing up to several hundred α-synuclein molecule (Conway et al., 2001; Norris et al., 2005).

The source of toxicity is still controversial, although a widely accepted hypothesis is that protofibrils are cytotoxic whereas fibrillar aggregates could be cytoprotective. A possible mechanism of toxicity has been proposed by Lansbury and colleagues, who showed that α-synuclein oligomers can form elliptical or circular pores in cell membranes, resulting in the release of their content and cell death due to increased calcium permeability (Campioni et al., 2010; Conway et al., 2000a, 2000b).

Changes in protein concentration and cellular localization can contribute to initiate aggregation. Higher production of the protein or impairments in protein degradation and quality control machinery directly increase intracellular α-synuclein concentration and consequently favor autonomous aggregation and seeding by exogenous α-synuclein. However, also the localization of the protein may be important. Indeed, mutant α-synuclein with impaired membrane binding ability results in the accumulation of unfolded monomers in the cytoplasmic compartment and a shifted equilibrium towards the formation of oligomeric and fibrillar species (Dettmer et al., 2015; Zhu and Fink, 2003).
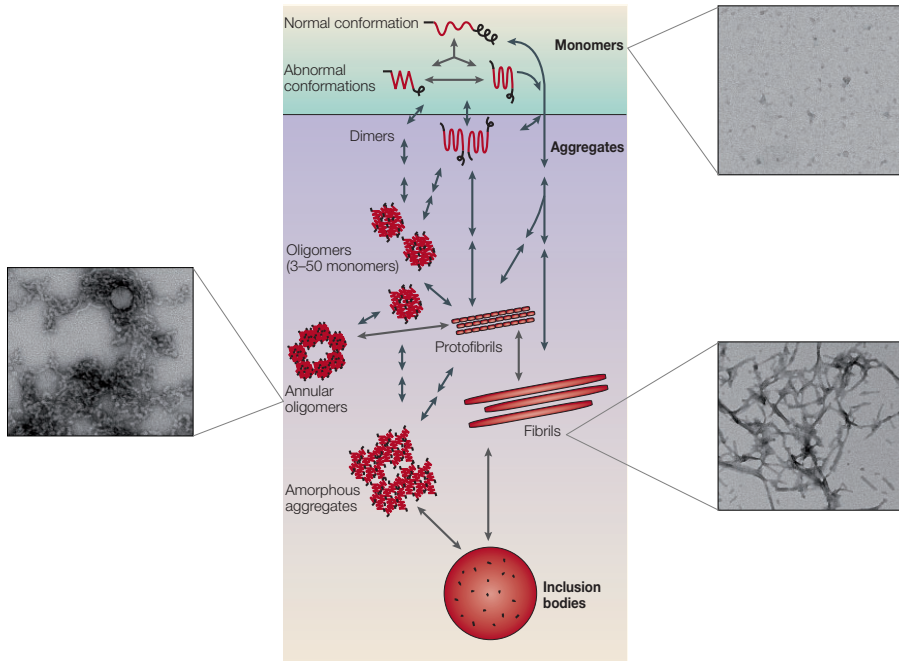
Figure 5. Possible pathways of α-synuclein aggregation and formation of inclusion bodies with electron microscopy images of monomeric α-synuclein, 4-hydroxy-2-noneal (HNE)-induced α-synuclein oligomers and α-synuclein fibrils obtained *in vitro*. [adapted from (Roberts et al., 2015; Ross and Poirier, 2005)]

b. Prion-like properties of pathologic α-synuclein

Prions are proteins that undergo a self-propagating conformational switch that can be transmitted to other proteins, which adopt a misfolded state. Although in fungi they play a crucial role in epigenetic inheritance (Aguzzi and Polymenidou, 2004), in mammals they are considered as infectious agents that can cause neuronal pathologies (e.g. Creutzfeldt-Jakob disease).

Several studies clearly point to a prion-like behavior of α-synuclein. *Post-mortem* histopathological examination of fetal mesencephalic neurons transplanted into PD patients show that these cells develop Lewy bodies. This suggests that the initiation factor of pathology had been conferred to healthy neurons by neighboring affected cells (Kordower et al., 2008). In line with this evidence, it has been

observed that brain homogenates containing α-synuclein aggregates can induce LB formation in the CNS of recipient animals (Luk et al., 2012a). Moreover, aggregation develops at very distant sites from the injection site indicating *in vivo* propagation of the misfolding process (Luk et al., 2012b; Masuda-Suzukake et al., 2013).

The mechanism of propagation of the disease is still unclear. Among possible routes, endocytosis appears to be a key mechanism mediating misfolded α-synuclein entry into neurons, as demonstrated by the observation that blocking endocytosis prevents cell-to-cell transfer of pathology (Desplats et al., 2009; Hansen et al., 2011). Another potential mechanism for spreading of the pathology are nanotunnels between cells which have been shown to be capable of spreading prion proteins, but this has not been yet demonstrated for α-synuclein (Gousset et al., 2009).

In addition, α-synuclein is found in several body fluids such as cerebrospinal fluid (CSF) and plasma, but the way the protein is released from cells remains unknown as well (El-Agnaf et al., 2003). Besides vesicles exocytosis, other non-conventional forms of exocytosis, such as exosome release and exophagy, an autophagosome mediated exocytosis, are currently being addressed (Emmanouilidou et al., 2010; Hasegawa et al., 2011).

c. α-synuclein and dopamine-oxidative stress

Alterations of functional α-synuclein levels impair neurotransmitter vesicles trafficking leading to accumulation o dopamine in the cytosol. Dopamine auto-oxidation metabolites promote the accumulation of cytotoxic protofibrillar species of α-synuclein, which cause vesicular membrane perforation with subsequent leakage of dopamine and further accumulation in the cytosol. The increase of reactive oxygen and nitrogen species perpetuates a toxicity loop, which can lead to neuronal degeneration (Conway et al., 2001; Jenner, 2003).

d. α-synuclein and mitochondrial dysfunction

Mitochondrial dysfunction has been largely implicated in the pathogenesis of PD. Indeed, Reeve AK. and co-workers demonstrated that α-synuclein accumulation and aggregation within mitochondria leads to inhibition of complex I, decrease of mitochondrial membrane potential ($\Delta\Psi_m$) and reduction of respiration and ATP production

(Reeve et al., 2015). This causes an increase in reactive oxygen species (ROS) production with deleterious consequences on α-synuclein aggregation and cellular metabolism (Luoma et al., 2004; Orth and Schapira, 2002). In parallel, this leads to the opening of the mitochondrial permeability transition pore (mPTP), release of cytochrome c and activation of apoptosis.

e. α-synuclein and ubiquitin-proteasome system impairment

The ubiquitin-proteasome system (UPS) play important roles in neuronal homeostasis (e.g. control of synaptic morphology and plasticity as well as electrical activity) by helping the equilibrium between protein degradation and synthesis, which are not confined in the cell body but occur also at the synapse (Bingol and Schuman, 2006; Ehlers, 2003; Jiang and Schuman, 2002). Moreover, the elimination of damaged proteins, such as oxidized or misfolded proteins, is particularly crucial for terminally differentiated cells that do not divide as neurons. The first indication of an implication of the UPS in PD, as well as other neurodegenerative disease, was the detection by ubiquitin immunohistochemistry of ubiquitylated proteins in LB and other protein inclusions. The second indication came from the identification of Parkin, a ubiquitin ligase enzyme, and UCHL-1, a deubiquitylating enzyme, as PD-associated genes. Although parkin only interacts with a glycosylated for of α-synuclein, it has been shown to exert a neuroprotective effect including against toxic α-synuclein, by rescuing proteasomal function (Feany 2003). Moreover, α-synuclein protofilaments, but not monomers or dimers, inhibit the catalytic activity of the 26S proteasome *in vitro* (Zhang et al., 2008).
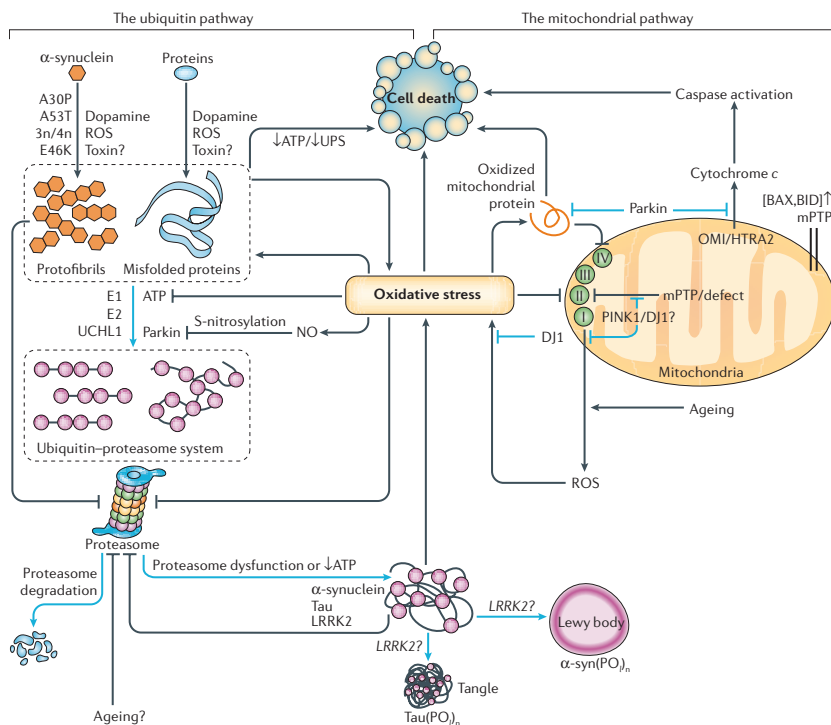
Figure 6. Pathways to Parkinons's disease and contribution of PD-associated genes [from (Abou-Sleiman et al., 2006)].

2.4 α-synuclein and Parkinson's disease

A missense mutation (A53T) in the *SNCA* gene encoding α-synuclein protein was the first PD-causing mutation that was identified in 1997 in a PD family with autosomal dominant inheritance (Polymeropoulos et al., 1997).

A53T, as well as E46K and H50Q have been reported to accelerate aggregation, while mutations A30P and G51D are instead associated with slower fibril formation, suggesting that their pathogenic effect might be related to soluble oligomers formation (Conway et al., 2000b; Greenbaum et al., 2005; Khalaf et al., 2014; Porcari et al., 2015). Patients carrying *SNCA* point mutations generally manifest an L-dopa-responsive parkinsonism with relatively early age of onset, rapid progression and high prevalence of dementia (Kiely et al., 2015; Spira et al., 2001).

Duplications and triplications of wild-type *SNCA* locus have also

been associated with autosomal dominant PD (Chartier-Harlin et al., 2004; Singleton et al., 2003). **The presence of multiple copies of the gene has been shown to cause an increase of α-synuclein mRNA expression in the frontal cortex and protein levels in whole blood samples.** Interestingly, the degree of overexpression was found to correlate with the severity of the disease and age of onset (Miller et al., 2004).

The role of *SNCA* locus has now been extended also to common sporadic forms of PD. Single nucleotide polymorphisms (SNPs) within *SNCA* locus have been associated to sporadic PD in the two largest genome-wide association studies (GWAS) performed to date (Satake et al., 2009; Simón-Sánchez et al., 2009).

2.5   *SNCA*   transcriptional   and   post-transcriptional regulation

The human gene encoding α-synuclein (*SNCA*) maps on chromosome 4q21.3-q22 and spans a region of 111 kb.

SNCA gene contains seven exons, five of which constitute the coding region, which is highly conserved between vertebrates (Siddiqui et al., 2016). *SNCA* gene generates various alternatively spliced transcripts, including the full-length transcript, commonly known as SNCA-140 from the length of the encoded protein, and three additional splicing variants known as, SNCA-126, SNCA-112 and SNCA-98, which are generated by in-frame excision of exon 3, 5, or both. SNCA-126 isoform lacks the N-terminal membrane interaction domain, SNCA-112 is significantly shorter in the unstructured C-terminal region, while SNCA-98 isoform results in a truncated protein composed almost only of the central NAC region (Beyer et al., 2008).

SNCA-126 has lower aggregation propensity, while C-terminus truncated SNCA-112 is expected to have higher tendency to aggregate. In addition to results showing α-synuclein overexpression in dementia with Lewy bodies brain, several studies have proved that C-terminal truncated α-synuclein enhances aggregation (Crowther et al., 1998; Daher et al., 2009; Murray et al., 2003). In contrast with this, a lower aggregation propensity for all shorter isoforms has been recently demonstrated *in vitro* (Bungeroth et al., 2014).

As mentioned before, next to missense mutations and gene

duplication and triplication responsible for alterations of protein intracellular concentration and aggregation propensity, a number of disease-associated *SNCA* variants have been identified by GWAS, but their link to disease remains unclear (Farrer et al., 2001; Maraganore et al., 2006; Satake et al., 2009). Possible effects of SNPs include alteration of the level of transcription, regulation of alternative splicing or alteration of mRNA stability through post-transcriptional mechanisms.

a. Transcription regulation

REP1 is a polymorphic dinucleotide repeat site located 10 kb upstream of *SNCA* transcription start site. Five REP1 alleles associated to PD-risk have been identified (Touchman et al., 2001; Xia et al., 1996). In particular, one of these alleles has been shown to regulate *SNCA* expression in neuronal cell culture (Chiba-Falek and Nussbaum, 2001) and in transgenic mouse model of PD (Cronin et al., 2009), and is in linkage disequilibrium with SNPs identified at the 3'end of *SNCA* locus. In a gene reporter assay, Chiba-Falek O. and colleagues, measured a mild to high increase of expression of the reporter gene depending on the size of the microsatellite "CA" repeat. They suggest a model of two regulatory regions, one upstream and another downstream of the REP1, where transcription factors bind and regulate *SNCA* transcription. REP1 might modulate their interaction with different effects depending on which allele is present in the locus.

b. Alternative splicing regulation

Alteration of the expression profile of *SNCA* splicing isoforms has been registered. All four transcripts are overexpressed in PD frontal cortex, with significant upregulation of SNCA-126 compared to healthy controls (Beyer et al., 2008). Only the three shorter transcripts are overexpressed in PD substantia nigra (Cardo et al., 2014; McLean et al., 2012). Interestingly, higher SNCA-112 ratio levels observed in frontal cortex samples of about 100 PD cases, have been associated with risk-associated SNPs rs2736990, rs356165 and rs356219 located at the 3'end of intron 4, at the 3'UTR of *SNCA* gene and at the 3' of *SNCA* gene respectively (McCarthy et al., 2011). In particular SNP rs356219 "G" risk allele and "A" protective allele correlated in an additive manner with higher ratio levels of SNCA-112, with a 2-fold difference between the two "GG" and "AA homozygous genotypes.

A *cis*-regulatory effect of these polymorphisms on splicing mechanism has been proposed, although any of these SNPs is positioned at splice sites. A bioinformatics analysis spotted potential enhancer/silencer *cis*-elements within the sequences surrounding the SNPs and, additionally, SR protein binding motifs (in particular for SRp40) that might be created or disrupted by the SNPs, were identified. However, the exact molecular mechanism through which these SNPs modulate *SNCA* splicing needs to be elucidated.

c. Post-transcriptional regulation by microRNAs targeting *SNCA* 3'UTR.

The 3'UTR of *SNCA* gene is known to contain target binding sites for two microRNAs, miR-7 and miR-153, which are mainly expressed in neurons and induce downregulation of α-synuclein expression (Doxakis, 2010; Junn et al., 2009). The presence, in this region of the transcript, of a cluster of three PD-associated SNPs with the most significant association, suggests that post-transcriptional regulation of mRNA stability, possibly through the binding of miRNAs, might determine disease susceptibility. More specifically, SNPs rs356165, which lies in a long interspersed nuclear element (LINE) in the 3'UTR of *SNCA*, and rs11931074, which map 3'downstream of *SNCA* gene, were associated to the risk of developing PD and are in strong linkage disequilibrium between them. However, *in silico* analysis predict that rs356165 would not affect the binding of known miRNAs. Another possibility is that SNPs within *SNCA* locus associated with PD are not actually functional, but lie in linkage disequilibrium with functional variants of surrounding loci. As an example, *SNCA* is flanked at the 5' by the G protein-regulated inducer of neurite outgrowth-3 (GRIN3) gene, which belongs to a family of proteins that participate in the regulation of synapsis transmission and energy metabolism, two processes that could be impaired in PD (Cardo et al., 2012).
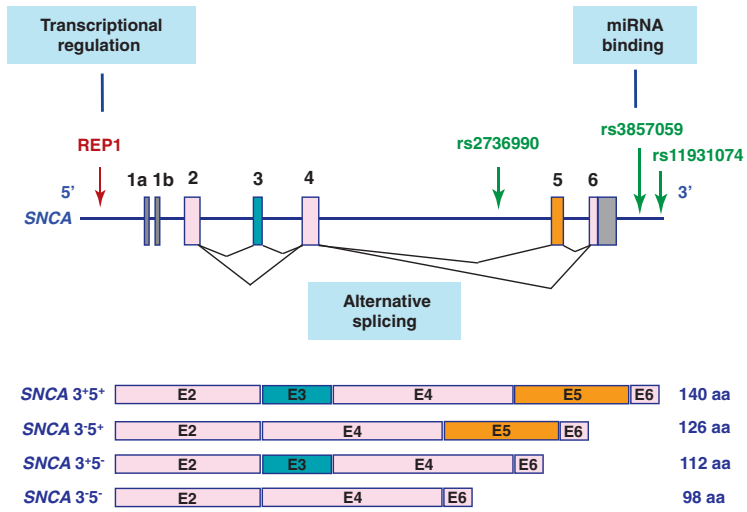
Figure 7. Schematic representation of *SNCA* gene structure, PD-associated polymorphisms (SNPs), miRNA-binding sites and alternative splicing isoforms [from (Venda et al., 2010)].

3. Post-transcriptional regulation of gene expression by 3'UTR binding factors: the key role of alternative polyadenylation

Neurons are the most complex cells in the mammalian organism. Their extremely polarized morphology, with formation of short and long processes that develop from the cell soma, namely dendrites and axons, require a particularly diversified proteome. In addition, neurons are highly interconnected among each other and need to quickly respond to electrochemical changes in the extracellular environment by rapidly adapting their proteome to the changing needs (e.g. expression of surface receptors and ion channels, enzymes and proteins for the synthesis, storage and release of neurotransmitters).

To fulfill these requirements, neurons make extensive use of post-transcriptional regulation. **Alternative splicing** (AS) and **alternative cleavage and polyadenylation at the 3'end** (APA) of pre-mRNA allow the cell to produce more than one mRNA isoform from a given gene. The isoforms can vary in their coding capacity and/or in their *cis*-acting regulatory elements. Despite the fact that these steps are traditionally described sequentially, they occur co-transcriptionally in the nucleus. Indeed, many mRNA processing factors are recruited to the C-terminal domain of the RNA polymerase II (Fong and Bentley, 2001). Moreover, all steps of pre-mRNA processing are in a controlled crosstalk between each other. For instance, polyadenylation is affected by transcription rate, chromatin state and spicing machinery.

In the cytoplasm, mRNA translation is also tightly controlled, most often during the assembly of the translation complex but also during the elongation phase. mRNAs are also actively transported to the subcellular domains where the encoded protein is needed in order to guarantee cellular functional compartmentalization. Finally, mRNA degradation can efficiently downregulate gene expression (Moore and Proudfoot, 2009).

All these regulatory steps are carried by *trans*-acting factors, including RNA-binding proteins (RBPs) and microRNAs (miRNAs) that target specific *cis*-acting sequence or structure elements that are particularly enriched in the 5' and 3'UTRs.

3.1 Alternative polyadenylation (APA)

The 3'end of most eukaryotic pre-mRNAs undergoes a two-step nuclear process that consists of (1) an endonucleolytic cleavage of the transcribed transcript, followed by (2) the addition of a poly adenosine tail. This process is essential for nuclear export and stability of mature transcripts and for their efficient translation in the cytoplasm (Proudfoot, 2011; Sachs, 1990).

This process requires several *cis*-acting RNA elements and several core and auxiliary proteins. The key *cis*-acting element that dictates the cleavage is the polyadenylation signal (PAS), a 'AAUAAA' hexamer which can adopt more than ten sequence variants and is located 15-30 nucleotides upstream of the cleavage site. Nearby there are also a U/GU-rich region, known as the dowstream sequence element (DSE), and the less well-defined upstream sequence elements (USEs), which enhance cleavage efficiency (Colgan and Manley, 1997; Millevoi and Vagner, 2010). The cleavage and polyadenylation specificity factor (CPSF) and cleavage stimulating factor (CSTF) are two complexes that recognize the PAS and DSEs, respectively, to promote cleavage between these two elements. CPSF consists of six polypeptides, named CPSF4, CPSF2, CPSF1, CPSF3, FIP1L1 and WDR33, while CSTF contains three subunits, namely CSTF1, CSTF2 and CSTF3 that are implicated in PAS selection. Additional factors that participate to the process are the highly evolutionary conserved poly(A) polymerase (PAP), the scaffold protein simplekin and cleavage factor Im (CFIm) and CFIIm. CFIm is composed of two subunits, CPSF6 and CFIm25, that bind UGUA motifs upstream of the cleavage site (Mandel et al., 2008; Yang et al., 2011).
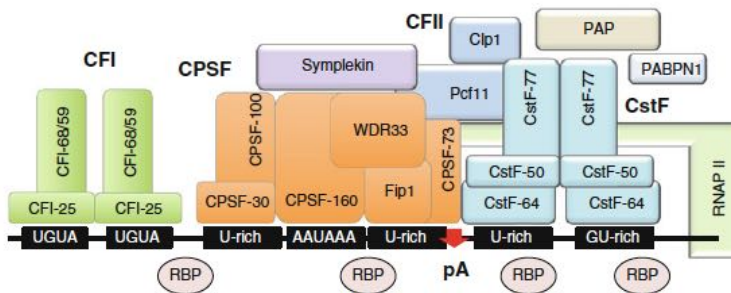
Figure 8. Schematic representation of the cleavage and polyadenylation machinery [from (Zheng Dinghai, 2014)]

The CP machinery can cleave and polyadenylate at multiple sites at the distal end of a gene, a process defined as alternative polyadenylation (APA). More than 50% of human genes undergo APA according to most recent genome-wide analysis of mRNA 3'termini, thus yielding multiple 3'UTRs. Notably, 3'UTR diversity has been recently recognized to be particularly widespread in the central nervous system (CNS) of Drosophila and mammals.

Depending on their configuration, APA events can be classified into four groups (Elkon et al., 2013) (Fig. 9):

- **tandem 3'UTR APA**, which involves the presence of alternative poly(A) sites within the same terminal exon and therefore generates isoforms that differ in their 3′UTR length without affecting the protein encoded. This is the most frequent APA;
- **alternative terminal exon APA**, in which alternative splicing generates isoforms that differ in their last exon and, consequently, in the availability of PAS sites;
- **intronic APA**, which involves cleavage at the cryptic intronic poly(A) signal, extending an internal exon and making it the terminal one;
- **internal exon APA**, which involves premature polyadenylation within the coding region.
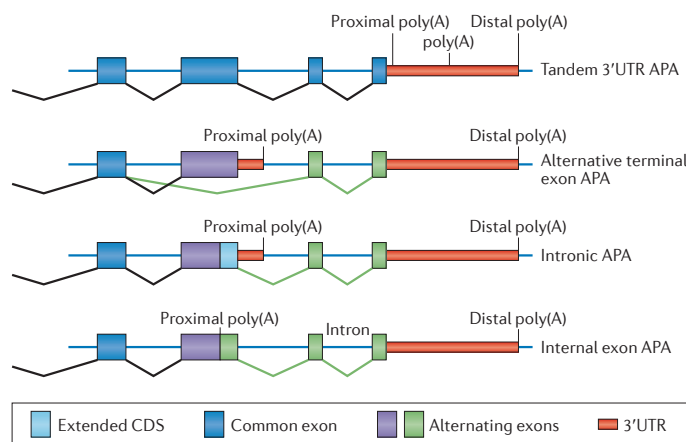
Figure 9. The four types of alternative polyadenylation [from (Elkon et al., 2013)]

By generating isoforms that differ in coding sequence or in 3'UTRs, APA strongly contributes to the complexity of the transcriptome. In the first case, APA can change the function of the encoded protein, while in the second case APA potentially regulates stability, cellular localization and translation efficiency of target RNAs.

Transcriptome-wide analysis of alternative 3'UTRs across several human tissues and cell lines reveal two classes of genes: one producing only one 3'UTR (**single-UTR genes**), and another producing alternative 3'UTR isoforms (**multi-UTR genes**) (Lianoglou et al., 2013). These two classes differ in architecture, function and tissue specificity. Single-UTR genes have a median 3'UTR length of 600 nt, in contrast with multi-UTR genes whose 3'UTRs are 2300 nt long on average. The majority of genes expressed in only one tissue have single 3'UTRs, while more than half of ubiquitously transcribed genes are multi-UTR genes. Ubiquitously transcribed single-UTR genes are enriched in housekeeping functions such as ribosome biogenesis, translation and energy metabolism, while ubiquitous multi-UTR genes generally play regulatory functions such as transcription, RNA binding, kinase or phosphatase activities, RNA and protein transport (Lianoglou et al., 2013)

3.2 Mechanisms of neuron-specific APA favoring 3'UTR lengthening

Several studies show that 3'UTR length is negatively correlated with the **abundance of poly(A) factors** in different cell types. Since the proximal poly(A) site is the first to be encountered by the cleavage machinery during transcription elongation, it is reasonable to think that sequence features surrounding this site and the availability of cleavage factors are crucial to decide whether the first poly(A) site will be bypassed or not (Ji and Tian, 2009; Ji et al., 2009; Ulitsky et al., 2012; Zhang et al., 2005a). However, experimental evidences of this hypothesis are contradictory. For instance, reduction of CstF-64 level did not introduce bias towards more proximal APA events; in contrast, decrease of CFIm68 levels had a broad effect on the transcriptome with a strong bias towards proximal PAS usage (Martin et al., 2012; Yao et al., 2012).

RNA polymerase activity may affect APA. Indeed, an RNA Pol II mutation that impair transcription elongation rate was linked to preferential usage of proximal polyA sites in Drosophila (Pinto et al.,

2011). Indeed, in mammalian cells transcription levels positively correlate with proximal poly(A) site usage (Ji et al., 2011). Also the chromatin status might influence PAS, as suggested by the observation of a biased nucleosome positioning around human PAS (Spies et al., 2009).

RBPs compete with poly(A) factors for the binding of sequence elements surrounding poly(A) sites. This is the case, for instance, of Drosophila Sex-Lethal (SXL), a protein that interferes with the usage of proximal sites by masking proximal DSEs, and promotes polyadenylation at distal sites. Also poly(A) binding protein 1 (PABPN1) acts through a similar competition mechanism and suppresses proximal PAS usage for more than 500 genes in human cells (Jenal et al., 2012). Finally, mammalian Hu proteins are well known to regulate RNA stability in the cytoplasm, but they can also affect 3'end processing in the nucleus (Zhu et al., 2007). HuB, HuC and HuD are neuron-specific, differently from the fourth member of the family, HuR, that is expressed ubiquitously. Interestingly, during neuron differentiation, all members of the family, including HuR itself, can modulate HuR APA and increase the expression of a less stable 6 kb long 3'UTR isoform of HuR transcript (Dai et al., 2012; Mansfield and Keene, 2012). This results in the downregulation of HuR protein necessary to favor expression of differentiation factors versus proliferation genes.

3.3   Functional roles of alternative 3'UTRs

a. Regulation of mRNA localization

Due to neuron peculiar morphology, the cellular sites of protein function are distant from the *nuclei*. Given that protein transport from the nucleus to the dendrites (or to synaptic terminals) is energetically very expensive for the cell, the most favorable strategy is to transport mRNA to the cellular compartment where protein function is needed. Yet, there is strong experimental evidence for local protein synthesis in neuronal dendrites. Asymmetrical distribution of the mRNAs is used not only to establish cell polarity, as in the case of *oskar* RNA which is localized to the posterior pole of the Drosophila oocyte during oogenesis by Mago Nashi-Tsunago protein complex (Mohr et al., 2001), but also to direct asymmetrical cell division, as for *ASH1* mRNA in budding yeast (Chartrand et al., 1999), or sequester protein activity, like observed for Ca(2+)-calmodulin-dependent protein

kinase II (*CaMKII α*) mRNA that localizes at the dendrites of mammalian neurons (Mayford et al., 1996).

Another example is the APA of the brain derived neurotrophic factor (BDNF), a neurotrophin important for synaptogenesis and activity-dependent synaptic plasticity. APA of the *BDNF* transcript generates two main 3'UTRs with remarkably different length: the short 3'UTR isoform localizes *BDNF* mRNA and protein to the soma of neurons, but the long 3'UTR, which contains the localization elements, is necessary for transport of the *BDNF* mRNA to the dendrites. Mice lacking the long 3'UTR had impaired long-term potentiation of hippocampal neurons (An et al., 2008). However, most of the *trans*-acting factors that mediate differential localization of neural 3'UTR isoforms remain to be identified.

Interestingly, new evidence suggest that mRNAs carrying long 3'UTRs might accumulate in ribonucleoprotein granules, membraneless cytoplasmic assemblies where a number of enzymatic reactions take place, including translation inhibition and mRNA degradation. Notably, granules-associated transcripts were enriched in gene ontology categories related to axon, dendrites and synapses composition and function (Han et al., 2012).

b. Regulation of mRNA translation

Alternative polyadenylation also determines the inclusion or exclusion of *cis*-elements targeted by RBPs that regulate translation (e.g. Pumilio, Maskin, TIAR, Musashi-1, FMRP, etc.,), and therefore generates 3'UTR mRNA isoforms with different translation potential (Battelli et al., 2006; Mazan-Mamczarz et al., 2006; de Moor and Richter, 2001). This is again the case of *BDNF*, whose short 3'UTR isoform is translated in unstimulated hippocampal neurons thus providing basal BDNF levels, whereas a translational switch in favor of the long 3'UTR isoform is produced by neuronal activation. This mechanism guarantees the activity-dependent increase of local BDNF synthesis (Lau et al., 2010).

c. Regulation of mRNA stability

The alternative 3'UTR isoforms can control protein abundance through the inclusion or exclusion of *cis*-elements that are targeted by RBPs regulating RNA stability or microRNAs-binding sites. AUF1,

TTP and KSRP or ELAVln, for instance, are RBPs that typically recognize AU-rich elements at the 3'UTRs and induce mRNA degradation or stabilization, respectively (Chen and Shyu, 1995). In addition, miRNAs recruit Ago proteins resulting in mRNA destabilization and shorten of mRNA half-life (Jonas and Izaurralde, 2015). Many proteins that need to be tightly controlled are regulated at the level of mRNA stability, including oncogenes, cytokines, cell cycle regulators and signaling proteins (Brewer, 1991; Liao et al., 2007; Schiavi et al., 1992; Stoecklin et al., 2003).

Tissue specific modulation of proteins encoded by ubiquitously transcribed genes can be achieved through the differential usage of proximal or distal APA sites in order to allow or avoid the interplay with specific miRNAs (Lianoglou et al., 2013). As an example, the mRNA of Pax-3, an important regulator of myogenesis, is targeted for degradation by miR-206. Despite the high levels of miR-206, considerable levels of Pax-3 protein are obtained in a subset of muscle stem cells through the selective expression of short 3'UTR isoforms that do not contain the binding site for miR-206 (Boutet et al., 2012)b. It is generally described that ubiquitously transcribed genes that produce alternative 3'UTRs are enriched in miRNA-binding sites for ubiquitously expressed miRNAs, while ubiquitous genes that produce only one 3'UTR are enriched in binding sites for tissue-specific miRNAs (Lianoglou et al., 2013).

It has been shown that shorter 3'UTRs of several oncogenes were more stable than the corresponding long 3'UTR isoforms and produced up to 40-fold more proteins (Mayr and Bartel, 2009a). IGF2BP1 (IMP-1) is an oncogene that if expressed with short 3'UTR generates higher protein amounts that induce fibroblast oncogenic transformation in soft agar assay or in mice (Tessier et al., 2004). By contrast, the expression of its long 3'UTR isoform had no transforming abilities. However, only a weak anti-correlation between the length of the 3'UTR and mRNA stability was found in transcriptome-wide studies performed in steady-state conditions and absence of stress.

d. Regulation of protein localization

Recently it was shown that the 3'UTR can act as a scaffold for the recruitment of proteins to the site of translation, which enables the formation of protein complexes for the transport of the nascent

protein to its final cellular localization (Berkovits and Mayr, 2015).

CD47 gene, encoding a lymphocyte surface antigen, generates alternative 3'UTR isoforms. In particular, CD47 protein produced by the short CD47 3'UTR isoform is predominantly retained in the endoplasmic reticulum, whereas the protein generated by the isoform carrying the long 3'UTR efficiently localizes to the plasma membrane, despite the fact that both RNAs have the same localization (Berkovits and Mayr, 2015). The difference is explained by the observation that the long 3'UTR binds the RBP HuR, which recruits the protein SET to the site of translation. SET is transferred to the nascent protein and, by forming a complex with RAC1, mediates the active translocation of CD47 to the plasma membrane (ten Klooster et al., 2007). This also influences protein function because the colocalization of CD47 with RAC1 at the plasma membrane also results in RAC1 hyperactivation, formation of lamellipodia and cell migration.

It is not known how the scaffold function of 3'UTRs is a widespread feature. It has been speculated that the same mechanism might be used for the translocation of other transmembrane proteins, such as G protein-coupled receptors, but this might also be applied to cytosolic or nuclear proteins (Dunham and Hall, 2009). We might even think that scaffold 3'UTRs could also influence protein folding by exerting a chaperone-like activity, or assist the formation of multiprotein complexes by helping protein-protein interactions, or mediate the recruitment of effector enzyme for the post-translational modification of nascent peptides.

3.4 Implication of polyadenylation in neurological disorders

A number of human diseases including hematological disorders (e.g. α- and ß-thalassemia), immunological (e.g. Wiskott-Aldrich syndrome, osteoarthritis and scleroderma), oncological (e.g. breast cancer, glioblastoma) and endocrine conditions (e.g. diabetic nephropathy and type II diabetes) have been related to alterations of polyadenylation events due to either mutations of APA *cis*-elements or to dysfunction of components of the polyadenylation machinery (Curinha et al., 2014).

Since broad neural 3'UTR lengthening is a property of adult mammalian brains, it is reasonable to assume that defective neural

APA might be associated with neurological syndromes. One emblematic case is the autosomal dominant oculopharyngeal muscular dystrophy (OPMD), a progressive adult onset disorder characterized by dysphagia, ptosis and proximal limb weakness (Davies et al., 2006). Most OPMD patients suffer cognitive decline, depression and psychosis. The disease is caused by a GCG expansion in the coding region of polyadenylation-binding protein nuclear 1 (PABPN1), which is translated into a N-terminal polyalanine tract of 12-17 amino acids that induces protein aggregation into intranucleus inclusion in skeletal muscle fibers. PABPN1 normally binds to poly(A) tails of the mRNAs stimulating progressive polyadenylation forming part of the complex that tethers poly(A) polymerase to the 3'end of mRNA (Abu-Baker and Rouleau, 2007). In the case of OPMD, mutated PABPN1 sequesters polyadenylated mRNAs into inclusion bodies, altering their expression (Fan et al., 2003).

The fragile X mental retardation 1 (FMR1) gene contains three pA signals, one is the canonical pA signal, and the other two are weaker PAS. It was observed that premutations in the 5'UTR (CGG repeats extended from 55 to 200) linked to fragile X-associated immature ovarian insufficiency (FXPOI) (Toniolo and Rizzolio, 2007) and fragile X-associated tremor and ataxia syndrome (FXTAS) (Hagerman and Hagerman, 2004), affect polyadenylation causing a decrease of isoforms produced by the weak pA signals (Tassone et al., 2011).

U1A, a subunit of U1 spliceosomal small nuclear ribonucleoproteins (snRNPs) complex, which has a main function in splicing, also intervenes in PA inhibiting polyadenylation through its interaction with PAP at the distal PAS of the bovine papilloma virus (BPV) pre-mRNA (Gunderson et al., 1998). Recently, it has been shown that U1A also inhibits polyadenylation of the survival motor neuron (SMN) pre-mRNA, resulting in a decrease in SMN protein production (Workman et al., 2014). This event is a key process in the development of Spinal Muscular Atrophy (SMA) (Lefebvre et al., 1995). Moreover, extracellular aggregation of U1snRNP components causing defects in RNA processing, has been described in the brain of AD patients (Bai et al., 2013).

Alterations of cyclooxygenase 2 (COX-2) polyadenylation have been also hypothesized in AD. COX-2 levels, which increase during inflammation, are regulated by APA through the production of two 3'UTR isoforms (2.8 kb and 4.6 kb), with the longer one being more

unstable (Ristimäki et al., 1994, 1996). It has been demonstrated that the neocortex, that is strongly affected in AD, expresses high levels of 4.6 kb COX-2 mRNA (Lukiw and Bazan, 1997).

Finally, the serotonin transporter (SERT) has two 3'UTR APA isoforms, the longer of which has been implicated in anxiety disorders (Hartley et al., 2012; Yoon et al., 2013).

3.5   *SNCA* alternative polyadenylation

The sequence of *SNCA* 3'UTR was first defined in 2009 by Sotiriou S and co-workers by means of EST bioinformatics analysis and RT-qPCR on RNA extracted from brain of human *SNCA* transgenic mice. They identified four different polyadenylation events and measured that about 95% of *SNCA* mRNA contain a 574 nucleotides long 3'UTR, suggesting that the first 574 nt are the most relevant for human physiology. rs17016074 SNP is located between the two most frequently used polyA sites, immediately upstream of a downstream sequence element (DSE), and could therefore affect polyadenylation efficiency at the upstream polyA signal. rs356165 is located in a LINE element at the downstream regions of the 3'UTR, between 800 and 1000 bases, and can therefore have a direct effect on the expression of only a small minority (about 5%) of *SNCA* mRNA in which is present, according to Sotiriou et al. (Sotiriou et al., 2009).

Alternative *SNCA* transcript isoforms usage has been suggested as a potential convergent mechanism in Parkinson's disease pathology (Rhinn et al., 2012). Specific transcript isoforms of *SNCA* with an extended 3'UTR (>574 nt) show an increased preponderance with respect to shorter isoforms (<574 nt) in cerebral cortex samples of *post-mortem* PD patients (Fig.10). A similar effect was observed in laser-dissected substantia nigra dopaminergic neurons of PD patients. Moreover, the presence of the extended 3'UTR impact accumulation of α-synuclein protein, which appears redirected away from synaptic terminals and towards mitochondria (Rhinn et al., 2012). This might be relevant to disease processes as mitochondrial dysfunction is implicated in the onset of Parkinson's disease neuropathology, as discussed before (Su et al., 2010). Interestingly, in the same study it was shown that the level of the *SNCA* isoform carrying the extended 3'UTR increased upon dopamine treatment in midbrain dopaminergic neurons, indicating that the neurotransmitter can modulate *SNCA* APA.

In addition, significantly lower levels of *SNCA* mRNA with the extended 3'UTR were quantified by digital expression analysis in peripheral blood in a cohort of 202 cases of *de novo* motor Parkinson's disease, thus envisaging its clinical role as potential accessible marker of diagnosis (Locascio et al., 2015).
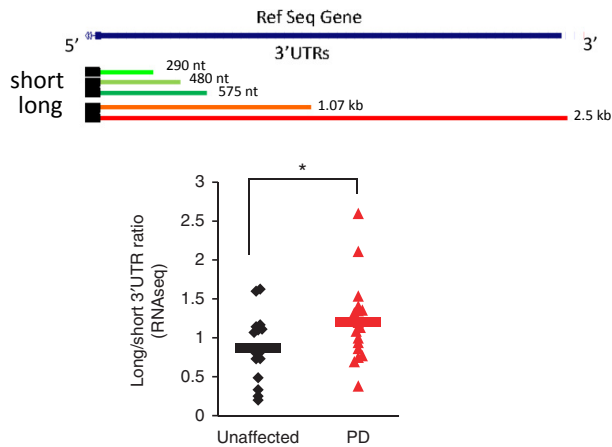
Figure 10. Increase of the *SNCA*-3'UTR long isoforms (1.07 and 2.5 kb) versus *SNCA*-3'UTR short isoforms (<575 nt) measured by pA-RNA sequencing in cortical samples of unaffected individuals (n=17) and PD patients (n=17). [adapted from Rhinn H. et al., 2012].

4.   Objective of the study

In the light of these observations, I hypothesized that post-transcriptional regulation of *SNCA* expression by *trans*-acting factors targeting the 3'UTR of its mRNA might have a strong impact on protein accumulation, localization and function. Although changes in expression levels produced by post-transcriptional regulation are usually lower than the order of magnitude caused by the regulation at the transcriptional level, we know that α-synuclein is highly concentrated at the pre-synaptic terminals of neurons in normal conditions (70-140 uM estimated) and even small fluctuations of its concentration can induce aggregation (van Raaij et al., 2008). A switch of alternative polyadenylation favoring the expression of minor *SNCA* isoforms with longer 3'UTRs in PD-brain, might represent a causative event responsible for the alteration of α-synuclein expression and function, leading to the initiation of the disease. Alternatively, the usage of distal polyadenylation sites could be a compensatory event activated in response to altered cellular environment (e.g. oxidative stress, α-synuclein aggregation, mitochondrial dysfunction, etc.). Both possible scenarios point to the relevance of the post-transcriptional regulation of *SNCA* expression by factors targeting upstream or downstream 3'UTR sequence elements.

Moreover, the emerging evidence that neurological disorders, traditionally considered as proteinopathies, are often caused by alterations of RNA processing events (which impose their re-definition as 'ribonucleopathies'), support the idea that Parkinson's disease, as other synucleinopathies, could be initiated by dysregulation of post-transcriptional processes.

I hypothesize that the regulation coordinated by RBPs and microRNAs is fundamental for the control of α-synuclein cellular level, mobilization and turnover in response to various environmental *stimuli*. **In the present work I address the question of what RBPs are able to bind the 3'UTR of *SNCA* gene and affect its expression.** Following the discovery of protein interactors by means of a large-scale *in vitro* screening, **I focused my attention on two RBPs, ELAVL1 and TIAR, that are known to target the 3'UTRs of mRNAs and influence their stability, translocation and translation efficiency**. Both proteins are ubiquitously expressed in human and might be essential components of a larger network of

factors that regulate various steps of *SNCA* expression.

MATERIAL AND METHODS

Herein I present the experimental procedures used for my experimental work. Details about primers sequence and antibodies used are in Appendix.

5.1 *SNCA* 3'UTRs cloning into pBSK vector

Genomic DNA extracted from human lymphocytes with QiaAMP DNA Mini kit (Qiagen) was used as a template to amplify the sequence of the three *SNCA* 3'UTRs of interest (570 bp, 1.07 kb and 2.5 kb):

- short 3'UTR (570 bp) was amplified with primers containing ApaI and NotI restriction sites. KOD polymerase (Millipore) was used following manufacturer's amplification conditions with annealing temperature (T_a) of 72°C. The amplicon corresponding to the correct size was purified from gel band using QIAquick gel extraction (Qiagen). PCR product and pBluescript-SK(+) empty plasmid were double digested with ApaI and NotI restriction enzymes. Dephosphorylation of the linearized plasmid was performed with FastAP enzyme (Fermentas). The insert and the plasmid were ligated with T4 DNA ligase (ThermoFisher Scientific) and transformed into DH5α compentent cells (Life Technologies).

- medium 3'UTR (1.07 kb) was amplified with primers containing ApaI and BamHI restriction sites. Phusion polymerase (New England Biolab) was used according to manufacturer's instructions with annealing temperature (T_a) of 62°C and with the addition of 3% DMSO to the reaction. PCR product was purified with MinElute PCR purification kit (Qiagen). PCR product and pBSK plasmid were double digested with ApaI and BamHI restriction enzymes. The linearized plasmid was dephosphorylated with FastAP enzyme (Fementas). Insert and plasmid were ligated T4 DNA ligase (ThermoFisher Scientific) and transformed into DH5α competent cells (Life Technologies).

- Due to amplification difficulties, long 3'UTR (2.5 kb) was amplified with a nested PCR approach. First a larger DNA

fragment was amplified using primers that anneal to the genomic regions flanking the 3'UTR of *SNCA*. Amplification reaction was done with KOD polymerase (Millipore) for 20 cycles in order to minimize mutation insertion, with T_a of 65°C and the addition of 1 M Betaine. The PCR product was used as template for a second amplification reaction with primers specific for the long 3'UTR containing ApaI and NotI restriction sites. KOD polymerase (Millipore) was used and the reaction was run according to manufacturer's instructions with T_a of 62°C and addition of 5% DMSO. The PCR product was purified with MinElute PCR purification kit (Qiagen). PCR product and pBSK plasmid were double digested with ApaI and NotI restriction enzymes. The linearized plasmid was dephosphorylated with FastAP enzyme (Fementas). Insert and plasmid were ligated with T4 DNA ligase (ThermoFisher Scientific) and transformed into Stbl2 competent cells, which are suitable for cloning of unstable inserts as the long 3'UTR that contains large stretches of poly(U), poly(UC) and poly(A) repeats.

White colonies, representing recombinants, were screened for the presence of the insert by colony PCR with T7 forward primer and reverse primer annealing at the 3'end of the insert. For positive colonies, the correctness of the construct was confirmed by sequencing.

Verified positive colonies were used for plasmid DNA amplification and purification with PureLink HiPure Plasmid Filter Maxiprep kit, according to manufacturer's instructions (Invitrogen).

Sequences of primers used for cloning are listed in Appendix.

5.2. Human Protein Array

The RNA probes of the *SNCA* long 3'UTR (3'UTRL) were synthesized by *in vitro* transcription (IVT) with the T7 RNA polymerase (Agilent) from a pBSK plasmid vector carrying a T7 (sense) or T3 (antisense) promoter and fluorescently labeled with *Label* IT μArray Cy5 labeling kit (Mirus) applying some modifications to manual instructions.

Briefly, 5 ug of RNA were mixed with 5 ul of 1:5 *Label* IT Cy5 reagent and incubated in a final volume of 25 ul at 37°C for 1 hour. The reaction was stopped by adding 2.5 ul of 10X Stop buffer and RNA was purified with Agencourt RNAclean XP magnetic beads and resuspended in 18 ul of RNase-free water. The RNA concentration and labeling density were measured with Nanodrop 1000 spectrophotometer (Thermo Scientific) and calculated as follows.

Only reactions with an RNA labeling density of 1 Cy5 dye per 700-900 nt were used.

$$\text{Base:dye} = (A_{base} * \varepsilon_{dye})/(A_{dye} * \varepsilon_{base})$$
$$A_{base} = A_{260} - (A_{dye} * CF260)$$

Constants:
$\varepsilon_{dye} = 250000$
$CF260 = 0.05$
$\varepsilon_{base} = 8250$

RNA integrity was verified by Agilent 2100 Bioanalyzer.

ProtoArray® Human Protein Microarrays v5.2 (Life Technologies) were probed with the Cy5 labeled RNA of interest as previously reported (Siprashvili et al., 2012). The dry slides were scanned at 635 nm (Cy5) using a GenePix 4000B Microarray scanner (Molecular Devices) immediately after or at least within 2 h of the completion of the hybridization.

The intensity of the signal at 635 nm wavelenght at each spotted protein location was determined with GenePix Pro 6.1 software (Molecular Devices). To quantify RNA-protein interactions, the local background intensity (B635) was subtracted from the intensity (F635)

at each of the duplicate spots for a given protein. Data was filtered based on signal to background ratio for each of the duplicate feature to be greater than 2.5 fold and Z-Score ≥ 3 from the global mean signal from all the spotted proteins. The intersection of 3 technical replicates was taken. In order to select sense-specific protein interactions, significant hits from the antisense were subtracted from the significant hits in the sense RNA.

The software developed by our group, catRAPID omics (Agostini et al. 2013, Bioinformatics) was used to compute the interaction propensity of *SNCA* long 3'UTR with the candidate proteins selected with ProtoArrays. catRAPID omics ranks predictions based on predictive score as well as presence of motifs and RBDs. For proteins >750 aa a 'uniform fragmentation' (i.e., division in shorter sequences) procedure was applied. Candidates were sorted by the median value of catRAPID omics ranking score.

5.3 RNA affinity purification

1. The RNA probes of the *SNCA* short 3'UTR (3'UTRS) and long (3'UTRL) were synthesized by *in vitro* transcription from a linearized pBSK plasmid vector carrying a T7 promoter. Biotin-14-CTP (Life Technologies) was added to the reaction with a ratio of 1:10 with CTP.
2. Biotinylated RNA was purified using Agencourt RNAclean XP magnetic beads and resuspended in 30 ul of RNase-free water. RNA concentration and integrity were verified by NanoDrop 1000 spectrophotometer (Thermo Scientific) and by denaturing agarose gel electrophoresis of the RNA. Successful biotinylation was checked using the Chemiluminescent Nucleic Acid Detection Module kit (Thermo Scientific).
3. 33 pmoles of biotinylated RNA were bound to Streptavidin magnetic beads (Dynabeads M-280, Invitrogen) previously blocked with 100 ng/ul of tRNAs in NT2 buffer (50 mM Tris-HCl pH 7.5, 150 mM NaCl, 1 mM MgCl$_2$, 0.05% NP-40, 1 mM DTT). As a negative control, beads in absence of RNA were used.
4. 2 mg of SH-SY5Y total cell extracts were added and incubated for 1 hour at room temperature, in the presence of 1X Protease Inhibitors cocktails (Sigma Aldrich), 320 ng/ul Heparin (Sigma Aldrich), 4.3 ug/ul of Creatine Phosphate and 80 ng/ul of Creatine Kinase.

5. Samples were cross-linked with 6000x100 uJ/cm^2 of energy using a UVP CL-1000 crosslinker with 254 nm wavelength.
6. Beads with RNA-protein complexes were washed two times with each of the following buffers in order to remove unbound proteins: NT2 (50 mM Tris-HCl pH 7.5, 150 mM NaCl, 1 mM MgCl2, 0.05% NP-40, 2 mM Vanadyl ribonucleoside complexes, 1% Triton X-100, 10% glycerol), HSB300 (50 mM Tris-HCl pH 7.5, 300 mM NaCl, 1 mM EDTA, 1% NP-40, 1% Triton X-100, 320 ng/ul heparin, 10% glycerol), HSB500 (50 mM Tris-HCl pH 7.5, 500 mM NaCl, 1 mM EDTA, 1% NP-40, 1% Triton X-100, 320 ng/ul heparin, 10% glycerol) and HSB1000 (50 mM Tris-HCl pH 7.5, 1 M NaCl, 1 mM EDTA, 1% NP-40, 1% Triton X-100, 320 ng/ul heparin, 10% glycerol).
7. Samples were resuspended with elution buffer (10 mM Tris-HCl pH 7.2, 1 mM MgCl2, 40 mM NaCl) RNase cocktail digestion was used to elute proteins bound to the RNA.
8. All volume eluted from 3'UTRS RNA, 3'UTRL RNA and negative control samples were used for western blot for the detection of specific target proteins previously identified by protein arrays, such as ELAVL1/HuR and TIAR (FMR1 was used as a negative control on the basis of protein array results, fold change < 1.7 and and Z-score < 0, and catRAPID score of interaction with *SNCA* 3'UTRs (Z-score of 0.18 with a interaction strength of 59% for the 3'UTRS).

The RNA affinity purification was done in technical triplicates and the protein bands for each of the RNAs were quantified by densitometry using ImageJ analysis software (Schneider et al., 2012). Statistical significance of the difference between 3'UTRS and 3'UTRL, as well as with respect to the negative control, were determined by a Student's T-test.

5.4 Luciferase gene reporter assay

SNCA short 3'UTR (570 bp), medium (1.07 kb) and long (2.5 kb) were sub-cloned by Gibson cloning strategy from the pBSK(+) plasmid to pGL4-TK-*Firefly* luciferase (pGL4-TK-FL) plasmid vector. *SNCA* 3'UTRs were cloned at the 3'end of the *Firefly* luciferase coding sequence and before the SV40 poly(A) signal.

Subsequently, pGL4-TK-FL was linearized by PCR with Ex Taq DNA polymerase (Takara), while short 3'UTR, medium and long were amplified from pBSK plasmid with forward and reverse primers containing 20 bases flanking regions annealing to the pGL4 plasmid at the site of insertion. Linearized pGL4 plasmid and amplified 3'UTRs with overlapping DNA extremities were incubated with Gibson mix which creates single-stranded 3´ overhangs that facilitate the annealing of the fragments that share complementarity (exonuclease), fills in gaps within each annealed fragment (DNA polymerase) and seals nicks in the assembled DNA (DNA ligase).

The reaction was used to transform DH5α competent cells (Life Technologies) and colonies were screened by colony-PCR for the presence of the insert. Recombinant colonies were then sequenced to verify the correctness of the constructs.

The proximal polyadenylation signals within the sequence of the exogenously expressed constructs carrying the long 3'UTR could be recognized by the endogenous CP machinery and prematurely cleaved thus producing a heterogeneous mix of RNAs with different length. To guarantee the expression of the long or medium 3'UTR isoforms only, the proximal polyadenylation sites (PAS), present within the sequence of the 3'UTRs, were deleted by Gibson cloning at position 262-267 nt, 468-473 nt, 529-553 nt and 1054-1059 nt (taken from Sotiriou S. et al., 2009). Indeed, a total of two, three and four PAS were deleted from the short 3'UTR, medium and long respectively by amplification of the constructs with primers annealing to sequences flanking the deletion sites. After amplification, the reaction was incubated with Gibson mix to seal the two DNA overlapping extremities. The correctness of the deleted constructs was verified by Sanger sequencing (GATC biotech).

The dual luciferase assay is commonly used to study cellular events coupled to gene expression such as promoter activity, intracellular signaling, mRNA processing, etc. It exploits the activity of the reporter gene, which encodes for an enzyme, the Firefly luciferase, that catalyzes the luciferin oxidation using ATP: Mg^{2+} as a co-substrate. The reaction produces the emission of light that can be measured using a luminometer. The intensity of light emitted is linearly proportional to the level of gene expression over eight orders of magnitude.

HeLa cells (courtesy of Di Croce's Lab) were seeded at a density of 8×10^5 cells per well in 24-well plates (triplicate wells per condition) with DMEM supplemented with 10% fetal calf serum (FBS), 2 mM L-glutamine without antibiotics. Cells at 80% confluence were transfected with Lipofectamine2000 (Life Technologies) according to manufacturer's instructions. pGL4-TK-FL plasmid carrying the sequence of the short medium or long 3'UTR, was co-transfected with pGL4-TK-*Renilla* luciferase plasmid (pGL4-TK-RL), used as internal control reporter activity to normalize for differences in transfection efficiency.

In addition, pGL4-TK-FL empty plasmid was used to compare the effect of *SNCA* 3'UTRs on reporter gene activity, and a GFP expressing vector (Puro IRES GFP, PIG) was used to check for transfection efficacy. Due to large size differences among the four contructs, cotransfection was performed with a fixed number of moles (130 fmoles) of pGL4-TK-FL construct (empty or carrying 3'UTRs), with 50 ng of pGL4-TK-RL.

48 h after transfection, the dual luciferase activity was measured using Dual-Luciferase reporter assay system (Promega). Briefly, cells were lysed with 1X Passive lysis buffer for 15 min at room temperature with gentle shaking. Lysates were diluted 1:10 with lysis buffer and the activity of the *Firefly* and *Renilla* luciferase was measured by sequentially adding the two substrates of enzymatic activity (LAR II and Stop&Glo reagents) and recording luminescence with a plate reader (Tecan Infinite M-200). Not transfected cells were used for estimating background noise. *Firefly* luciferase activity was normalized with *Renilla* luciferase activity for each sample and then normalized *Firefly* luciferase activity of pGL4-TK-FL-*SNCA* 3'UTRs constructs was compared with the activity of pGL4-TK-FL vector.

From a duplicate 24-well plate RNA was purified with *RNeasy* Mini kit and reverse transcribed with SuperScript III First-Strand synthesis SuperMix for qRT-PCR (Invitrogen). Real-time PCR was performed with 10 ng of cDNA template, 250 uM forward and reverse primers and 1X Sybr Green PCR master mix (Applied biosystem). The mRNA of *Renilla* luciferase was used to normalize *Firefly* luciferase mRNA levels. Primers used are listed in Appendix.

In the case of luciferase assay performed with RNA transfection, the RNA corresponding to FL, FL-SNCA 3'UTR S, FL-SNCA 3'UTR M, FL-SNCA 3'UTR L and RL (*Renilla* luciferase) was synthesized *in vitro* with a T7 MegaScript kit (Ambion) following manufacturer's instructions and pre-incubating the reaction with a unmethylated Cap Analog G (5′)ppp(5′)G (NEB), which is essential to protect the RNA from degradation. RNA was purified with Agencourt RNAclean XP magnetic beads and its concentration was measured at Nanodrop 1000 spectrophotometer (Thermo Scientific). The integrity and size of the RNAs were checked by denaturing agarose gel electrophoresis.
500 fmoles of each *Firefly* luciferase construct were co-transfected with 100 ng of the *Renilla* luciferase RNA, by using TransMessenger Transfection kit (Qiagen) following manufacturer's instructions. 4 hours after transfection cells were lysed with Passive lysis buffer and processed as decribed before for dual luciferase assay.

5.5 RNA 3'end sequencing

500 ng of total RNA isolated from HeLa and *in vitro* differentiated SH-SY5Y cells with RNeasy Mini kit (Qiagen) were used for the first strand cDNA synthesis with OligodT carrying a 5' flanking region containing the sequence of the Unique Molecular Identifier (UMI) and the R2 sequencing adaptor. Then a first PCR amplification was performed with a pool of forward PCR specific primers annealing to different regions of the 3'UTR and carrying 5' flanking regions containing the R1 sequencing adaptor, and the Index primer, annealing to the R2 adaptor. This was followed by a second PCR amplification with Universal PCR primer and TS Oligo 2. After purification with AMPure WP Beads, the quality of the library was assessed on a Agilent Bioanalyzer DNA 1000 Chip. DNA libraries were subjected to 50 bases pair end sequencing. Around $1,5 \times 10^{6}$ reads

per sample were obtained and 66% of them mapped to *SNCA* transcript.

The procedure used for the bioinformatics analysis was the following: the unique molecular identifier (UMI) was transferred from the second read pair to the first one's header and the left pair read was mapped to the gene of interest. The UMI in the header was used for checking the PCR duplicates and for grouping together reads with multiple mapping. In that case only the read with the biggest coordinates was counted. Every mapping smaller than 25 nt was removed and a tolerance of +8 bases for reads count was admitted in order to avoid PCR artifacts. Finally the ratio on the total number of reads mapping to those intervals was calculated.

The same analysis was also applied to HeLa control, TIAR knockdown and ELAVL1 knockdown cells in three biological replicates knockdown experiments and the average results were compared across cell lines in order to assess changes in the

5.6 Measurement of expression level in frontal motor cortex of Parkinson's disease (PD) and Multiple System Atrophy (MSA) patients

The human *post-mortem* motor cortex brain tissue stored at -80°C was obtained from the Brainbank from Institut d'Investigacions Biomèdiques August Pi I Sunyer (IDIBAPS)-Biobank, with the corresponding informed consent signed by donors or relatives. Approval of the local ethics committee was requested for the use of brain tissue and for access to medical records for research purposes. The tissue samples were dissected and used in a manner compliant with the Declaration of Helsinki. Brain tissue of five Parkinson's disease (PD) patients, five Multiple System Atrophy (MSA) patients and five healthy control individuals was used in this study. The three groups were matched for age of onset and age of death, gender and severity of the disease. Total RNA was extracted by using the *RNeasy Lipid Tissue Mini Kit according to manufacturer's instructions.* RNA concentration and integrity were verified by NanoDrop 1000 spectrophotometer (Thermo Scientific) and Agilent 2100 Bioanalyzer.

500 ng of RNA were used for reverse transcription with the SuperScript III First-Strand synthesis SuperMix for qRT-PCR (Invitrogen) and real-time PCR was performed with 10 ng of cDNA template, 250 uM forward and reverse primers and 1X Sybr Green PCR master mix (Applied biosystem).

The expression levels of the following genes was measured: *ELAVL1*, *TIAR*, *SNCA* total isoforms, *SNCA* (1.07 kb and 2.5 kb isoforms), *SNCA* (2.5 kb isoform). Primers used are listed in the Appendix. Cq values for each gene were normalized using *GAPDH* as endogenous reference gene (DeltaCq). The mean Cq values between biological replicates was calculated. The relative expression value was calculated using the delta Ct formula (Vandesompele et al., 2002). Student's *T*-test was performed to assess the three groups (PD, MSA and control) for significant differences in gene expression.

Total proteins were extracted from frontal motor cortex frozen tissue of five PD, five MSA and five control individuals (see above). The tissue was lysed with RIPA buffer (50 mM Tris-HCl pH 7.4, 150 mM NaCl, 1% Triton-X100, 0.5% sodium deoxycholate, 0.1% SDS, 1X Protease and Phosphatase Inhibitors) and homogenized with the help of pellet pestles. After sonication with bioruptor sonifier (Branson) at medium power for five min, 30 sec ON/OFF, samples were centrifuged at 16000 g for 15 min.

Supernatants were transferred to other tubes and protein concentration was measured with Bradford reagent (Sigma Aldrich). 20 ug of total cell lysate were used for SDS-PAGE and transferred to nitrocellulose membrane with iBLOT dry transfer system (Invitrogen). After blocking with 5% milk with 1X TBS-T, the membrane was incubated overnight at 4°C with the primary antibody in 2.5% milk with 1X TBS-T. After washing with 1X TBS-T, the membrane was incubated with HRP-conjugated secondary antibody for 1 h at room temperature and washed again with 1X TBS-T. ECL solution (Luminata Classico Western HRP substrate, Millipore) was added and exposure to photographic film (GE Healthcare) during a variable time depending on protein expression level allowed proteins bands detection. Human α-tubulin was used as internal reference protein for normalization with ImageJ (Schneider et al., 2012).

The list of commercial antibodies used can be found in Appendix.

5.7 TIAR and ELAVL1 knockdown

Adherent HeLa cells (courtesy of Di Croce's lab) were cultured under standard conditions. TIAR and ELAVL1 short hairpin RNA (shRNA) constructs were generated by annealing single stranded complementary oligonucleotides (Sigma Aldrich) containing the shRNA sequence flanked by sequences that are compatible with the sticky ends of EcoRI and AgeI. pLKO.1 TRC-puro plasmid was digested with AgeI and EcoRI and purified from gel band. The annealed oligos were then ligated with digested pLKO.1 TRC-puro plasmid by T4 DNA ligase and transformed into DH5α competent cells (Life Technologies). The sequence of shRNAs, listed in the Appendix, was chosen from Sigma short hairpin RNA library, according to the validated mean knockdown levels.

Hek293T cells were used as lentivirus packaging system. Cells were cultured in 10 cm^2 dishes under standard conditions (DMEM supplemented with 10% heat-inactivated FBS, L-glutamine and antibiotics). By using calcium phosphate transfection method, cells at 60% confluence were transfected with 7 ug of pLKO-shRNA (TIAR shRNA, ELAVL1 shRNA) or pLKO-empty vector (negative control), 5 ug of pCMV-VSV-G and 6 ug of pCMVDR-8.91 plasmids, to produce pLKO-shRNA-containing lentivirus. Medium containing lentivirus was collected after 40 and 48 h, filtered, supplemented with 5 ug/ml polybrene (Sigma Aldrich) and used to infect HeLa cells.

The day after infection, HeLa cells were selected with 2.5 ug/ml puromycin (Sigma Aldrich) for effective infection. After 24 h of selection cells were split and checked for efficacy of the knockdown by real-time PCR and western blot. Samples collected 3 days after selection were used to check the level of expression of α-synuclein at the mRNA and protein level.

RNA was isolated with *RNeasy* Mini kit (Qiagen) and reverse transcribed with SuperScript III First-Strand synthesis SuperMix for qRT-PCR (Invitrogen). Real-time PCR was performed with 10 ng of cDNA template, 250 uM forward and reverse primers and 1X Sybr Green PCR master mix in a 7900HT system (Applied biosystem). Cq values for each gene were normalized using ACTB reference gene (ΔCq) and the relative expression values were calculated using the delta Ct formula. Average values of biological replicates were

calculated and a *T*-test was performed to assess for significant differences in gene expression between knockdown and control cells.

Proteins were extracted by lysing the cells with Pierce lysis buffer (Thermo Fisher Scientific) supplemented with Protease and Phosphatase Inhibitors (Thermo Fisher Scientific). After sonication, samples were centrifuged at 20,000 g. Protein concentration was measured by Bradford reagent (Sigma Aldrich) from supernatants.
30 ug of total proteins were used for SDS-page transferred to nitrocellulose membrane with a wet electroblotting system (Bio-rad).
After blocking with 5% milk with 1X TBS-T, the membrane was incubated overnight at 4°C with the primary antibody in 2.5% milk with 1X TBS-T, washed with 1X TBS-T and incubated with HRP-conjugated secondary antibody for 1 h at room temperature. After additional washes with 1X TBS-T, proteins were detected using an ECL solution (Luminata Classico Western HRP substrate, Millipore) and exposing to photographic films (GE Healthcare) during a variable time depending on protein expression levels. Human α-tubulin was used as internal reference protein for normalization with ImageJ (Schneider et al., 2012).

5.8 TIAR and ELAVL1 overexpression

Hela cells were seeded in 6-well plate at a density of $4,8x10^5$ cells per well using DMEM supplemented with 10% FBS and L-glutamine, without antibiotics. 80-90% confluent cells were transiently transfected with 2 ug of pCMV-AC-ELAVL1 (OriGene Technologies) for ELAVL1 overexpression or pEGFP_G-TIAR (Clontech, courtesy of Valcarcel's Lab) for TIAR overexpression, using Lipofectamine 2000 according to manufacturer's instructions. pcDNA3.1-EGFP was used as a control plasmid for both overexpression experiments. Cells were collected 24 h and 48 h after transfection and *SNCA* mRNA and protein levels were checked upon ELAVL1 and TIAR overexpression by real-time PCR and western blot (see above). The mean values of technical triplicates were calculated.

5.9 RNA stability assay

Hela cells (control, TIAR and ELAVL1 knockdown) were seeded in 12-wells plate at a density of $1,6x10^5$ cells per well. The stability of *SNCA* mRNA was assessed by the addition of the general transcription inhibitor actinomycin D (Sigma Aldrich) at a concentration of 5 ug/ml for 0, 4, 8 and 12 h.

Total RNA was isolated with Maxwell 16 LEV simply RNA cells kit (Promega) and analyzed by RT-qPCR. ACTB was used as a reference gene for normalization (ΔCt), and the ΔCt of each time point was compared to time 0 h ($\Delta\Delta$Ct). For each experiment the average of triplicate wells per condition was calculated and used to determine mean values and standard deviation of three biological replicates. A Student's *T*-test was performed to assess for significant differences of RNA decay rate between the three conditions (TIAR or ELAVL1 knockdown and control cells).

5.10 Measurement of microRNAs expression level

Total RNA was extracted from HeLa control and ELAVL1 knockdown cells with RNeasy Micro kit (Qiagen) and quantified with Nanodrop 1000 spectrophotometer (Thermo Scientific). 10 ng of total RNA were used for reverse transcription reaction with miR7, miR153 and U6 RT specific primers by using the TaqMan MicroRNA Reverse Transcription kit (Applied Biosystem) following manufacturer's inscructions. Real-time amplification reaction was performed with TaqMan Universal PCR master mix (Life Technologies) and TaqMan probe assay for human miR-7, miR-153-3p and U6 snRNA, which was used as a control for normalization. In the case of miR7, for which we obtained C_t around 30, we normalized to U6 reference gene (ΔCt) and compared ELAVL1 knockdown to control samples ($\Delta\Delta$Ct). The mean values and standard deviation of five replicates was calculated. A Student's *T*-test was performed to assess for significant differences between the two conditions. As for miR153, threshold cycles above 33 were obtained.

5.11 Polysome profiling

HeLa control, TIAR and ELAVL1 knockdown cells were grown in 10 cm^2 plates under standard conditions. Incubation with the translation inhibitor cycloheximide (100 ug/ml) was performed at 70% cell confluence, for 15 min at 37°C. Cells were washed with cold 1X PBS and lysed on ice with 250 ul/plate of Polysome lysis buffer (10 mM Tris-HCl pH 7.4, 100 mM KCl, 10 mM MgCl$_2$, 1% Triton-X 100, 2.5 U/ml Turbo DNase, 2 mM DTT, 1X protease inhibitors, 100 ug/ml cycloheximide, 200 U/ml Superase In).

Lysates from three 10 cm^2 dishes were transferred to a tube containing 425-600 microns glass beads (Sigma). After vortex and centrifugation for 5 min at 5,000 g at 4°C, lysates were transferred to new tubes and immediately snap-frozen in liquid nitrogen. A 1:40 dilution of cell lysates was used to measure absorbance at 260 nm with Nanodrop 1000 spectrophotometer (Thermo Scientific). 9-12 OD$_{260}$ were loaded onto a 10-50% sucrose gradient in a Beckman SW 41Ti rotor and subjected to ultracentrifugation for 150 min at 35,000 g at 4°C using a Beckman Optima XL-100 K centrifuge. The gradients were fractioned by upward displacement with a 60% sucrose solution using a gradient fractionator connected to a BioRad Econo UV monitor, peristaltic pump, and fraction collector. Sixteen fractions were collected with a speed of 0.8 ml/min. 5 ng of *in vitro* synthesized *firefly* luciferase RNA were added to each fraction as an internal control for RNA precipitation efficiency. Samples were precipitated overnight at -20°C with 100% ethanol and then the pellets were washed with 80% ethanol and resuspended before isolating RNA using Maxwell 16 LEV simply RNA cells kit (Promega).

A fixed volume of RNA was used for reverse transcription with the SuperScript III First-Strand synthesis SuperMix for qRT-PCR (Invitrogen) and real-time PCR was performed with 250 uM forward and reverse primers and 1X Sybr Green PCR master mix (Applied biosystems). In order to have a standard curve-based relative quantification, we used serial dilutions of a cDNA sample to which we assigned arbitrary values for each of the genes of interest (e.g. 100 AU to 12.5 ng, 10 AU to 1.25 ng, 1 AU to 0.125 ng, etc.). The values of *SNCA* for each polysomal fraction (x_1, x_2, …x_{16}) obtained by interpolation with the standard curve, were then normalized to the

Firefly luciferase signal, which was used as internal control RNA to correct for differences in RNA precipitation efficiencies.

The total amount of *SNCA* in all fractions was calculated as the sum of the corrected values. The ratio $(x_{n=1-16}/\sum x_n)$ against the total for each fraction was calculated and represented as percentage of *SNCA* mRNA in each polysomal fraction. The average and standard deviation of biological triplicates were calculated for each condition (control, TIAR kd and ELAVL1 kd) and the results were compared. ACTB was used as a negative control since its distribution along the polysomal fractions is not affected by TIAR or ELAVL1 knockdown.

RESULTS

6. Identification of RNA-binding proteins interacting with *SNCA*-3'UTR

6.1 Human protein array

We used commercially available human protein arrays to identify proteins interacting with a transcript of interest. Protein arrays have been relatively recently used to test the binding of proteins to long non coding RNAs or protein coding RNAs with an average length of 1200 nt (Siprashvili et al., 2012), making them a suitable technique for our RNA of interest, *SNCA*-long 3'UTR (2500 nt). The method has the advantage to allow the screening of about 10000 human proteins in less than a day, and with relatively few amount of RNA required.

We performed a total of three technical replicates, hybridizing sense and antisense RNAs on separate chips, and obtained Pearson's correlations between replicates of 0.87 and 0.72 (replicates1 and 2), 0.88 and 0.93 (replicates2 and 3), 0.89 and 0.77 (replicates1 and 3), for sense and antisense RNA respectively (Fig.1). The antisense RNA was used as a control for specificity.
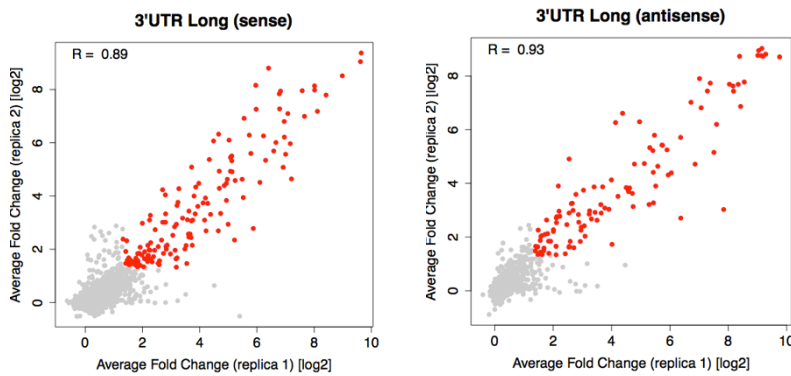

Figure 1. Correlation plot between two replicates of the protein array of *SNCA* long 3'UTR sense (left) and long 3'UTR antisense (right).

To identify significant protein-RNA binding events, we selected proteins with fold change (signal to background ratio) above 2.5 and Z-score above 3, obtaining around 100 proteins per experiment.

By taking the intersection of the three replicates, and removing all interactions that were in common between sense and antisense RNAs, we filtered out unspecific binders.

Our analysis led to a list of 27 proteins shown in Table 1.

Protein	Uniprot ID	RNA binding domain	Annotated function
ELAVL1	Q15717	+	mRNA stability trough binding to 3'UTR, pre-mRNA splicing
HNRNPUL1	Q9BTB7	+	transcriptional regulator, nucleocytoplasmic RNA transport
PTBP2	Q9UKA9	+	pre-mRNA splicing, regulation of translation
RBM9/RFOX2	O43251	+	pre-mRNA splicing
ZC3H14	Q6PJT7	+	poly(A) tail length control
CUGBP1/CELF1	Q92879	+	pre-mRNA alternative splicing, mRNA translation and stability (mediates deadenylation)
RALYL	Q86SE5	+	unknown
CUGBP2/CELF2	O95319	+	pre-mRNA alternative splicing, mRNA translation and stability
CSTF2	P33240	+	subunit of the complex required for mRNA 3' cleavage and polyadenylation
HNRPA1/ROA1	P09651	+	mRNA packaging into hnRNP particles and nuclear export, splicing (putative)
SUB1/TCP4	P53999	+	transcriptional activator
LSM6	P62312	+	subunit of the nuclear LSM2-LSM8 complex involved in mRNA splicing, and of the cytoplasmic complex LSM1-LSM7 involved in RNA decapping and degradation
RBM22	Q9NW64	+	pre-mRNA splicing
MOV10	Q9HCE1	+	RNA helicase involved in miRNA-mediated gene silencing by RISC complex
TIAL1/TIAR	Q01085	+	component of stress granules, translation inhibition, apoptosis
PUF60	Q9UHX1	+	pre-mRNA splicing, apoptosis, transcription regulation
PABPC5	Q96DU9	+	binds to poly(A) tail of mRNA, maybe involved in cytoplasmic regulatory process of mRNA metabolism
RBM39	Q14498	+	transcriptional coactivator, pre-mRNA alternative splicing

C12orf41/KANSL2	Q9H9L4	-	part of the NSL complex it is involved in acetylation of nucleosomal histone H4
SNAPC5	O75971	-	part of the SNAPc complex required for the transcription of both RNA polymerase II and III small-nuclear RNA genes.
SERPINA3/AACT	P01011	-	its physiological function is unclear, it can inhibit neutrophil cathepsin G and mast cell chymase
RAB4A	P20338	-	protein transport, vesicular trafficking
DECR2	Q9NUI1	-	regulation of lipid metabolism (peroxisomal 2,4-dienoyl-CoA reductase)
APOBEC3G	Q05JX5	-	DNA cytidine deaminase
COLEC12	Q5KU26	-	scavenger receptor that displays several functions associated with host defense
STK40	Q8N2I9	-	may be a negative regulator of NF-kappa-B and p53-mediated gene transcription
KCNAB1	Q14722	-	cytoplasmic potassium channel subunit that modulates the characteristics of the channel-forming α-subunits

Table 1. List of 27 candidate protein interactors of *SNCA*-3'UTR RNA

Using catRAPID omics (Agostini et al., 2013), we computed the interaction propensity of *SNCA* long 3'UTR and the 27 candidates selected with protein arrays. Candidates were sorted by the median value of catRAPID omics ranking score. As MOV10 (1003 aa) and HNRL1 (856 aa) are >750 aa, they have been fragmented. The top five proteins with highest propensity to bind the sequence of *SNCA*-3'UTR are TIAR, CELF1, ELAVL1, KANL2 and CSTF2 (Fig. 2).
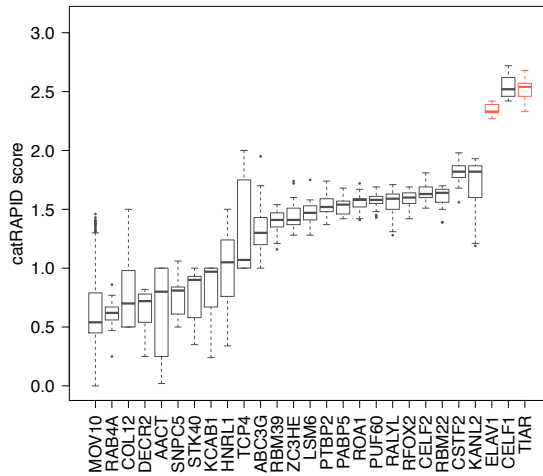
Figure 2. Median value of catRAPID omics ranking score of top 27 protein interactors of *SNCA*-3'UTR at protein array screening. ELAVL1 and TIAR are highlighted in red.

Besides KANSL2, or KAT8 regulatory NSL complex subunit 2, which is part of the NSL (nonspecific lethal) complex, involved in the acetylation of nucleosomal histone H4, all other four proteins are known RNA binding proteins involved in various aspects of RNA metabolism.

Due to their documented ability to bind RNAs at the 3'UTR, the commonalities of their binding modes, and the key role in the regulation of mRNA stability and translation, ELAVL1 and TIAR were considered the two most interesting candidates among the five top candidate proteins for further investigation (Cok et al., 2003; Izquierdo, 2006; Kim et al., 2011; Subramaniam et al., 2011; Suswam et al., 2005a; Wigington et al., 2015). In addition, the Atlas of UTR regulatory activity (AURA) database, a manually curated database of UTR cis- and trans-regulatory elements, reports ELAVL1 and TIAR, but not CELF1 and CSTF2, as *SNCA* 3'UTR binders.
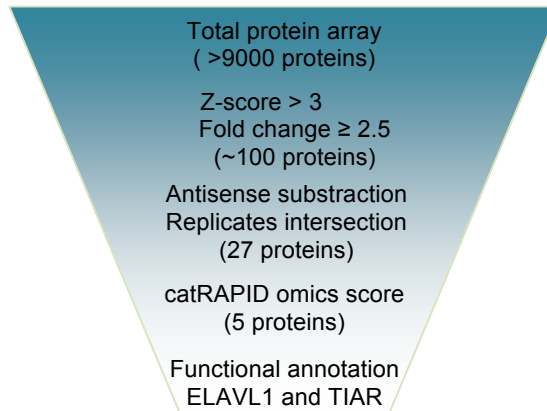
Figure 3. Scheme of the analysis of the protein array data and selection of candidate proteins for validation.

6.2 TIAR and ELAVL1 are able to bind *SNCA* 3'UTR *in vitro*

We tested the *in vitro* binding capability of TIAR and ELAVL1 to the *in vitro* synthesized and biotinylated long 3'UTR (2.5 kb) and short (575 nt) by an RNA affinity purification assay in cross-linking conditions.

As shown in Fig. 4, ELAVL1 was found to interact with both UTRs, with a significant higher binding avidity for the long 3'UTR. The protein was not recovered when we used streptavidin beads in absence of RNA, thus confirming the specificity of the signal. This result is in agreement with published CLIP data (Kishore et al., 2011; Mukherjee et al., 2011) that report the presence of a single binding site within the sequence of the short 3'UTR, and four additional binding sites in the downstream regions proper of the long 3'UTR (Fig.5).

By contrast, similar amounts of TIAR interact with long and short 3'UTR, in accordance with CLIP binding sites that are mapped only in the first 600 nt of the sequence (Wang et al., 2010) indicating equal binding avidity for both 3'UTRs (Fig.4-5). Also in this case the beads without RNA, which were used as a control for background, didn't bind the protein of interest.

The results confirm the ability of ELAVL1 and TIAR to bind *SNCA* 3'UTR *in vitro*. In particular, when the binding to two 3'UTRs with different length (575 nt and 2.5 kb) was compared, I observed that ELAVL1 has a higher binding propensity for the long 3'UTR with respect to the short, while TIAR shows similar binding abilities. The difference can be explained by the multivalency of the long 3'UTR, which contains at least five ELAVL1 binding sites along its sequence. These results also suggest that the binding is conserved in the first 575 nt.
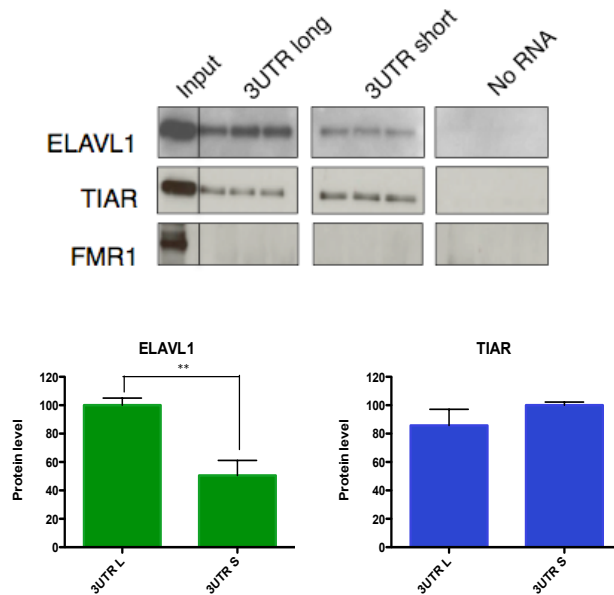
Figure 4. **RNA affinity purification**. ELAVL1 and TIAR were co-purified with the *in vitro* synthesized RNA of *SNCA*-long 3'UTR, *SNCA*-short 3'UTR (western blot in the upper panel). ELAVL1 binds to the long 3'UTR with significant more avidity with respect to the short 3'UTR, while TIAR shows similar binding ability for both 3'UTRs (p-value < 0.05, Student's T-test).
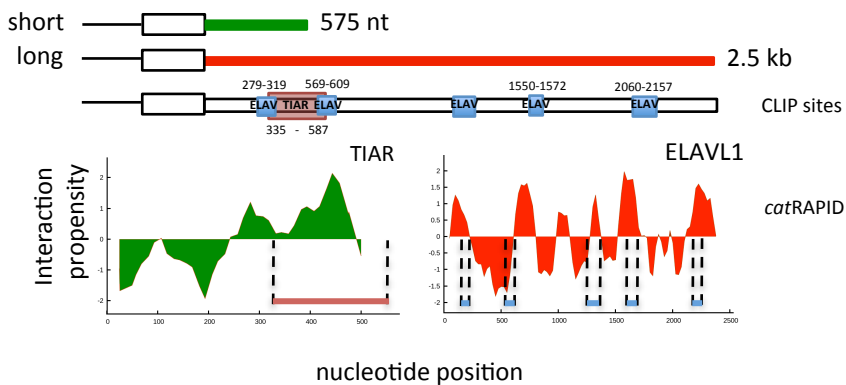
Figure 5. CLIP identified binding sites along the sequence of *SNCA*-3'UTR. ELAVL1 binding sites are represented with blue boxes and TIAR binding sites are represented with a pink box (upper part). Scheme of *cat*RAPID interaction profile for TIAR and ELAVL1 proteins with the sequence of *SNCA*-3'UTR short (green) and *SNCA*-3'UTR long (red) respectively (lower part). The interaction profile represents the values of the interaction score for the protein of interest (Y axis) along each nucleotide of the RNA target sequence (X axis).

In addition, to prove that the interactions observed were not due to technical artifacts of the UV cross-linking, the RNA affinity purification assay was performed in absence of cross-linking. Indeed, the binding was detected also in absence of cross-linking and with washing conditions used (300 mM NaCl, 1% NP-40, 1% Triton X-100), indicating that the affinity of the interactions is high enough to resist those concentrations of salt and detergents (Fig. 6). The amount of protein recovered under nonphysiological 500 mM NaCl washing conditions was lower with respect to 300 mM NaCl washing buffer (data not shown).
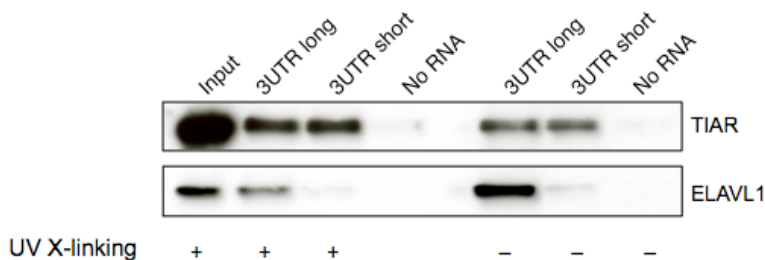
Figure 6. RNA affinity purification in presence or absence of UV cross-linking.

6.3 *SNCA* carrying a short 3'UTR is the predominant isoform in SH-SY5Y and HeLa cells

In order to quantify the abundance of the five previously identified 3'UTR isoforms (Rhinn et al., 2012) of *SNCA* mRNA, we performed a modified sequencing protocol to which we will refer as gene specific-3'end RNA sequencing.

The analysis was done using two different cell lines, HeLa cells and human neuroblastoma cells (SH-SY5Y). HeLa cells are human cervix adenocarcinoma cells commonly used for laboratory research due to the ease of growth and manipulation. SH-SY5Y cells were *in vitro* differentiated towards a dopaminergic neuron-like phenotype by treatment with retinoic acid (RA) for 4 days and 12-O-tetradecanoyl-phorbol-13-acetate (TPA) for 3 days, in order to recapitulate the biochemical and genetic settings typical of *substantia nigra* dopaminergic neurons, which are mainly affected in Parkinson's disease (Korecka et al., 2013). The goal of this analysis was to quantify the relative abundances of different *SNCA* mRNA APA isoforms and compare the results of the two cell lines. According to the observation that the process of alternative polyadenylation (APA) contributes to tissue specificity (Zhang et al., 2005a) and that an extensive lengthening of the 3'UTRs has been measured in the brain (Miura et al., 2013), the two cell lines selected, which come from different tissues and originate from different embryonic germ lines, might express different levels of *SNCA* 3'UTR isoforms.

Around $1,5x10^6$ reads per sample were obtained and 66% of them mapped to *SNCA* transcript. HeLa cells express 51.5% of the *SNCA* mRNA carrying the 3'UTR of 575 nt, followed by 24.8% of the 290 nt long 3'UTR, 17% of the 1074 nt UTR, 5.6% of the 2.5 kb 3'UTR and 1.1 % of the 480 nt long 3'UTR.

Similarly for SH-SY5Y cells 41.3% of the total *SNCA* polyadenylated mRNA is represented by the isoform carrying the 3'UTR of 575 nt (short), followed by 23.1% of the 1074 nt 3'UTR, 20.8% of the 290 nt long 3'UTR, 14% of the 2,5 kb 3'UTR (long) and 0.7 % of the 480 nt (see Fig. 7).

We notice a difference in the expression level of the isoform carrying the 3'UTR 2.5 kb long, that is expressed 2.5 times more in SH-SY5Y

than HeLa cells. Still, **we can conclude that the overall most abundant isoform in both cell lines is the one carrying the short 3'UTR (575 nt) that represents around half of the total *SNCA* mRNA.** The least prominent isoforms are those carrying 480 nt and 2.5 kb long 3'UTR (Fig. 7).

Thus, it is likely that the isoform expressing the short 3'UTR is the main responsible for protein expression and its deregulation might be relevant for pathology.
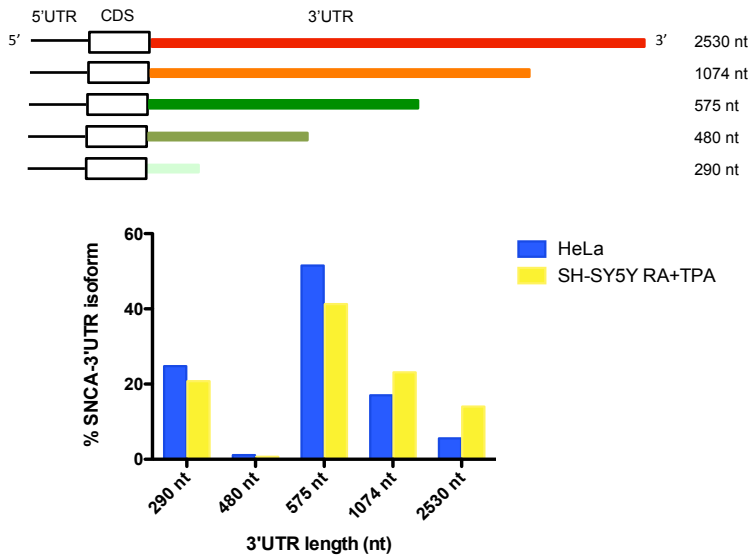

Figure 7. **Quantification of the five 3'UTR isoforms of *SNCA* mRNA.** (a) scheme of the five isoforms with different length of the 3'UTR ranging from 290 nt (light green) to 2.5 kb (red). (b) % of each of the 3'UTR-isoforms of *SNCA* transcript in HeLa cells (blue) and *in vitro* differentiated SH-SY5Y cells (yellow) measured by gene-specific 3'end RNA sequencing.

6.4 The size of the 3'UTR influences the expression of the protein

To assess if the size of the 3'UTR influences the expression of the α-synuclein protein, we performed a dual luciferase gene reporter assay. To guarantee the expression of the long or medium 3'UTR isoforms and avoid premature cleavage, the proximal polyadenylation sites (PAS), present within the sequence of the 3'UTRs, were deleted.

The relative firefly luciferase activities obtained for the constructs carrying the sequence of the short 3'UTR (575 nt) and medium 3'UTR (1.07 kb) are more than 3.5 and 2 times higher than the one of the firefly luciferase empty vector, respectively, while the construct carrying the long 3'UTR (2.5 kb) displays around 10 times less luciferase activity with respect to the control empty vector (Fig. 8). **overall, the construct carrying the long 3'UTR is 17.5 times less active than the construct carrying the short 3'UTR.** This suggests that, as expected due to its length, the long 3'UTR contains a higher number of sequence elements targeted by *trans*-acting factors, such as microRNAs and destabilizing RBPs, which promote RNA degradation or inhibit its translation.

A similar trend is observed also at the RNA level, with the RNA carrying the short 3'UTR being 2 times more abundant than the control vector carrying only the luciferase coding sequence (FL). However, the difference between FL-*SNCA* 3'UTR S and FL-*SNCA* 3'UTR L mRNA level is much smaller than the difference of their enzymatic activities (1.7 fold versus 17.5 fold), suggesting that the rate of translation is probably majorly contributing to the differences observed between constructs expression, rather than the mRNA stability and decay rate.
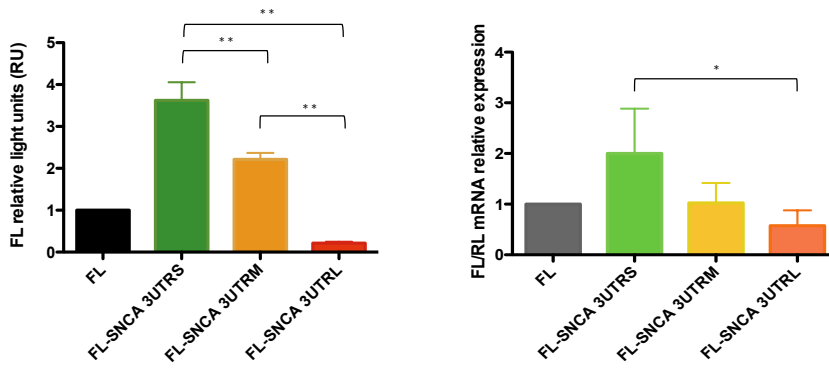
Figure 8. **Dual luciferase gene reporter assay**. The Firefly luciferase relative to Renilla luciferase activity is compared between the constructs carrying the sequence of *SNCA*-3'UTRs of different length (3'UTRS, 575 nt, 3'UTRM, 1.07 kb and 3UTRL, 2.5 kb) with respect to the control empty vector (left panel). Relative mRNA abundances are also represented (right panel).

∗∗ P-value < 0.01 calculated with Student's T test

∗ P-value < 0.05 calculated with Student's T test

7. Functional study of TIAR and ELAVL1 regulation of *SNCA* expression

7.1 TIAR expression is altered in frontal motor cortex of PD and MSA affected individuals

As TIAR and ELAVL1 interact with *SNCA*-3'UTR, we questioned whether their abundance is altered in pathological conditions that are associated with alteration of α-synuclein expression and solubility.

To answer this question we have measured the expression level of α-synuclein, TIAR and ELAVL1 in frontal motor cortex of *post-mortem* Parkinon's disease (PD) and Multiple System Atrophy (MSA) affected individuals with respect to non-affected control individuals:

- At the RNA level we observe a small downregulation of α-synuclein total RNA (*SNCA*-3UTR all) in PD patients (fold change 0.87), similarly to TIAR for which we measure a fold change of 0.61 and 0.77 in PD and MSA respectively. No change of expression is detected for ELAVL1 mRNA (see Fig. 1).

- At the protein level TIAR is significantly downregulated in PD patients and upregulated in MSA patients with respect to control individuals (fold change=0.65, fold change=1.36). This result correlates with α-synuclein protein expression, which is decreased in PD (fold change=0.49) and increased in MSA (fold change=2.57) with respect to controls (p-value<0.05). No alteration of ELAVL1 expression is observed in PD affected individuals, while a 1.5 fold upregulation is measured in MSA patients if compared to controls (see Fig. 2).

Individuals from the three different groups were chosen in order to ensure the best match for gender, age of onset and age at death and severity of the disease. Nevertheless, we notice a strong expression heterogeneity among individuals of the same group, which might be caused by several factors such as: presence of concomitant pathologies (e.g. initial stages of dementia or aging), variations in treatment strategies, oxidative stress conditions due to type of death of the subjects, *post-mortem* delay for brain sampling, or presence of specific single nucleotide polymorphisms associated with other conditions, etc.

This heterogeneity is particularly pronounced for α-synuclein and TIAR proteins. Due to this intra-group variability and to small sample size, it is difficult to postulate that the differences in expression that we observe are actually related to the presence of the pathology.

Nevertheless, we note that α-synuclein and TIAR expressions correlate at both RNA and protein level, suggesting a possible functional relationship between the two genes.
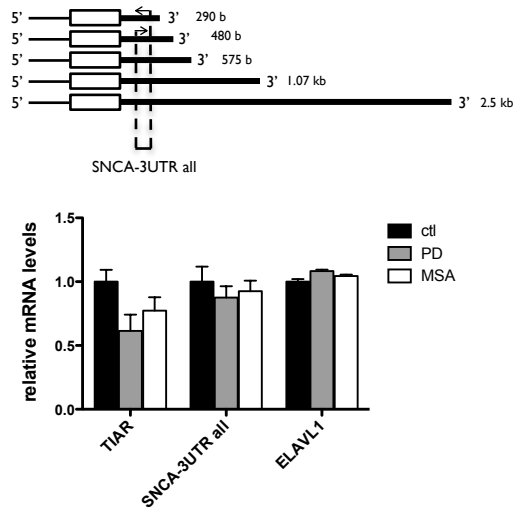
Figure 1. Scheme of primers used for real-time PCR to detect different 3'UTR isoforms of *SNCA* mRNA (upper panel). mRNA level of *SNCA*, TIAR and ELAVL1, relative to GAPDH, in total RNA isolated from frontal motor cortex of *post-mortem* control individuals, Parkinson's disease (PD) and Multiple System Atrophy (MSA) affected patients (lower panel).
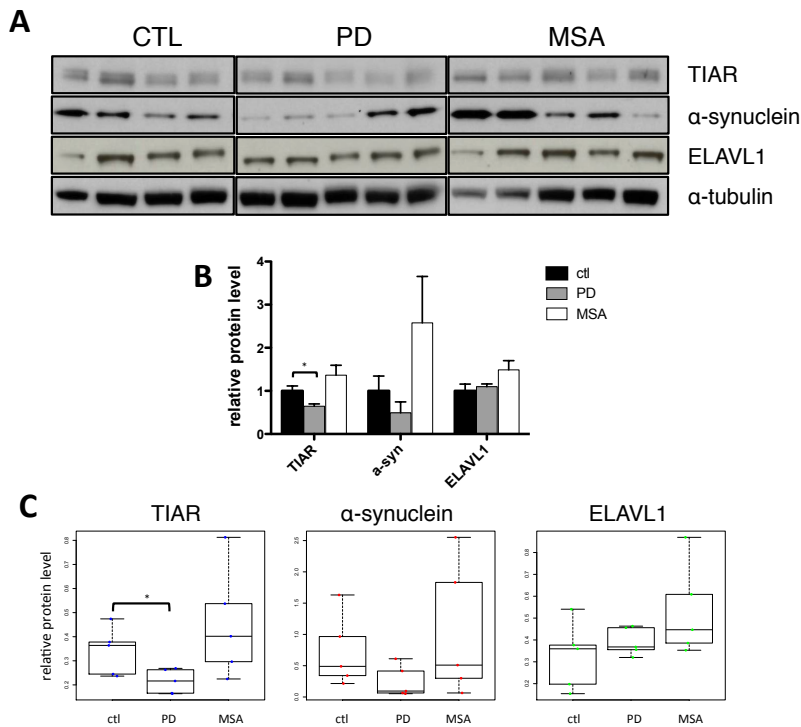
Figure 2. Western Blot of α-synuclein, TIAR and ELAVL1 proteins from frontal motor cortex tissue of *post-mortem* control individuals, PD and MSA patients. α-tubulin was used as a loading control for normalization (panel A). Bar plot (panel B) and box plot (panel C) representing normalized values of TIAR, α-synuclein and ELAVL1 protein abundances in the three groups of individuals. Normalized values of each individual are represented in the boxplot as blue, red and green dots for TIAR, α-synuclein and ELAVL1 respectively. *p-value < 0.05, Student's T-test.

7.2 TIAR and ELAVL1 knockdown downregulates α-synuclein

I validated the hypothesis of a functional relation between TIAR (or ELAVL1) and α-synuclein expression by measuring α-synuclein RNA and protein level upon stable knockdown of the two RBPs in HeLa cells.

We decided to use HeLa cells because, in addition to its ease of manipulation, growth and transfectability, they have a very similar distribution of *SNCA* 3'UTR-isoforms expression at the 3'end RNA-seq (see section 6.3) with respect to neuron-like SH-SY5Y cells, which makes them suitable to study the effect of TIAR and ELAVL1 on the expression of α-synuclein through the regulation of its 3'UTR.

The comparison with control samples infected with virus carrying pLKO empty vector reveals around 90% depletion of both proteins. **Upon knockdown of TIAR we observed a significant decrease of endogenous α-synuclein expression at the RNA level** with a fold change of 0.63 for primer pairs detecting all 3'UTR isoforms, 0.72 for primers detecting *SNCA*-3'UTR 1.07 kb (medium) and 2.5 kb (long) RNA isoforms, and 0.68 for *SNCA*-3'UTR 2.5 kb (long) only (p-value<0.01) (Fig.3). This is consistent with the presence of TIAR binding sites within the first 500 bases of the 3'UTR and, consequently, with equal binding capability of TIAR to all 3'UTR isoforms of *SNCA* mRNA.

Notably, also α-synuclein protein is decreased (fold change 0.5, p-value < 0.01) upon TIAR KD as measured by western blot (Fig.4).

When we knockdown ELAVL1 we observe a moderate effect on endogenous α-synuclein expression with a fold change of 0.87 at the RNA level for primer pairs detecting all 3'UTR isoforms as well as for primers detecting *SNCA*-3'UTR 1.07 kb and 2.5 kb RNA isoforms. No change is observed for the longest 3'UTR isoform of *SNCA* mRNA (Fig.3). Similarly, also the protein is decreased, with a fold change of 0.78, upon knockdown of ELAVL1 with respect to control (Fig.4).

Overall, the results show that depletion of TIAR and ELAVL1 protein in HeLa cells causes a moderate (ELAVL1) and high (TIAR) down-regulation of endogenous α-synuclein at the RNA and protein level. This suggests that the two RBPs might act as post-transcriptional positive regulators of α-synuclein expression, although additional experiments are necessary to prove a direct regulation through the binding of TIAR and ELAVL1 at the 3'UTR of *SNCA* mRNA.
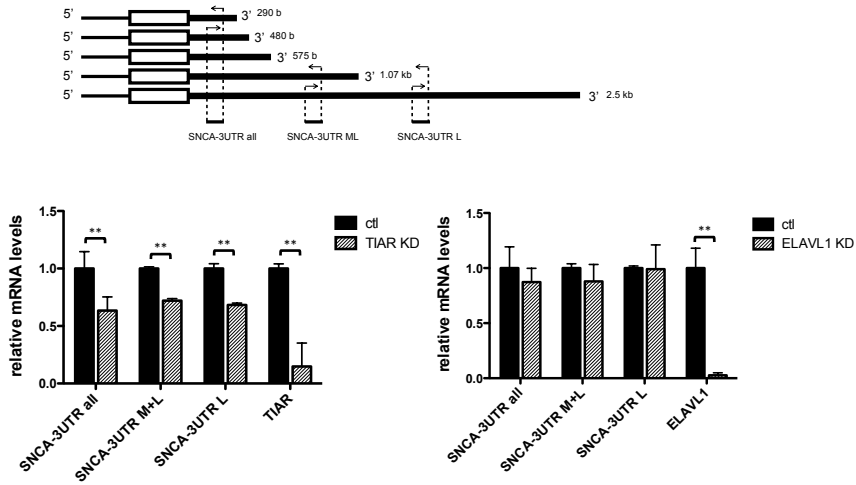
Figure 3. **TIAR and ELAVL1 knockdown**. mRNA level of SNCA-3UTR all isoforms, SNCA-3UTR M+L, SNCA-3UTR L and TIAR (relative to ACTB) in total RNA isolated from HeLa control cells and HeLa stably infected with shRNA against TIAR (left panel). mRNA level of SNCA-3UTR all isoforms, SNCA-3UTR M+L, SNCA-3UTR L and ELAVL1 (relative to ACTB) in total RNA isolated from HeLa control cells and HeLa stably infected with shRNA against ELAVL1 (right panel). Average and standard deviation of seven biological replicates are represented. ∗∗p-value < 0.01, Student's T-test.
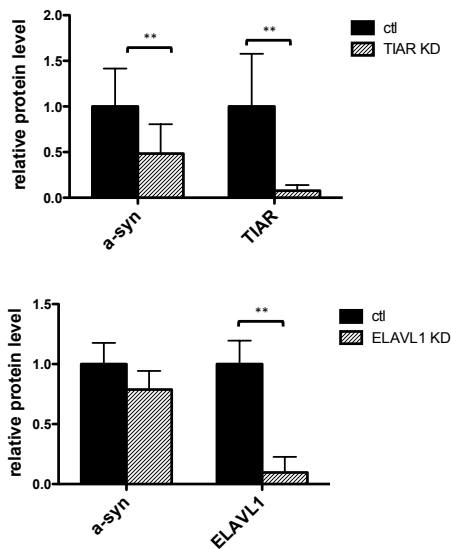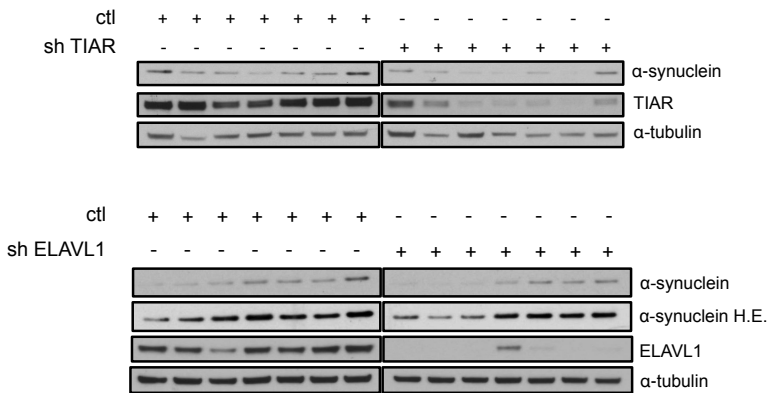
Figure 4. **TIAR and ELAVL1 knockdown**. Western Blot of α-synuclein, TIAR and ELAVL1 proteins from HeLa total cell extracts prepared from control cells and cells stably infected with shRNAs against either TIAR (upper panel) or ELAVL1 (lower panel). H.E. states for High Exposure. Average and standard deviation of seven biological replicates are represented in the bar plot.

7.3 TIAR and ELAVL1 knockdown do not alter the relative abundance of *SNCA*-3'UTR isoforms

Using the same 3'end gene-specific sequencing strategy that was previously used to quantify the alternative polyadenylation isoforms of *SNCA* mRNA in HeLa and SH-SY5Y differentiated cells, we compared the relative abundances of the different APA isoforms upon TIAR or ELAVL1 depletion with respect to control HeLa cells. The results, represented in Fig. 5, are the average % abundances of three knockdown experiments. No significant change of the relative abundance of *SNCA* APA mRNA isoforms was detected when comparing knockdown cells to control cells, meaning that depletion of TIAR and ELAVL1 causes approximately the same degree of decrease for all 3'UTR isoforms without any substantial alteration of the proportion among 3'UTR isoforms. This is consistent with what we observed by real-time PCR using primers *SNCA*-3UTR M+L and *SNCA*-3UTR L.
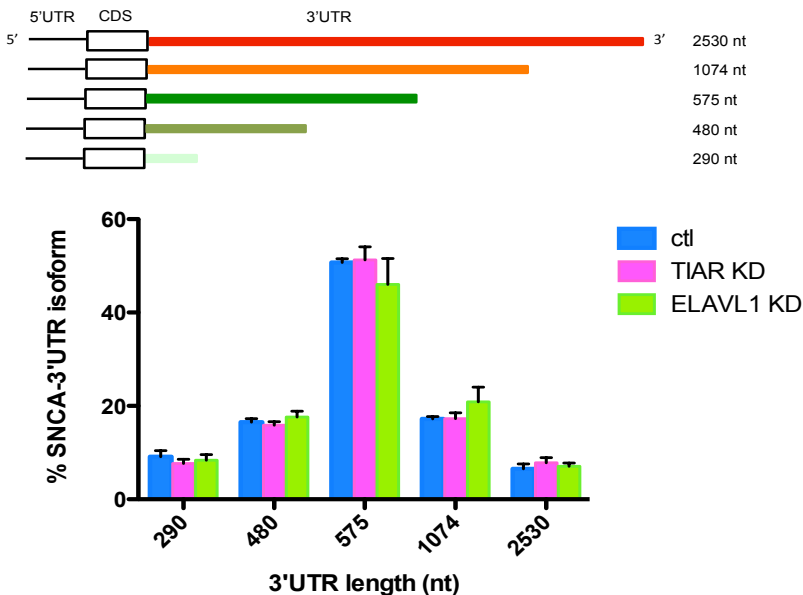
Figure 5. **Quantification of the five 3'UTR isoforms of *SNCA* mRNA.** Scheme of the five isoforms with different length of the 3'UTR ranging from 290 nt (light green) to 2.5 kb (red) (upper panel); average % and standard deviation of *SNCA*-3'UTR isoforms in three TIAR (purple) and ELAVL1 (green) knockdown biological

replicates compared to HeLa control cells (blue) measured by gene-specific 3'end RNA sequencing (lower panel).

7.4 TIAR and ELAVL1 overexpression upregulates α-synuclein expression

To confirm that the change of α-synuclein expression is a direct consequence of TIAR and ELAVL1 depletion rather than being an indirect and/or unspecific effect of the knockdown, we measured the RNA and protein level of α-synuclein upon overexpression of the two proteins in HeLa cells.

48 h after transfection we obtain a 6.2 fold overexpression of a GFP-tagged TIAR protein. In line with our hypothesis, α-synuclein RNA is upregulated with 2.2 fold increase of *SNCA*-3UTR all, 1.7 fold increase of *SNCA*-3UTR M+L, and a 2 fold increase of *SNCA*-3UTR L (average of three replicates). Consistent with this result, we found an average 1.6 fold increase at the protein level (Fig. 6).
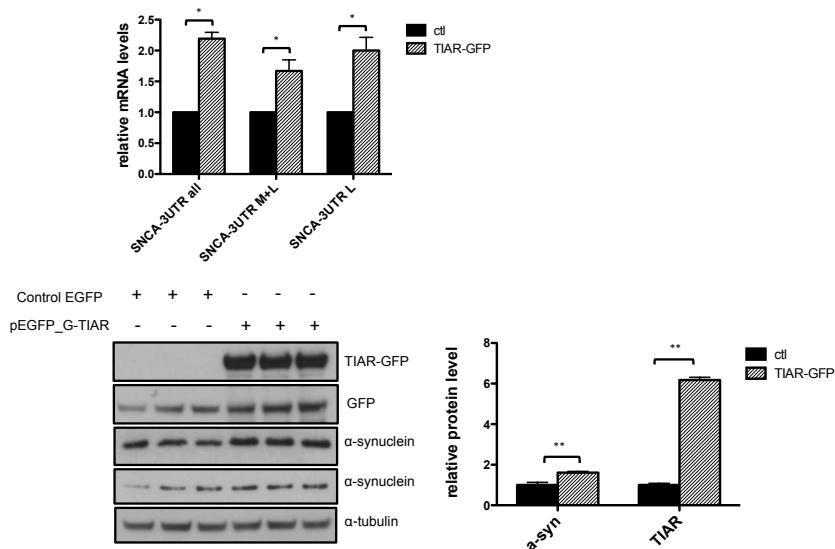
Figure 6. **TIAR overexpression**. Relative mRNA level of *SNCA*-3UTR all, *SNCA*-3UTR M+L and *SNCA*3UTR L in TIAR-GFP and control GFP overexpressing HeLa cells. Average and standard deviation of three replicates is represented (upper panel). Western Blot of α-synuclein, TIAR and GFP from total cell extract of TIAR-

GFP and control GFP overexpressing HeLa cells 48h after transfection; α-synuclein and TIAR protein quantification. ∗∗P-value<0.01, ∗P-value<0.05, Student's T-test.

We observe a 1.52 fold increase of α-synuclein protein upon overexpression of ELAVL1 by transient transfection of HeLa cells with a pCMV-AC-ELAVL1 plasmid vector. However, this effect was not accompanied by a significant change of *SNCA* mRNA level with respect to GFP control vector (Fig.7).

The results overall confirm that TIAR and ELAVL1 play a positive regulatory role on α-synuclein expression. In particular, **TIAR overexpression significantly increases the level of α-synuclein RNA and protein, doubling its expression. Instead, ELAVL1 seems to have a milder effect when overexpressed, leading to a 1.5 upregulation of the protein and with no apparent changes of the RNA level**.
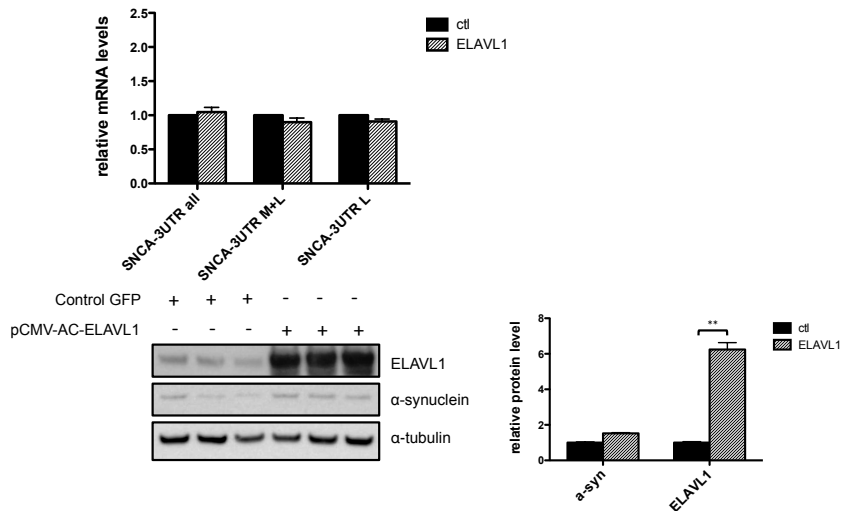
Figure 7. **ELAVL1 overexpression**. Relative mRNA level of *SNCA*-3UTR all, *SNCA*-3UTR M+L and *SNCA*3UTR L in ELAVL1 and control GFP overexpressing HeLa cells. Average and standard deviation of three replicates are represented (upper panel). Western Blot of α-synuclein and ELAVL1 from total cell extract of ELAVL2 and control GFP overexpressing HeLa cells 48 h after transfection; α-synuclein and ELAVL1 protein quantification. ∗P-value<0.05, Student's T-test.

7.5 ELAVL1 regulation of α-synuclein requires the presence of the 3'UTR of *SNCA* mRNA

To understand whether the regulation by TIAR and ELAVL1 is mediated by the 3'UTR of *SNCA* transcript, we performed a dual luciferase reporter assay with the constructs carrying the sequence of the *SNCA* short 3'UTR (575 nt), medium (1.07 kb) and long (2.5 kb), in TIAR and ELAVL1 depleted cells and compared to control cells.

For each of the recombinant constructs (FL-*SNCA* 3UTRS, FL-*SNCA* 3UTRM and FL-*SNCA* 3UTRL) we see that the normalized firefly luciferase enzymatic activity is significantly decreased in ELAVL1 knockdown condition when compared to control cells with fold-changes of 0.5, 0.46 and 0.54, respectively. Although we detect a decrease of the luciferase signal also for the FL empty vector, this change is not significant (Fig. 8).

This result confirms that the regulation of α-synuclein expression by ELAVL1 requires the sequence of the 3'UTR *SNCA* transcript that contains ELAVL1 binding regions. More specifically, all three 3'UTRs tested are targeted by ELAVL1 with similar effect on the expression of the reporter gene.

As for TIAR, we obtained a significant decrease of the luciferase activity for all tested constructs, including the control FL empty vector, meaning that the effect observed is most likely due to a general alteration of cell metabolism and transcription, rather than being specifically associated to TIAR depletion (Fig. 8).

To remove possible confounding factors caused by changes in the transcriptional efficiency of the exogenous constructs, we repeated the assay by co-transfecting HeLa control and TIAR KD cells with the *in vitro* synthesized RNA corresponding to each of the four constructs together with the *Renilla luciferase* RNA, and tested the dual luciferase activity 4 h after RNA transfection. This approach allowed us to exclusively monitor the 3'UTR-dependent regulation by TIAR at the post-transcriptional level.

At a first preliminary experiment, **we confirmed the down-regulatory effect of TIAR knockdown on the expression of the reporter gene containing the sequence of all three *SNCA***

3'UTRs tested, while the control vector containing only the sequence of the firefly luciferase was not affected by the depletion of TIAR protein (Fig. 9). Nevertheless, this result needs to be further confirmed with additional biological replicates.
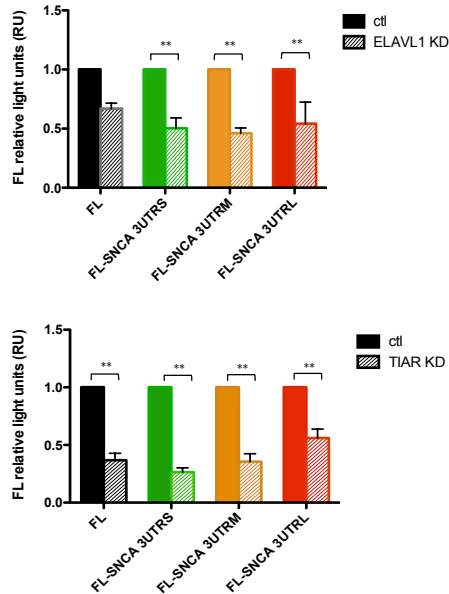
Figure 8. **Luciferase gene reporter assay with ELAVL1 knockdown and TIAR knockdown HeLa cells**. The Firefly luciferase relative to Renilla luciferase activity for each constructs containing the sequence of three different SNCA-3'UTRs (3'UTRS, 575 nt, 3'UTRM, 1.07 kb and 3UTRL, 2.5 kb) is compared between ELAVL1 knockdown (upper panel) or TIAR knockdown cells (lower panel) and control HeLa cells. Average values and standard deviation of three biological replicates are represented. ∗∗ P-value < 0.01 calculated with Student's T test.
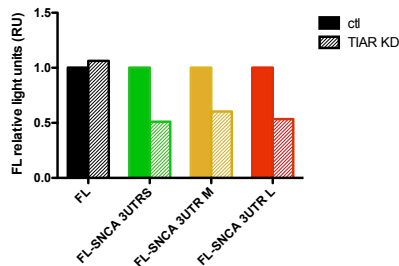
Figure 9. **Dual luciferase assay with RNA transfection.** Relative luciferase enzymatic activity of the four constructs (FL, FL-SNCA 3UTRS, FL-SNCA 3UTRM and FL-3UTRL) measured 4 h after RNA transfection of control and TIAR KD HeLa cells.

7.6 TIAR and ELAVL1 knockdown decreases *SNCA* mRNA stability

The decrease of *SNCA* mRNA upon knockdown of TIAR and, to a less extent, of ELAVL1, suggests that one of the possible mechanisms of regulation by the two proteins could be the stabilization of the mRNA through direct binding at the 3'UTR and interference with RNA degradation factors such as microRNAs and other RBPs.

As a matter of fact, the role of ELAVL1 as an RNA stabilizing factor is extensively documented in the literature (Brennan and Steitz, 2001; Peng et al., 1998). In the case of TIAR, the protein is mainly known for its effect on translation regulation (Kedersha et al., 1999; Mazan-Mamczarz et al., 2006; Podszywalow-Bartnicka et al., 2014) but we cannot exclude that the protein might play other functions in mRNA metabolism.

In order to address this question we measured the stability of *SNCA* mRNA in TIAR and ELAVL1 depleted versus control HeLa cells. The synthesis of new RNA was blocked by treating cells with the general transcription inhibitor actinomycin D. Samples were taken at different time points (0 h, 4 h, 8 h and 12 h) in order to measure the rate of decay of *SNCA* mRNA in the three different conditions. As a result, we measured a statistically significant difference of *SNCA* mRNA rate of decay when we compare TIAR or ELAVL1 depleted HeLa cells to control cells. In particular, the difference between knockdown and control cells is already detectable at 4 h after actinomycin D treatment, with ELAVL1 and TIAR depleted cells showing a decay rate of around 43% and 30% respectively, while in control cells only 5% of *SNCA* mRNA is decayed (p-value < 0.05). We cannot observe the same effect for *SNCA* mRNA isoforms carrying larger 3'UTRs (1.07 and 2.5 kb) (Fig.10). VEGF mRNA was used as a control for the effectiveness of the actinomycin D treatment since it was previously reported to have a short half-life, compatible with our time of treatment with actinomycin D (Onesto et al., 2004).
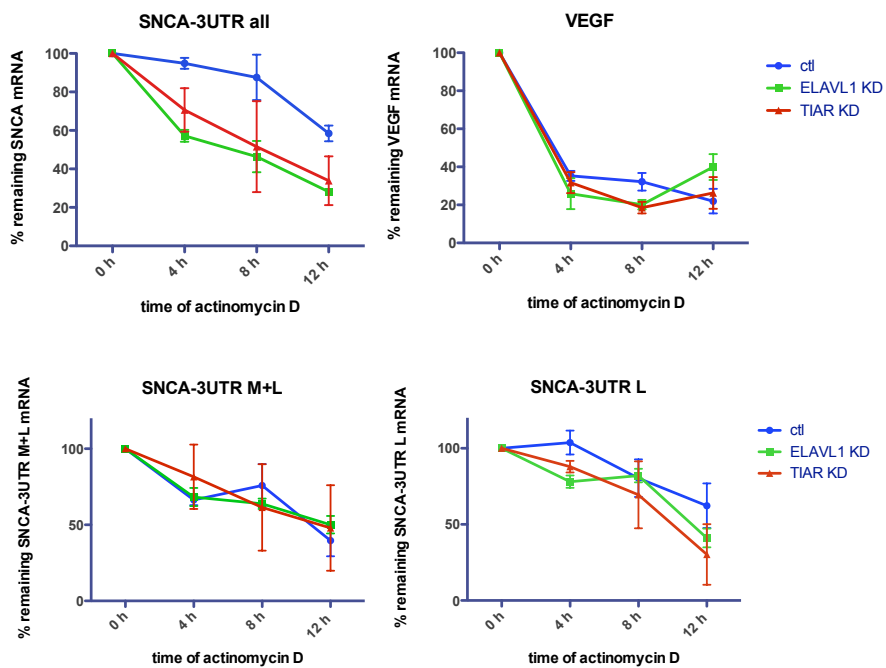
Figure 10. **mRNA stability assay.** Percentage of remaining mRNA (SNCA-3UTR all, SNCA-3UTR M+L, SNCA-3UTR L and VEGF) measured by real-time PCR after transcription inhibition with actinomycin D in control, ELAVL1 KD and TIAR KD HeLa cells. Mean and standard deviation of three independent experiments are shown.

7.7 *SNCA* mRNA stabilization by ELAVL1 and TIAR is not achieved by competition with miR-7 and miR-153 in HeLa cells

We know form previous evidence that α-synuclein expression is downregulated by two microRNAs, namely miR7 and miR153, which are expressed at high level in brain (Doxakis, 2010). Interestingly, although miR7 binding site does not overlap with CLIP defined ELAVL1 or TIAR binding regions, we know that ELAVL1 inhibits miR7 expression by preventing pre-miR7 maturation (Choudhury et al., 2013; Lebedeva et al., 2011). We therefore tested the hypothesis that ELAVL1 stabilization effect could be mediated by miR7 downregulation. However, when we measured miR7 expression upon ELAVL1 knockdown we found that miR7 was significantly downregulated, in contrast with what we expected (Fig. 11). More generally miR7 expression level was very poor in both HeLa control and knockdown cell lines, therefore its involvement in *SNCA* regulation is very unlikely. As for miR153, its binding site overlaps with TIAR target regions, so the two factors might physically compete for the binding to *SNCA* mRNA and regulate its expression with antagonistic effects. Nevertheless, also miR153 expression was barely detectable in HeLa cells thus excluding its involvement in a competition mechanism with TIAR protein.

In conclusion, we can rule out the participation of miR7 and miR153 in α-synuclein regulation by ELAVL1 and TIAR proteins in HeLa cells. However, we cannot exclude their implication in other cell lines, such as neurons, where both miRNAs are expressed at higher levels.
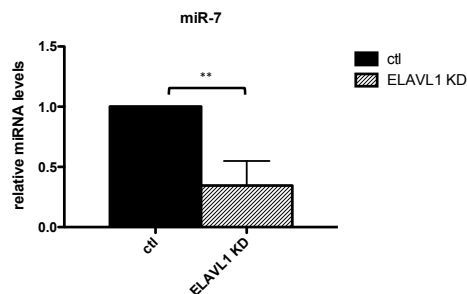
Figure 11. miR7 relative expression level in HeLa cells upon ELAVL1 knockdown. Average and standard deviation of five biological replicates are represented. ∗∗P-value<0.01, Student's T-test.

7.8 TIAR knockdown causes an inhibition of *SNCA* mRNA translation

Since TIAR and ELAVL1 have been reported to be involved also in translation regulation, with TIAR having a major translational inhibitory effect in presence of stress conditions (Kedersha et al., 1999; Mazan-Mamczarz et al., 2006; Podszywalow-Bartnicka et al., 2014), and ELAVL1 having dual roles depending on the target mRNA (Mazan-Mamczarz et al., 2003; Katsanou et al., 2005; Bhattacharyya et al., 2006), we tested the hypothesis that TIAR and ELAVL1 could also participate to the translation of *SNCA* mRNA.

To this aim, we performed a polyribosome profiling experiment with HeLa control, TIAR and ELAVL1 knockdown cells and measured *SNCA* mRNA in total RNA isolated from all polyribosomal fractions. By this approach we were able to separate the translationally inactive monosomes fraction (80S, fraction 5, Fig. 12) from the active polysomal fractions (fractions 7-15, Fig. 12). We traced the distribution of *SNCA* mRNA across these fractions, in order to compare the translation activity of the specific mRNA in TIAR and ELAVL1 knockdown cells with respect to control cells. As a negative control we used ACTB mRNA, whose distribution along polyribosomal fractions doesn't change upon TIAR and ELAVL1 knockdown.

In all three conditions the majority of *SNCA* mRNA (70-75%) is distributed between fractions of 3 to >7 ribosomes (fractions 10-13). However, we measure that while in control cells 27.5% of *SNCA* mRNA co-sediments with 5 ribosomes (fraction 13), only 12.9% of *SNCA* mRNA co-sediment with the same polysomal fraction in cells that were depleted of TIAR protein (Fig. 13). On the other hand, 28.9% of *SNCA* mRNA co-sediment with about 3 ribosomes (fraction 10) in TIAR KD cells, while only 11.8% of the mRNA co-sediment with the same fraction in control cells (Fig. 13).

Overall, we observe a substantial shift of *SNCA* mRNA in cells depleted for TIAR protein, from the 'more' translationally active polysomal fraction 12, corresponding to 5 ribosomes, to the 'less' translational active fraction 10, which corresponds to 3 ribosomes. In contrast, no relevant change was observed upon knockdown of ELAVL1.

It is difficult to estimate to which extent this shift of *SNCA* mRNA from the '5 ribosome-fraction' to the '3 ribosome-fraction' affects the total *SNCA* mRNA translational rate. Nevertheless, we can conclude that TIAR knockdown causes a partial inhibition of *SNCA* translation.

With this evidence we can conclude that, **besides stabilizing *SNCA* mRNA, TIAR also promotes *SNCA* mRNA translation through a mechanism that is not known and needs to be furhter elucidated. Differently, ELAVL1 seems to play a main role in *SNCA* mRNA stabilization, in agreement with its very well documented function in RNA metabolism**. Yet, it doesn't have any relevant effect on its translation efficiency.
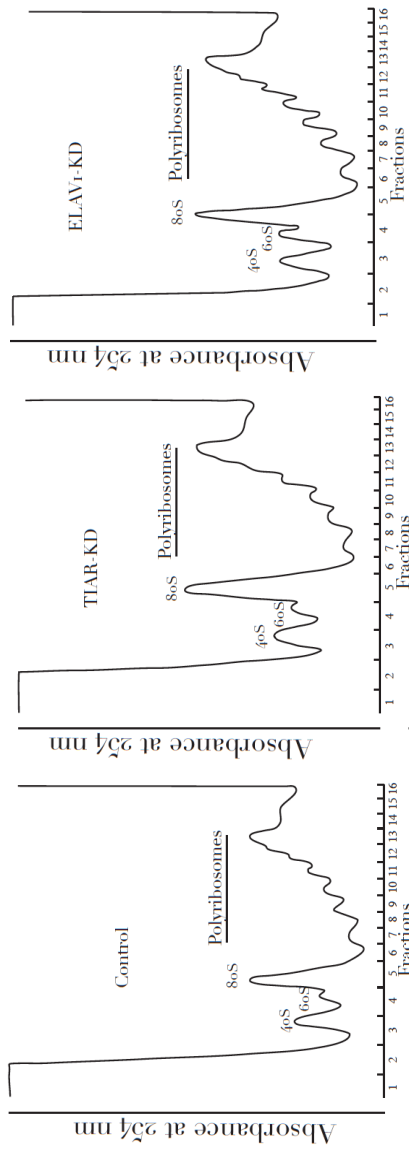
Figure 12. Polyribosome profile of Hela control, TIAR KD and ELAVL1 KD cells.
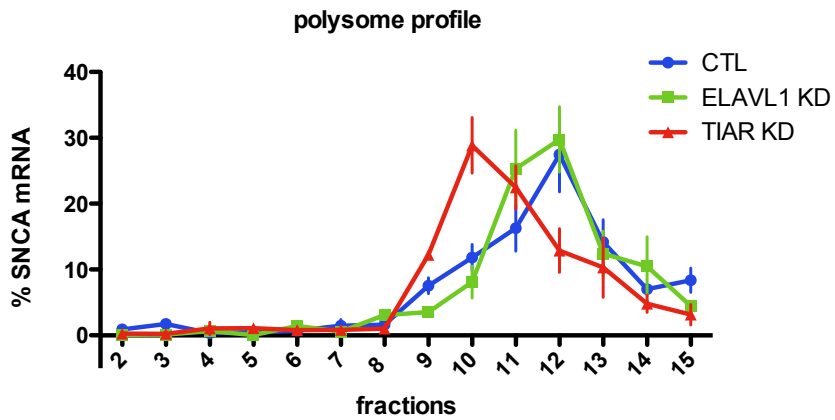
Figure 13. Relative *SNCA* mRNA distribution across polyribosome gradient in HeLa control, TIAR knockdown and ELAVL1 knockdown conditions. Data shown are mean with standard deviation of three independent experiments. Ribosome fractions distribution corresponds to franctions represented in Fig. 12 above.

8. Review on experimental and computational approaches for the characterization of protein-RNA interactions

In this Chapter I present a review that describes the latest advances of experimental and computational methods for the investigation of protein-RNA interactions. Some of these methods were applied in the study presented in Chapters 6 and 7.

Along its journey the RNA is accompanied by a number of RNA-binding proteins that assemble into ribonucleoprotein complexes and regulate RNA processing, transport, editing, translation and degradation. Many protein-RNA assemblies are observed in the nucleoplasm and cytoplasm of all cells and play fundamental roles in growth, development, and homeostasis (e.g. Cajal bodies, P-bodies, stress granules, etc.).

Thanks to the combination of cross-linking chemistries and sequencing technologies, it has been possible to develop new procedures for the identification of protein-RNA interactions on a large scale. In addition, progresses in microscopy and structural biology fields allowed the characterization of specific complexes, their structural features and dynamicity. Many useful computational tools for the prediction of RNA-binding proteins, RNA binding domains and protein-RNA interactions have been developed as well. These methods complement experimental approaches and help the researcher in the discovery of new targets in RNA datasets as well as in the identification of binding residues.

Despite all these advancements, many questions remain open: how many proteins have RNA-binding ability? What are their target and functional pathways? How ribonucleoprotein complexes assemble in response to external *stimuli*? What is the composition of RNA granules and what features contribute to their dynamicity? What are the determinants of granules toxicity in disease?

Marchese D, de Groot NS, Lorenzo Gotor N, Livi CM, Tartaglia GG. Advances in the characterization of RNA-binding proteins. Wiley Interdiscip Rev RNA. 2016 Nov;7(6):793–810. DOI: 10.1002/wrna.1378

9. Principles of self-association in biological pathways: a hypothesis on the autogenous regulation of α-synuclein

Since the early 1980 the first cases of proteins association with their cognate RNAs (autogenous interactions) were documented. Such known cases include yeast maturase, which splices its own mRNA (Lazowska et al., 1980), yeast L32 ribosomal protein (Dabeva et al., 1986), Drosphila *per* gene (Hardin et al., 1990) or the heat-shock protein 70 (Hsp70) gene (Yost et al., 1990). These autogenous interactions provide the cell with a fast and sensitive mechanism to control protein production in response to transient *stimuli*, as hormones or cell cycle changes. Indeed, the interaction of a protein with its own mRNA can exert a negative feedback loop by inducing mRNA destabilization or by inhibiting translation.

How general this mechanism is in eukaryotes is still unknown, but the existence of a pool of proteins bound to their cognate mRNA, as postulated by Kyprides and Ouzounis in the '*autoregulation model'* proposed in 1993, would confer to the cells remarkable advantages (Kyrpides and Ouzounis, 1993). Instead of retaining a huge number of specific nucleases or proteins able to recognize and control the expression of various mRNA molecules, which in turn would need to be regulated, there could be a self-regulated architecture, with transcriptional control activated only when the needs over-exceed the capacity of this system. Thus, the cell could enhance its ability to sense environmental changes, and respond very fast in order to fulfill metabolic needs and to rapidly return to normal state once the conditions are stabilized again. If a specific protein function is required, the protein can be mobilized from the self-associated pool with consequent release of the repressed mRNAs, which in turn can be translated to produce more protein (Kyrpides and Ouzounis, 1993). Also the 'mutation tracking' would be an important aspect of this regulatory mechanism: any mutation disrupting protein conformation or function, might cause an accumulation of the protein in the cytoplasm leading to final inhibition of its mRNA, given that the protein can still recognize its mRNA and interact in a specific manner. Obviously, this theory cannot be extended to all proteins. Protein localization limits RNA accessibility, as in the case of proteins that are secreted or localized into confined intracellular compartment as the endoplasmic reticulum. Moreover, only few proteins have evolved the

capacity to interact with nucleic acids (although the catalogue might be larger than expected).

In this article we investigated the occurrence of autogenous associations in the human proteome. By means of *cat*RAPID (Bellucci et al., 2011), we have interrogated the occurrence of autogenous interactions in biological networks, and found an enrichment in pathways such as 'Amyloids' or 'α-synuclein signaling', suggesting a possible role in the control of aggregation-prone proteins, as well as in pathways related to metabolic regulation such as 'amine compound SLC transporters', 'metabolism of nitric oxide', 'iron uptake and transport', etc. envisaging a contribution of self-associations to the rapid response to cellular needs. This work also highlights the contribution of protein structural disorder in the formation of autogenous associations, thus suggesting that RNA could protect unstructured domains from aberrant and promiscuous interactions or aggregation.

Interestingly, we predicted that α-synuclein is able to establish an interaction with the 5'UTR of its own mRNA, compatibly with a negative feedback regulation that could help preventing protein accumulation at the presynaptic terminals. In addition, previous studies describe that interaction with 'GC' rich DNA molecules induces conformational changes of α-synuclein protein and also increases its amyloidogenicity (Cherny et al., 2004; Hegde and Rao, 2007). One could speculate that α-synuclein interaction with its mRNA could have a broader effect, controlling not only protein synthesis but also folding and aggregation propensities. However, there isn't any evidence about the RNA binding ability of α-synuclein, therefore experimental proof is required to determine the binding affinity of α-synuclein for RNA molecules and evaluate whether the interactions with its own mRNA actually occurs *in vivo*.

Zanzoni A, Marchese D, Agostini F, Bolognesi B, Cirillo D, Botta-Orfila M, et al. Principles of self-organization in biological pathways: a hypothesis on the autogenous association of alpha-synuclein. Nucleic Acids Res. 2013 Dec;41(22):9987–98. DOI: 10.1093/nar/gkt794

10. DISCUSSION

Transcriptional regulation is the main mechanism used by prokaryotic organisms to regulate protein synthesis. However, eukaryotic organisms have evolved a wide variety of post-transcriptional mechanisms to regulate gene expression. Post-transcriptional regulation occurs in the nucleus where the pre-mRNA undergoes maturation which involves the addition of a 7-methyguanosine cap at the 5'end, splice-out of intronic regions as well as the addition of a poly(A) tail at the 3'end of the message, or in the cytoplasm where mRNA transport, editing, storage, stability and translation contribute to modulate protein synthesis and function (Moore and Proudfoot, 2009). All these steps are highly interconnected among each other and are assisted by RNA-binding proteins (RBPs) and noncoding RNAs (microRNAs and long non coding RNAs). In particular, the cytoplasmic control of mRNA turnover and translation has been shown to be very effective to achieve rapid adaptive responses to environmental stresses (e.g. oxidative stress, heat shock, inflammation or immune responses, osmotic shock and ER stress), during which the cell needs to prioritize specific stress-induced transcripts for cell survival (Darnell, 2013; Keene, 2007; Kong and Lasko, 2012).

One peculiar mechanism of post-transcriptional regulation that has been observed for a number of genes, including ribosomal proteins and splicing factors, involves the interaction of a protein with its own mRNA with consequent negative feedback regulation by induction of mRNA splicing, de-adenylation and degradation by nucleases, or through translation inhibition (Boelens et al., 1993; Mosner et al., 1995; Sureau et al., 2001; Schaeffer et al., 2003; Malygin et al., 2007; Ayala et al., 2011). Post-transcriptional mechanisms have been reported to be altered in many diseases, from cancer and inflammation to neurological disorders. This points to the importance of post-transcriptional regulation in the maintenance of cell and organism homeostasis (Anthony and Gallo, 2010; Linder et al., 2015; Brinegar and Cooper, 2016).

Parkinson's disease (PD) is a neurodegenerative movement disorder mainly characterized by the progressive loss of *substantia nigra* dopaminergic neurons (Dauer and Przedborski, 2003). PD is traditionally considered as a proteinopathy caused by abnormal accumulation and aggregation of α-synuclein protein (Conway et al.,

2000b). Although most of the efforts have been so far addressed to the investigation of α-synuclein biochemical properties, its interaction with membranes and other cellular components, and the biophysics of its aggregation, few studies showed the implication of the regulation of α-synuclein expression at the transcriptional and post-transcriptional level for the development of the disease (Beyer et al., 2008; Doxakis, 2010; McCarthy et al., 2011; Cardo et al., 2014; Locascio et al., 2015). Recent articles reported an alteration of specific *SNCA* 3'UTR transcript isoforms levels in patients affected by PD (Locascio et al., 2015; Rhinn et al., 2012). In one case, the authors measured an increase of *SNCA* isoforms with extended 3'UTRs in cortical brain samples of PD affected individuals, and associated this alteration to a change of cellular protein synthesis and localization (Rhinn et al., 2012). In the other case a decrease of the same 3'UTR isoform was measured in peripheral blood in cases of *de novo* motor PD (Locascio et al., 2015).

Given the importance of *trans*-acting factors targeting the 3'UTR, namely RNA-binding proteins (RBPs) and microRNAs, for the determination of mRNA translation and turnover, we decided to address the question of which RBPs bind the 3'UTR of *SNCA* transcript and regulate its expression. By using a platform of human protein arrays, we have tested the binding of almost 10000 proteins to the *SNCA*-3'UTR and identified 27 physical interactions. Protein arrays are usually employed to detect protein-protein, protein-small molecules or protein-DNA interactions, and their application for the discovery of protein-RNA interactions is relatively new (Scherrer et al., 2010; Siprashvili et al., 2012). The technique presents some limitations given the fact that the use of entirely recombinant proteins precludes the detection of RNA-protein interactions that 1) require post-translational modifications of the protein, 2) involve macro-complexes, and 3) take place with proteins that are not present on the array or are present in another folding state. Despite these limitations, the array provides a powerful approach for the simultaneous screening of thousands of proteins with minimal amounts of RNA and in a very short time (3-4 days approximatively). In addition, considering the scarce availability of reliable methods for testing protein binding with long RNAs, we chose this strategy as a method to complement the biotin RNA pulldown, which suffers from a high background noise with increasing RNA size (Michlewski and Cáceres, 2010).

Out of 27 significant interactors, 18 proteins contain known RNA binding domains (RBDs) and 4 proteins are nuclear factors involved in transcription, DNA editing and histone modifications (see section 6.1). Considering the last discoveries in the field, which report that a number of DNA-binding domains have also ability to interact with transcripts (Castello et al., 2012), it is not hard to believe that this group of proteins might bind RNA. The majority (>80%) of proteins detected have nucleic acids binding capability demonstrating the good reliability of the method. Many of these proteins intervene in essential processes of RNA metabolism. In particular ELAVL1, PTBP2, ZC3H14, CUGBP1, CSTF2, HNRPA1, MOV10, TIAR and PABPC5 have all been previously reported to bind at 3'UTR of transcripts and regulate mRNA polyadenylation, stability, transport and translation, thus they represent good candidates for further validation (Lebedeva et al., 2011; Xu and Hecht, 2007; Masuda et al., 2012; Kandala et al., 2016; Glisovic et al., 2003; Gregersen et al., 2014; Liao et al., 2007).

By applying *cat*RAPID (Agostini et al., 2013) to predict protein-RNA interactions, we were able to narrow down the list of candidates to five proteins: TIAR, CELF1, ELAVL1, CSTF2 and KANSL2 which show the highest score of interaction with *SNCA*-3'UTR (see section 6.1). *cat*RAPID is a sequence-based method that exploits physico-chemical properties of nucleotide and amino acid chains such as secondary structure, hydrogen bonding, and van der Waals' propensities to predict protein–RNA associations with a confidence of 80% or higher (Bellucci et al., 2011). The method has been previously applied for the investigation of protein interactions with coding and noncoding RNAs involved in neurodegenerative diseases such as amyotrophic lateral sclerosis, Alzheimer's and Parkinson's diseases, fragile X-associated tremor/ataxia syndrome, with results in agreement with experimental evidence (Cirillo et al., 2013). As for the performances of *cat*RAPID on the protein array, we observed an area under the ROC curve AUC > 0.7 on strong-signal cases (i.e., top 50 high-affinity vs bottom 50 low-affinity interactions), which indicates good reproducibility of experimental data.

TIAR and ELAVL1 are among the best characterized AU-rich element (ARE)-binding proteins (Kim et al., 2011). Although they share only 30% of sequence homology, the two proteins have similar domain architecture, with three classical RNA recognition motif (RRMs) at the N-terminus that interact with RNA (Cléry et al., 2008). Both are ubiquitously expressed in mammalian cells and nucleo-

cytoplasmic shuttling proteins performing a variety of roles at different stages of mRNA expression. Notably, TIAR and ELAVL1 have been found to bind to several common mRNAs including TNF-α, GM-CSF COX-2, β-F1-ATPase, PDCD4, IL-1β and β$_2$-AR but with different, and often opposite, effects (Cok et al., 2003; Izquierdo, 2006; Kim et al., 2011; Subramaniam et al., 2011; Suswam et al., 2005a; Wigington et al., 2015). Given their documented interplay and the commonality of binding modalities we decided to focus our study on TIAR and ELAVL1. We hypothesized that the two proteins might bind to *SNCA* mRNA and regulate its expression by modulating its stability and translation. In addition, TIAR and ELAVL1 are reported in AURA database (Dassi et al., 2012) as *SNCA* 3'UTR interacting factors, while CELF1, CSTF2 and KANSL2 are not present. Recently, a CLIP experiment in HeLa cells on CELF1 interactions has been published (Le Tonquèze et al., 2016). The study reports binding sites in the intronic regions of *SNCA* pre-mRNA, but the contacts are not conserved in replicate experiments (Le Tonquèze et al., 2016). The discrepancy between our *in vitro* / *in silico* findings and CLIP experiments on CELF1 can be explained by considering the interplay with factors present in the cellular context which might prevent the binding to occur.

The biotinylated RNA pulldown confirmed the capacity of TIAR and ELAVL1 to bind the 3'UTR of *SNCA* transcript *in vitro* and revealed differences in the binding ability to two different sized 3'UTRs. In particular, while TIAR shows similar propensities for the 3'UTR short (575 nt) and long (2.5 kb), ELAVL1 seems to preferentially bind the long 3'UTR, compatibly with published CLIP data that assign to TIAR a cluster of binding sites within the first 600 bases and to ELAVL1 at least 5 different binding sites, one of them in the first 600 bases and the additional four spread all over the 2.5 kb (Kishore et al., 2011; Mukherjee et al., 2011; Wang et al., 2010). This result suggests that ELAVL1 might exert different regulatory roles depending on the 3'UTR isoform and the availability of binding sites. The protein might spread along the sequence of the UTR and oligomerize, similarly to Drosophila orthologue HuR (Toba and White, 2008; Scheiba et al., 2014), and compete with miRNA binding or protect the RNA from the binding of RNA degradation proteins.

Our study also reveals that *in vitro* differentiated human neuroblastoma cells (SH-SY5Y) and HeLa cells mainly express the *SNCA* isoform

carrying the short 3'UTR (575 nt) that accounts for around 50% of total *SNCA* mRNA, while the longest 3'UTR isoform represent only a small portion of the total *SNCA* transcript, similarly to the other three isoforms that have been identified up to date (see section 6.3). Together with the observation that the 3'UTR short is almost 18 times more active than the long 3'UTR at a luciferase gene reporter assay (see section 6.4), our data indicate that the isoform that mainly contributes to protein synthesis is the one carrying the short 3'UTR. Our observation is compatible with previous evidence showing that shorter 3'UTRs are more stable than their corresponding longer isoforms and produce also more protein (Mayr and Bartel, 2009b). It is likely that the difference is due to the fact that longer UTRs can host more miRNAs binding sites that make them more susceptible to degradation. Thus, we hypothesized that the short 3'UTR isoform is the most relevant in the context of disease where an aberrant accumulation of α-synuclein with subsequent formation of aggregates and cell degeneration are among the main causes. Nevertheless, we cannot rule out that the long 3'UTR isoforms play different roles in the disease by activating compensatory events to contrast the degeneration process. These isoforms could be upregulated in PD in order to reduce protein synthesis or modulate protein localization and function.

The two RBPs under study, ELAVL1 and TIAR, showed similar effects upon stable knockdown and transient overexpression in HeLa cells, with the endogenous α-synuclein protein being downregulated upon depletion of the two proteins and upregulated in response to their overexpression (see Sections 7.2 and 7.4). More specifically, TIAR significantly affects both RNA and protein levels, while ELAVL1 only has a mild effect on α-synuclein protein levels. The effect of ELAVL1 on *SNCA* RNA at the steady state is negligible. When we quantified each 3'UTR isoform in knockdown and control cells with a more sensitive method, such as the 3'end RNA sequencing, we didn't obtain any difference in the proportion of the five 3'UTR isoforms, indicating that TIAR and ELAVL1 knockdown equally affect all isoforms independently from the number of binding sites available (see Section 7.3). This is somehow expected for TIAR that only binds in the first 600 bases, but was not as obvious for ELAVL1 that, according to CLIP data, can bind the long 3'UTR at five different sites implying a much higher

combinatorial power with different possible outcomes (Kishore et al., 2011; Mukherjee et al., 2011).

Overall**, our results strongly argue for a role of TIAR and ELAVL1 as positive regulators of α-synuclein expression**, although the mechanism through which they achieve this effect and the sequence regulatory elements involved are not known yet. Notably, ELAVL1 also binds intronic regions (e.g. intron 2 and 3) of *SNCA* mRNA, according to CLIP data (Kishore et al., 2011; Mukherjee et al., 2011), and could therefore affect other steps of its maturation, compatibly with its involvement in upstream regulatory events such as pre-mRNA splicing. Also TIAR was found to co-regulate transcription and splicing of pre-mRNAs in the nucleus during early biogenesis of RNAs (Suswam et al., 2005b), so we cannot exclude its participation in other upstream regulatory events although CLIP experiments failed to detect other binding sites outside the 3'UTR.

We obtained that the 3'UTR was necessary to achieve the down-regulation of a luciferase construct in ELAVL1 knockdown cells, suggesting that **the regulation observed endogenously might actually happen through the interaction of ELAVL1 with the 3'UTR** of the mRNA in agreement with our hypothesis (see Section 7.5). The same trend was obtained for TIAR knockdown when we directly transfected the RNA containing the sequence of *SNCA* 3'UTR, although additional biological replicates are needed.

Considering that the binding of ELAVL1 and TIAR to the 3'UTR generally affects mRNA translation and turnover, we decided to address these two possible avenues. In agreement with our hypothesis, the mRNA stability assay shows that **both RBPs significantly affect the decay rate of *SNCA* mRNA by protecting it from degradation** (see Section 7.6). This result is compatible with the well-documented role of ELAVL1 as RNA stabilization factor (Fig.1). Indeed, ELAVL1 interferes with ARE-dependent mRNA degradation by protecting the body of the mRNA from decay, rather than slowing down mRNA deadenylation (Peng et al., 1998). While it is generally assumed that ELAVL1 stabilized mRNAs primarily by competing with proteins designated to mRNA degradation such as AUF-1 in the case of COX-2 mRNA, or KSRP for IL-8 mRNA and TTP that binds ELAVL1 own mRNA (Cok et al., 2004; Suswam et al., 2005a; Dai et al., 2012), other mechanisms might be involved, as suggested by the

literature (Lu et al., 2014; Srikantan et al., 2012). A competition with microRNAs has been demonstrated for many genes. In the case of TOP2A coding for the topoisomerase II α, an enzyme that relieves tension form supercoiled DNA, its expression is higher in G2/M phase of cell cycle thanks to ELAVL1 competition with miR-548c and prevention of TOP2A mRNA recruitment to processing bodies (P-bodies) (Srikantan et al., 2011).

Lebedeva and colleagues found that microRNA binding sites are preferentially located toward the boundaries of 3'UTR as previously reported (Grimson et al., 2007; Nielsen et al., 2007) whereas ELAVL1 binding sites distribute uniformly along the 3'UTR except for regions surrounding the stop codon and the polyadenylation site (Lebedeva et al., 2011). When binding sites overlap, direct competition between miRNAs and the protein is possible, whereas in the context of non-overlapping sites, competition can occur either by steric hindrance or by non-steric hindrance involving changes in the secondary structure of the mRNA. Moreover, ELAVL1 was found to regulate microRNA expression by intervening in pri- or pre-miRNAs processing, as in the case of miR-16 or miR-7 (Xu et al., 2010; Choudhury et al., 2013). In particular, ELAVL1 down-regulates the expression of the mature miR7 by preventing pre-miR7 processing. Interestingly, miR-7 has been implicated in the down-regulation of *SNCA* expression, suggesting the possibility of a regulatory loop involving ELAVL1 inhibition of miR7 expression with consequent release of *SNCA* from miR7 binding and final increase of synuclein expression. This scenario is compatible with our observation of a down-regulation of *SNCA* upon ELAVL1 depletion, which might be mediated by miR7 upregulation. However, when we tested this hypothesis by measuring miR7 expression in ELAVL1 knockdown and control cells, we found that the general level of expression of miR7 in HeLa cells was very low and that it was instead downregulated upon ELAVL1 depletion. This result led us to exclude a possible role of miR7 in mediating ELAVL1 regulation of α-synuclein in our system, while the hypothesis of a competition with other destabilizing factors remains to be explored.

The reason why the decrease of *SNCA* mRNA stability was not evident when we measured mRNA level at the steady state is not clear. One possibility is that at the steady state the rate of transcription is greater than the rate of degradation, and changes in *SNCA* RNA decay rate are undetectable in these conditions. Indeed, the mRNA of

α-synuclein is globally very stable if compared to the average half-life of other mRNAs, as suggested by the observation that 12 hours after blocking transcription we still measured 60% of intact mRNA. Another explanation could reside in ELAVL1 intracellular localization. In normal conditions, the protein mainly localizes to the nucleus where it intervenes in pre-mRNA splicing and polyadenylation, but upon certain *stimuli* and post-translational modifications the protein translocates to the cytoplasm where it accomplishes its function of mRNA stabilization (Doller et al., 2008a). Interestingly, in 1998 Fan XC and Steitz J. observed a significant re-localization of ELAVL1 upon stress induced by inhibition of RNA Polymerase II transcription through actinomycin D (Fan and Steitz, 1998). We could speculate that only when we induce ELAVL1 export by treating cells with actinomycin D, thus favoring protein interaction with *SNCA*-3'UTR in the cytoplasm, the stabilizing effect becomes evident.

With respect to TIAR, there are lines of evidence on its involvement in the regulation of mRNA turnover by facilitation of mRNA deadenylation and stimulation of cap removal at the 5'end. Only in few cases, as for iNOS gene (Fechir et al., 2005), a positive regulation with increase of the mRNA level in response to TIAR overexpression, was registered. However, TIAR has been extensively characterized for its role in translation regulation. We know that together with TIA1 protein, TIAR is an important translational inhibitor in both development and stress response, but also in conditions of cell homeostasis (Kedersha et al., 1999; Mazan-Mamczarz et al., 2006). For this reason it is difficult to speculate about the mechanism through which the protein stabilizes *SNCA* mRNA. The overlap between TIAR binding site and the target region of miR153, a miRNA that has been identified to downregulate *SNCA* expression (Doxakis, 2010), suggests that a competition between the two factors could take place. However, miR153 expression is almost undetectable in HeLa cells, therefore its participation in α-synuclein downregulation upon TIAR depletion is very unlikely. Yet, we cannot exclude that miR153 could play a role in TIAR regulation in the nervous system, where this miRNA is more expressed.

We did not observe the same effect of ELAVL1 and TIAR knockdown on the decay rates of every *SNCA* isoforms (see Section 7.6). Yet, the two long isoforms account for 25% of total *SNCA* mRNA and the isoform carrying the 2.5 kb 3'UTR represents only 5%

of the total, which indicates that our assay might not be sensitive enough to quantify the decay rate of poorly expressed RNAs (C_t values above 30 at real-time PCR).

As mentioned, TIAR and ELAVL1 can regulate translation. In particular, ELAVL1 was found to activate translation of a number of mRNAs involved in cell cycle regulation, proliferation and cell survival, by targeting the 3'UTR, as in the case of prothymosin α (ProTα), B-cell leukemia (BCL-2), and cyclin A2 mRNA (Durie et al., 2011). In addition, ELAVL1 binds the 5' UTR of the hypoxia-inducible factor 1, α (HIF-1α) mRNA and promotes translation through a mechanism that has not been fully described, but imply coordination with internal ribosome entry sites (IRES) present in the 5'UTR of HIF-1α mRNA (Galbán et al., 2008). ELAVL1 can play dual role in translation regulation since cases of translation inhibition have been also observed, as for Wnt5a and p27 transcripts that are targeted at their 5'UTR and 3'UTR respectively (Kullmann et al., 2002; Leandersson et al., 2006). As for TIAR, we know that the protein is a major translation inhibitor together with TIA1. The two proteins modulate translation by binding the 48S complex in the place of eIF2-GTP-tRNA$^{\text{Met}}$, thereby promoting polysome disassembly and the concurrent routing of the mRNA into stress granules, cytoplasmic membraneless compartments where mRNAs are temporary stored in a translationally inactive state until the cell recovers from stress. The formation of stress granules depends on the auto-aggregation ability of the prion-like C-termini of TIA proteins, and this process is very dynamic and reversible (Gilks et al., 2004). When we measured changes in *SNCA* mRNA translation by polyribosome profiling in control and knockdown cells, we couldn't see any difference upon ELAVL1 depletion, but **we did detect a reproducible shift of *SNCA* mRNA content in TIAR KD cells, from the polysomal fraction corresponding to five ribosomes to the fraction corresponding to three ribosomes, indicating that translation is somehow slowed down in absence of the protein** (Fig.1). Although this result goes into opposite direction with respect to what is generally known about TIAR function (Mazan-Mamczarz et al., 2006), it provides a good explanation of the substantial down-regulation of endogenous α-synuclein observed upon TIAR depletion, especially if combined with the effect registered on RNA stability. At present, we do not have elements to explain TIAR behaviour in this particular case, but we don't consider surprising that the protein might

promote translation rather that suppress it, given the high degree of versatility of ARE-binding proteins, and more generally of all RBPs (Barreau et al., 2005). As described for ELAVL1, as well as for many other RBPs, given a certain sequence or structure binding propensity, many additional factors contribute to determine if a regulatory event will happen or not. RBPs generally work in complexes rather than alone; the availability of protein partners determines the final composition of ribonucleoprotein complexes and therefore the probability that the RBP of interest will bind or not its target RNA and will produce a determined outcome or the opposite effect. Moreover, a translational network composed of RRM-type RBPs that control each other's expression has been deciphered, with ELAVL1 representing the hub of this network, which confirms its role of 'regulator of regulators' (Dassi et al., 2013; Pullmann et al., 2007). Importantly, TIAR and ELAVL1 continuously shuttle between the nucleus and the cytoplasm, therefore the regulation of protein localization is also essential to ensure their functionality. The nucleo-cytoplasmic shuttling of the two proteins is triggered by various environmental stress *stimuli* (heat-shock, osmotic shock, oxidative stress, etc.,). More specifically, the transport of ELAVL1 across the nuclear envelope requires a specific domain, the nucleocytoplasmic shuttling domain or HNS, and several transport machinery components, including transportins 1 and 2, the chromosome region maintenance 1 (CRM1), and importin-1 (Fan and Steitz, 1998; Gallouzi and Steitz, 2001; Güttinger et al., 2004; Rebane et al., 2004). ELAVL1 nucleocytoplasmic transport is also influenced by kinases such as Cdk1, AMP-activated protein kinase (AMPK), PKC, and p38 that phosphorylate ELAVL1 and its transport proteins (Doller et al., 2007, 2008b; Kim and Gorospe, 2008; Kim et al., 2008a, 2008b; Wang et al., 2002). Also TIAR, which is in highest proportion nuclear at the equilibrium, goes into the cytoplasm in response to transcription block through a mechanism that is mediated by the RRM3 domain (Zhang et al., 2005b).

In addition to their practical advantage in terms of ease of growth and manipulation, the choice to use HeLa cells as a cellular model to investigate the mechanism of regulation of α-synuclein expression by ELAVL1 and TIAR was based on the observation that, not only the two RBPs of interest are ubiquitously expressed, but also the five different 3'UTR isoforms of *SNCA* mRNA are similarly represented in HeLa cells and *in vitro* differentiated neuroblastoma cells, a cell line

commonly used as a model of human dopaminergic neurons (Korecka et al., 2013). However, we have to take into account that HeLa cells do not accurately reproduce the conditions present in the brain regions where α-synuclein is mainly expressed. The lack of neuron-specific protein partners or microRNAs that might cooperate or compete with ELAVL1 and TIAR, or the absence of environmental *stimuli* that drive proteins shuttling from the nucleus to the cytoplasm and *viceversa* might have influenced our results. In the future, it would be interesting to monitor α-synuclein expression upon environmental stresses inducing ELAVL1 and TIAR protein export, and use different cellular models such as mouse primary neurons or *in vitro* neuronal differentiated mouse embryonic stem cells. I also speculate that ELAVL1 and TIAR could carry the mature mRNA while shuttling from the nucleus to the cytoplasm, thus influencing its availability for translation. If so, it would be important to test *SNCA* mRNA intracellular localization in presence or absence of the two proteins.

The mechanisms through which ELAVL1 and TIAR achieve the effects that we observed will need further investigation. *In vitro* experiments to characterize binding sites in *SNCA* 3'UTR and to address possible cooperation (or competition) between the two proteins will be performed. Nevertheless, our findings help to identify new important regulators of α-synuclein expression and explain their functional role in basal conditions.

Notably, **we also found that TIAR expression was altered in *post-mortem* brain samples of patients affected by Parkinson's disease and Multiple System Atrophy**. Interestingly, α-synuclein and TIAR expression correlate at both RNA and protein levels, in agreement with our findings describing TIAR as a positive regulator of synuclein expression. In particular, the two proteins were downregulated in frontal motor cortex of PD individuals and upregulated in the same brain region of MSA patients. MSA belongs, as PD, to the neurodegenerative group of α-synucleinopathies, which are characterized by abnormal accumulation of α-synuclein. Differently from PD, where α-synuclein-positive aggregates appear to be largely neuronal, oligodendroglia inclusion prevail in MSA (Cykowski et al., 2015; Halliday et al., 2011). The pathogenic mechanisms that lead to neurodegeneration in MSA are not well understood, but partially differ from PD since MSA patients show resistance to L-dopa treatment (Churchyard et al., 1993; Wenning et al., 1994). Yet in contrast to PD,

disease-causative genetic mutations responsible of monogenic forms of MSA have so far not been identified (Al-Chalabi et al., 2009; Houlden H., 2016; Scholz et al., 2009). The data on oligodendroglial dysfunction in MSA support the notion that neurodegeneration may occur secondary to demyelination and lack of trophic support by oligodendroglia bearing cytoplasmic inclusions. Neurodegeneration typically occur with a multisystemic distribution that partially differs from the one observed in PD. For this reason, we decided to examine the frontal motor cortex, that is generally affected with similar degree in both diseases at the late stages. In agreement with our results, Neystat et al. showed reduction of *SNCA* expression in *substantia nigra* of PD affected individuals (Neystat et al., 1999) and another group reported 50% reduction at the cellular level in *substantia nigra* neurons and frontal cortex neurons in PD (Kingsbury et al., 2004). On the other hand, oligodendrocytes isolated from MSA brains expressed elevated levels of *SNCA* compared to control (Asi et al., 2014), and a recent strand-specific RNA-sequencing analysis of MSA brain transcriptome reported a moderate increase of *SNCA* expression in frontal cortex of MSA patients compared to normal individuals (Mills et al., 2016), in agreement with our results.

Besides the fact that we compared the expression of *SNCA* in frontal motor cortex samples of patients affected by two synucleinopathies for the first time, the interesting aspect of our analysis resides in the fact that the expression of α-synuclein protein correlates with the expression of TIAR, thus supporting our results that describe this RBP as an important positive regulator of *SNCA* expression.

Given the small sample size and the intra-group variability, it is however difficult to assume that the changes in expression that we observed for the two genes are actually related to the presence of the pathology and functionally coupled between them. Enlarging our group of study and introducing a comparison with control brain areas (areas not affected by the disease) would certainly help to reduce the intra-group variability and reach more conclusive results. Nevertheless, given the promising results obtained from the analysis of *post-mortem* biopsies, the quantification of TIAR in peripheral tissues and fluids from PD and MSA patients, such as blood, cerebrospinal fluid (CSF), urine and fibroblasts, could be of interest for the clinical diagnosis of different synucleinopathies. Distinguishing MSA from PD initially can be difficult owing to PD-like features in MSA, including occasionally a

transient L-dopa response in some patients. Moreover, MSA is characterized by a prognosis of a markedly shorten life span with respect to PD (mean age of onset of 56 years, mean survival form symptoms onset of 6-10 years) (Jecmenica-Lukic et al., 2012; Petrovic et al., 2012), so a high level of accuracy in the diagnosis is needed but not yet available.

Moreover, ELAV1 and TIAR regulate a number of genes involved in pathways characteristic of PD and MSA neurodegeneration, such as inflammatory response, oxidative stress, mitochondrial stress and apoptosis. A significant increase in the level of innate immune components, including complement and cytokines (e.g., IL-1, IL-2, IL-6, and TNF), in the *substantia nigra* and CSF of PD patients has been observed (Liu and Hong, 2003). Microglial activation has been reported to parallel neuronal degeneration in MSA (Ishizawa et al., 2004) and increased expression of proinflammatory genes has been observed in *post-mortem* tissue from the rostral pons of MSA patients (Langerveld et al., 2007). Polymorphisms in proinflammatory genes such as IL-1β, IL-1α or TNF-α have been reported to be associated with increased MSA risk (Infante et al., 2005; Nishimura et al., 2002). In synergy with TIA proteins, ELAVL1 coordinates the expression of inflammatory genes such as TNF-α, IL-1β or TGFβ1 in mice macrophages in response to different *stimuli*. ELAVL1 has also been recently shown to play a neuroprotective role in mice hippocampal neurons following strong glutamatergic excitation, through the post-transcriptional orchestration of specialized genes involved in mitochondrial dysfunction, oxidative damage and programmed cell death (Skliris et al., 2015).

In the light of these considerations one could hypothesize a scenario in which the two RBPs synergistically control neuronal expression of entire sets of genes implicated in the etiopathological process of PD or MSA, including α-synuclein. Alterations of ELAVL1 and TIAR expression, intracellular localization and function would trigger a cascade of misregulation events leading to disease. It is therefore important to further investigate the functional interconnection of TIAR and ELAVL1 proteins with *SNCA* and other PD-associated genes. This would help to get some insights about new aspects of the disease that have been so far underestimated, meaning the post-transcriptional coordination of gene expression.
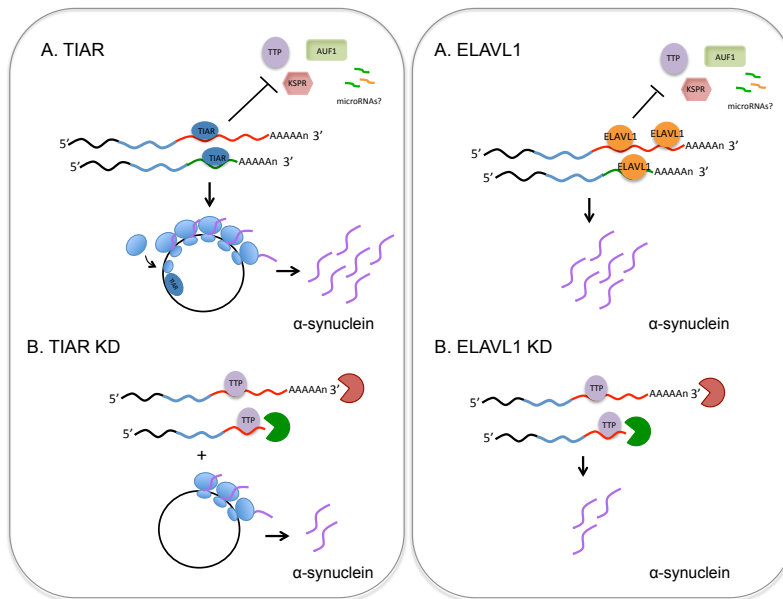
Figure 1. Scheme of the regulation of α-synuclein mRNA stability and translation by TIAR and ELAVL1 according to our results in HeLa cells. In normal conditions (A) TIAR and ELAVL1 protect *SNCA* mRNA from degradation by competing with degradation factors, such as RBPs and microRNAs. In addition TIAR promotes translation through a mechanism that is unknown. In absence of TIAR (B, left) there is a decrease of proteins synthesis due to a combination of mRNA destabilization and slower translation, while upon ELAVL1 depletion (B, right) only mRNA stability is affected.

Another aspect of α-synuclein gene regulation that we have addressed by means of computational tools, is the hypothesis of an autoregulatory mechanism involving the binding of α-synuclein to its own mRNA. *cat*RAPID predicts a high interaction propensity with a GC-rich region contained in the 5'UTR of the transcript, compatible with previous evidence of α-synuclein binding to GC-rich DNA molecules (Cherny et al., 2004; Hegde and Rao, 2007). Experimental evidence of autogenous interactions are available for other amyloidogenic proteins. As an example, TDP-43 binds to the 3'UTR of its transcript and induces RNA instability (Ayala et al., 2011). A second example is FMRP that is capable of interacting with its mRNA via a guanine-quartet (G-quartet) RNA motif at the 3'end of its coding region which can act as a splicing enhancer in a negative autoregulatory loop (Didiot et al., 2008; Schaeffer et al., 2001). Impairment of these feedback mechanisms could have consequences

for the onset of amyotrophic lateral sclerosis and fragile-X-syndrome respectively.

Interestingly, it has been shown that the intracellular concentrations of proteins that are likely to form aggregates is significantly lower than that of non-aggregation prone proteins (Tartaglia et al., 2007). It is likely that the cellular regulation of these proteins is different from the rest of the proteome and a combination of reduced transcript abundance, rapid protein turnover and translation regulation contributes to the low availability of aggregating proteins (Gsponer and Babu, 2012). In this perspective, the autogenous regulation might represent an additional strategy that the cell excogitates to keep intracellular level of potentially harmful proteins under tight control.

In the case of α-synuclein, the protein is normally unfolded and does not contain RNA binding domains, therefore its interaction with nucleic acids is difficult to postulate. Our preliminary *in vitro* experiments (data not shown in this manuscript) suggest a certain tendency of the protein to interact with RNA molecules at high protein concentrations compatible with intracellular levels, with some preferentiality for GC-rich sequences. Moreover, we know that the interaction of the N-terminal domain of the protein with the negatively charged phosphate groups in the polar head of membrane phospholipid induces a conformational change of α-synuclein with a disorder-to-order transition. Similarly, upon *in vitro* interaction with double or single stranded DNA, an increase in α-helical content of the protein was measured. Therefore, the interaction of the nascent peptide with its mRNA could play a role in the regulation of protein folding and aggregation propensity in addition to control expression. However, the specificity of this interaction and the evidence for the binding *in vivo* are needed to argue about its biological relevance.

In conclusion, we believe that the expression of dosage-sensitive genes, as those encoding aggregation-prone proteins associated to disease, undergoes distinct regulatory mechanisms. These comprise the post-transcriptional control by RBPs (*trans*-regulation) or the regulation by the protein itself that interacts with its own transcript (*cis*-regulation). The characterization of these regulatory networks is challenging due to their cell-specificity and extreme dynamicity, but it is fundamental for the understanding of the basis of diseases.

11. CONCLUSIONS

The work carried out during my PhD studies at Centre for Genomic Regulation (CRG) of Barcelona, has been compiled under the form of a thesis entitled "Post-transcriptional regulation of α-synuclein and link to Parkinson's disease". The thesis presents my personal contribution to the understanding of the regulation of α-synuclein expression by RNA-binding proteins that bind to the untranslated regions (UTRs) of its mRNA and control its stability and translation efficiency. Both experimental and computational tools have been employed for this purpose.

More specifically I can summarize the content of my thesis as follows:

1. Using a large-scale *in vitro* screening, new proteins potentially involved in the regulation of α-synuclein expression by targeting the 3'UTR of its mRNA were identified.

2. Two of these protein candidates, ELAVL1 and TIAR, also bind the 3'UTR of *SNCA* in a complementary *in vitro* assay with differences between previously identified 3'UTR isoforms of increasing size generated by alternative polyadenylation mechanism.

3. Among five different known 3'UTR isoforms of *SNCA* mRNA, the one carrying a short 3'UTR (575 bases) is the most abundant isoform in *in vitro* differentiated SH-SY5Y and HeLa cells, representing around 50% of total *SNCA* mRNA.

4. The short 3'UTR isoform is more 'active' when compared to two longer isoforms (1.07 and 2.5 kb 3'UTR) in a gene reporter assay and, potentially, the one mostly contributing to protein synthesis *in vivo*.

5. ELAVL1 and TIAR proved to be positive regulators of endogenous α-synuclein in knockdown and overexpression experiments conducted in HeLa cells.

6. The sequence of *SNCA* 3'UTR is required to mediate the regulation by ELAVL1, as demonstrated by the gene reporter assay preformed in ELAVL1 depleted cells with constructs

carrying the sequence of *SNCA* 3'UTRs, while additional proof is needed for TIAR.

7. The mechanism through which the two RBPs regulate *SNCA* mRNA expression implies the stabilization of the mRNA by both proteins, as shown by the RNA decay assay, and the enhancement of its translation in the case of TIAR, as demonstrated by the polyribosome profiling experiment. In our cellular model, the stabilization effect is not mediated by competition with miR7 or miR153 binding.

8. TIAR expression is altered in *post-mortem* brain tissue from patients affected by PD and MSA. In correlation with α-synuclein, we observed a downregulation in PD and an upregulation in MSA.

9. In parallel, we predicted the interaction of α-synuclein with its cognate mRNA in correspondence of a GC-rich region of the 5'UTR. We hypothesize that this autogenous regulation might be crucial to maintain α-synuclein intracellular concentration under tight control and prevent protein aggregation.

Appendix

Primer for SNCA 3'UTR cloning in pBSK plasmid

```
ApaI-Syn3UTR Fw
CGGGGCCCGGAAATATCTTTGCTCCCAGT

NotI-Syn3UTRS Rv
GCGCGGCCGCgTATTTTTGCAATGAGATAACGT

NotI-Syn3UTRL Rv
GCGCGGCCGCGTATTTTCATATATGTATATATT

BamHI-Syn3UTRM Rv
CGGGATCCCATGGTCGAATATTATTTATTG

Syn3UTRL flanking Fw
GAAGGGTATCAAGACTACGAACCTGAAGCC

Syn3UTRL flanking Rv
GAACAAGGGTTTTAGGAGCTCTTTGTAAG
```

Primers for Colony PCR

```
T7 promoter
TAATACGACTCACTATAGGG

NotI-Syn3UTRL Rv
GCGCGGCCGCGTATTTTCATATATGTATATATT

BamHI-Syn3UTRM Rv
CGGGATCCCATGGTCGAATATTATTTATTG
```

Primers for construct sequencing

```
T7 promoter      TAATACGACTCACTATAGGG
T3 promoter      GCAATTAACCCTCACTAAAGG
SYN3UTRLseq1     ACTGTTGTTTGATGTGTATG
Syn3UTRLseq2     GCCTAGAATTCATATATTTGGC
Syn3UTRLseq3     CCTAGAATTCATATATTTGGC
```

Primers for real-time PCR

```
HaSNCA all Fw    AGGGTGTTCTCTATGTAGG
HaSNCA all Rv    ACTGTCTTCTGGGCTACTGC
```

```
SNCA ML Fw AGCTTTGAAGAAGGAGGAAT
SNCA ML Rv CTTAAGGAACCAGTGCATACCA

SNCA L Fw  AAACATCGTTGGAACTACCAGAGTC
SNCA L Rv  GGGGAGTTAATAGATCTTCCCTGAA

TIAR Fw    GCCAATGGAGCCAAGTGTAT
TIAR Rv    CATATCCGGCTTGGTTAGGA

ELAVL1 Fw  AAAACCATTAAGGTGTCGTATGCTC
ELAVL1 Rv  CCTCTGGACAAACCTGTAGTCTGAT

GAPDH Fw   GACCACAGTCCATGCCATC
GAPDH Rv   TTCAGCTCAGGGATGACCTT

ACTB Fw    GGACCTGACTGACTACCTCAT
ACTB rv    CGTAGCACAGCTTCTCCTTAAT
```

Primers for Gibson cloning

pGL4-TK-FL linearization

```
pGL4-TK-FL Fw
CTTCGAGCAGACATGATAAGATACATTGATGAGTTT
pGL4-TK-FL Rv
TTATTACACGGCGATCTTGCCGC
```

3'UTRs amplification from pBSK plasmid

```
All_3UTRs_Gibs Fw
GCAAGATCGCCGTGTAATAAGAAATATCTTTGCTCCCAGT
3UTRS-Gibs Rv
CTTATCATGTCTGCTCGAAGTCCACCGTATTTTTGCAATGAGATAACGT
3UTRM-Gibs Rv
TTATCATGTCTGCTCGAAGCGGCGTGCATGGTCGAATATTATTTATTG
3UTRL-Gibs Rv
CTTATCATGTCTGCTCGAAGTATTTTCATATATGTATATATT
```

Primers/Gibson oligos for PAS deletion

```
Δ(262-267) Fw AACACCTAAGTGACTACCACTTATTTCTAAATC
Δ(262-267) Rv TTGTTTTAACATCGTAGATTGAAGCC

Δ(262-267)Gibson oligos
```

Fw:
GCTTCAATCTACGATGTTAAAACAAAACACCTAAGTGACTACCACTTATT
Rv:
AATAAGTGGTAGTCACTTAGGTGTTTTGTTTTAACATCGTAGATTGAAGC

Δ(468-473)Fw TACTAAATATGAAATTTTACCATTTTGCG
Δ(468-473)Rv GGTGCATAGTTTCATGCTCACAT

Δ(468-473)Gibson oligos
Fw:
ATATGTGAGCATGAAACTATGCACCTACTAAATATGAAATTTTACCATTT
Rv:
AAATGGTAAAATTTCATATTTAGTAGGTGCATAGTTTCATGCTCACATAT

Δ(529-553)Fw ACGTTATCTCATTGCAAAAATATT
Δ(529-553)Rv TACAAACACAAGTGAATAAAACACA

Δ(529-553)Gibson oligos
Fw:
TGTGTTTTATTCACTTGTGTTTGTAACGTTATCTCATTGCAAAAATATTT
Rv:
AAATATTTTTGCAATGAGATAACGTTACAAACACAAGTGAATAAAACACA

Δ(1054-1059)Fw TAATATTCGACCATGAATAAAA
Δ(1054-1059)Rv GTCAGAAAGGTACAGCATTCAC
Δ(1054-1059)Fw TAATATTCGACCATGCACGCCG (for 3UTRM)

Δ(1054-1059)Gibson oligos
Fw:
GGTGTGAATGCTGTACCTTTCTGACTAATATTCGACCATGAATAAAAAAA
Rv:
TTTTTTTATTCATGGTCGAATATTAGTCAGAAAGGTACAGCATTCACACC

Primers for real-time PCR of luciferase assay

Luc FW: ACCTTCGTGACTTCCCATTT
Luc RV: GGTACTGCCACTACTGTTCAT

Ren FW: TTGAATCATGGGATGAATGG
Ren RV: ATGTTGGACGACGAACTTCA

Luc-3UTRS FW: TGTGAGCATGAAACTATGCACCT
Luc-3UTRS RV: TCATGTCTGCTCGAAGTCCACC

Luc-3UTRM FW: TGGGGAACTGTTGTTTGATGTGT
Luc-3UTRM RV: CGGCGTGCATGGTCGAATATTA

```
Luc-3UTRL FW GTGAATGCTGTACCTTTCTGACTAAT
Luc-3UTRL RV CAGAGCCTTGAATGTGCTAATATGT
```

Short hairpin RNAs for knockdown

```
shTIAR-1 forward oligo :
CCGGCCCATATTGCTTTGTGGAATTCTCGAGAATTCCACAAAGCAATAT
GGGTTTTTG

shTIAR-1 reverse oligo:
AATTCAAAAACCCATATTGCTTTGTGGAATTCTCGAGAATTCCACAAAG
CAATATGGGT

shTIAR-2 forward oligo:
CCGGCTTCAGTTGTTCAGTCAGATTCTCGAGAATCTGACTGAACAACTG
AAGTTTTTG

shTIAR-2 reverse oligo:
AATTCAAAAACTTCAGTTGTTCAGTCAGATTCTCGAGAATCTGACTGAA
CAACTGAAGT

shELAVL1-1 forward oligo:
CCGGTACCAGTTTCAATGGTCATAACTCGAGTTATGACCATTGAAACTG
GTATTTTTG

shELAVL1-1 reverse oligo:
AATTCAAAAATACCAGTTTCAATGGTCATAACTCGAGTTATGACCATTG
AAACTGGTA

shELAVL1-2 forward oligo:
CCGGCGAGCTCAGAGGTGATCAAAGCTCGAGCTTTGATCACCTCTGAGC
TCGTTTTTG

shELAVL1-2 reverse oligo:
AATTCAAAAACGAGCTCAGAGGTGATCAAAGCTCGAGCTTTGATCACCT
CTGAGCTCG
```

Primers for 3'end RNA sequencing

```
R1-SNC608
CCCTACACGACGCTCTTCCGATCTtatgcctgtggatcctgaca
R1-SNC909
CCCTACACGACGCTCTTCCGATCTctgtggattttgtggcttca
R1-SNC1154
CCCTACACGACGCTCTTCCGATCTtgagcatgaaactatgcacct
```

R1-SNC1432
CCCTACACGACGCTCTTCCGATCTctgaagcaacactgccagaa
R1-SNC1713
CCCTACACGACGCTCTTCCGATCTttggtgtgaatgctgtacctt
R1-SNC2004
CCCTACACGACGCTCTTCCGATCTtgcctttaaacatcgttgga
R1-SNC2353
CCCTACACGACGCTCTTCCGATCTatatattgggcgctggtgag
R1-SNC2787
CCCTACACGACGCTCTTCCGATCTtgacggtaatttttgagcagtg
R1-SNC3013
CCCTACACGACGCTCTTCCGATCTggtcggctttaccaaaacag

R2-UMI-dT16
VNTTCAGACGTGTGCTCTTCCGATCTNNNNNNNNNNNTTTTTTTTTTTTTTT
TTTVN

Antibodies

Rabbit polyclonal anti-alpha Synuclein antibody
[ab93832]
Mouse monoclonal anti-HuR/ELAVL1 [ab54987]
Goat polyclonal anti-TIAR [sc-1749]
Rabbit polyclonal anti-FMRP [ab69815]
Mouse monoclonal anti-alpha Tubulin antibody
[ab7291]
Rabbit monoclonal anti-RALY [ab170105]

Protein G HRP-conjugate (Millipore, 18-161)
Rabbit polyclonal secondary antibody to Mouse
IgG-HRP [ab97046]

Bibliografia

Abeliovich, A., Schmitz, Y., Fariñas, I., Choi-Lundberg, D., Ho, W.H., Castillo, P.E., Shinsky, N., Verdugo, J.M., Armanini, M., Ryan, A., et al. (2000). Mice lacking alpha-synuclein display functional deficits in the nigrostriatal dopamine system. Neuron *25*, 239–252.

Abou-Sleiman, P.M., Muqit, M.M.K., and Wood, N.W. (2006). Expanding insights of mitochondrial dysfunction in Parkinson's disease. Nat. Rev. Neurosci. *7*, 207–219.

Agostini, F., Zanzoni, A., Klus, P., Marchese, D., Cirillo, D., and Tartaglia, G.G. (2013). catRAPID omics: a web server for large-scale prediction of protein-RNA interactions. Bioinforma. Oxf. Engl.

Aguzzi, A., and Polymenidou, M. (2004). Mammalian prion biology: one century of evolving concepts. Cell *116*, 313–327.

Ahn, B.-H., Rhim, H., Kim, S.Y., Sung, Y.-M., Lee, M.-Y., Choi, J.-Y., Wolozin, B., Chang, J.-S., Lee, Y.H., Kwon, T.K., et al. (2002). alpha-Synuclein interacts with phospholipase D isozymes and inhibits pervanadate-induced phospholipase D activation in human embryonic kidney-293 cells. J. Biol. Chem. *277*, 12334–12342.

Alavanja, M.C.R., Samanic, C., Dosemeci, M., Lubin, J., Tarone, R., Lynch, C.F., Knott, C., Thomas, K., Hoppin, J.A., Barker, J., et al. (2003). Use of agricultural pesticides and prostate cancer risk in the Agricultural Health Study cohort. Am. J. Epidemiol. *157*, 800–814.

An, J.J., Gharami, K., Liao, G.-Y., Woo, N.H., Lau, A.G., Vanevski, F., Torre, E.R., Jones, K.R., Feng, Y., Lu, B., et al. (2008). Distinct role of long 3' UTR BDNF mRNA in spine morphology and synaptic plasticity in hippocampal neurons. Cell *134*, 175–187.

Anthony, K., and Gallo, J.-M. (2010). Aberrant RNA processing events in neurological disorders. Brain Res. *1338*, 67–77.

Asi, Y.T., Simpson, J.E., Heath, P.R., Wharton, S.B., Lees, A.J., Revesz, T., Houlden, H., and Holton, J.L. (2014). Alpha-synuclein mRNA expression in oligodendrocytes in MSA. Glia *62*, 964–970.

Ayala, Y.M., De Conti, L., Avendaño-Vázquez, S.E., Dhir, A., Romano, M., D'Ambrogio, A., Tollervey, J., Ule, J., Baralle, M., Buratti, E., et al. (2011). TDP-43 regulates its mRNA levels through a negative feedback loop. EMBO J. *30*, 277–288.

Baba, M., Nakajo, S., Tu, P.H., Tomita, T., Nakaya, K., Lee, V.M., Trojanowski, J.Q., and Iwatsubo, T. (1998). Aggregation of alpha-synuclein in Lewy bodies of sporadic Parkinson's disease and dementia with Lewy bodies. Am. J. Pathol. *152*, 879–884.

Bai, B., Hales, C.M., Chen, P.-C., Gozal, Y., Dammer, E.B., Fritz, J.J., Wang, X., Xia, Q., Duong, D.M., Street, C., et al. (2013). U1 small nuclear ribonucleoprotein complex and RNA splicing alterations in Alzheimer's disease. Proc. Natl. Acad. Sci. U. S. A. *110*, 16562–16567.

Abu-Baker, A., and Rouleau, G.A. (2007). Oculopharyngeal muscular dystrophy: recent advances in the understanding of the molecular pathogenic mechanisms and treatment strategies. Biochim. Biophys. Acta *1772*, 173–185.

Baptista, M.J., O'Farrell, C., Daya, S., Ahmad, R., Miller, D.W., Hardy, J., Farrer, M.J., and Cookson, M.R. (2003). Co-ordinate transcriptional regulation of dopamine synthesis genes by alpha-synuclein in human neuroblastoma cell lines. J. Neurochem. *85*, 957–968.

Barreau, C., Paillard, L., and Osborne, H.B. (2005). AU-rich elements and associated factors: are there unifying principles? Nucleic Acids Res. *33*, 7138–7150.

Battelli, C., Nikopoulos, G.N., Mitchell, J.G., and Verdi, J.M. (2006). The RNA-binding protein Musashi-1 regulates neural development through the translational repression of p21WAF-1. Mol. Cell. Neurosci. *31*, 85–96.

Bellani, S., Sousa, V.L., Ronzitti, G., Valtorta, F., Meldolesi, J., and Chieregatti, E. (2010). The regulation of synaptic function by alpha-synuclein. Commun. Integr. Biol. *3*, 106–109.

Bellucci, M., Agostini, F., Masin, M., and Tartaglia, G.G. (2011). Predicting protein associations with long noncoding RNAs. Nat. Methods *8*, 444–445.

Berkovits, B.D., and Mayr, C. (2015). Alternative 3' UTRs act as scaffolds to regulate membrane protein localization. Nature *522*, 363–367.

Beyer, K., and Ariza, A. (2013). α-Synuclein posttranslational modification and alternative splicing as a trigger for neurodegeneration. Mol. Neurobiol. *47*, 509–524.

Beyer, K., Domingo-Sábat, M., Lao, J.I., Carrato, C., Ferrer, I., and Ariza, A. (2008). Identification and characterization of a new alpha-synuclein isoform and its role in Lewy body diseases. Neurogenetics *9*, 15–23.

Bhattacharyya, S.N., Habermacher, R., Martine, U., Closs, E.I., and Filipowicz, W. (2006). Relief of microRNA-mediated translational repression in human cells subjected to stress. Cell *125*, 1111–1124.

Bingol, B., and Schuman, E.M. (2006). Activity-dependent dynamics and sequestration of proteasomes in dendritic spines. Nature *441*, 1144–1148.

Boelens, W.C., Jansen, E.J.R., van Venrooij, W.J., Stripecke, R., Mattaj, I.W., and Gunderson, S.I. (1993). The human U1 snRNP-Specific U1A protein inhibits polyadenylation of its own pre-mRNA. Cell *72*, 881–892.

Boers, D., van Amelsvoort, L., Colosio, C., Corsini, E., Fustinoni, S., Campo, L., Bosetti, C., La Vecchia, C., Vergieva, T., Tarkowski, M., et al. (2008). Asthmatic symptoms after exposure to ethylenebisdithiocarbamates and other pesticides in the Europit field studies. Hum. Exp. Toxicol. *27*, 721–727.

Bolam, J.P., and Pissadaki, E.K. (2012). Living on the edge with too many mouths to feed: why dopamine neurons die. Mov. Disord. Off. J. Mov. Disord. Soc. *27*, 1478–1483.

Boutet, S.C., Cheung, T.H., Quach, N.L., Liu, L., Prescott, S.L., Edalati, A., Iori, K., and Rando, T.A. (2012). Alternative polyadenylation mediates microRNA regulation of muscle stem cell function. Cell Stem Cell *10*, 327–336.

Braak, H., Del Tredici, K., Rüb, U., de Vos, R.A.I., Jansen Steur, E.N.H., and Braak, E. (2003). Staging of brain pathology related to sporadic Parkinson's disease. Neurobiol. Aging *24*, 197–211.

Braak, H., Ghebremedhin, E., Rüb, U., Bratzke, H., and Del Tredici, K. (2004). Stages in the development of Parkinson's disease-related pathology. Cell Tissue Res. *318*, 121–134.

Brennan, C.M., and Steitz, J.A. (2001). HuR and mRNA stability. Cell. Mol. Life Sci. CMLS *58*, 266–277.

Brewer, G. (1991). An A + U-rich element RNA-binding factor regulates c-myc mRNA stability in vitro. Mol. Cell. Biol. *11*, 2460–2466.

Brinegar, A.E., and Cooper, T.A. (2016). Roles for RNA-binding proteins in development and disease. Brain Res. *1647*, 1–8.

Bungeroth, M., Appenzeller, S., Regulin, A., Völker, W., Lorenzen, I., Grötzinger, J., Pendziwiat, M., and Kuhlenbäumer, G. (2014). Differential aggregation properties of alpha-synuclein isoforms. Neurobiol. Aging *35*, 1913–1919.

Burré, J., Sharma, M., Tsetsenis, T., Buchman, V., Etherton, M.R., and Südhof, T.C. (2010). Alpha-synuclein promotes SNARE-complex assembly in vivo and in vitro. Science *329*, 1663–1667.

Cabin, D.E., Shimazu, K., Murphy, D., Cole, N.B., Gottschalk, W., McIlwain, K.L., Orrison, B., Chen, A., Ellis, C.E., Paylor, R., et al. (2002). Synaptic vesicle depletion correlates with attenuated synaptic responses to prolonged repetitive stimulation in mice lacking alpha-synuclein. J. Neurosci. Off. J. Soc. Neurosci. *22*, 8797–8807.

Campioni, S., Mannini, B., Zampagni, M., Pensalfini, A., Parrini, C., Evangelisti, E., Relini, A., Stefani, M., Dobson, C.M., Cecchi, C., et al. (2010). A causative link between the structure of aberrant protein oligomers and their toxicity. Nat. Chem. Biol. *6*, 140–147.

Canet-Avilés, R.M., Wilson, M.A., Miller, D.W., Ahmad, R., McLendon, C., Bandyopadhyay, S., Baptista, M.J., Ringe, D., Petsko, G.A., and Cookson, M.R. (2004). The Parkinson's disease protein DJ-1 is neuroprotective due to cysteine-sulfinic acid-driven mitochondrial localization. Proc. Natl. Acad. Sci. U. S. A. *101*, 9103–9108.

Cardo, L.F., Coto, E., de Mena, L., Ribacoba, R., Lorenzo-Betancor, O., Pastor, P., Samaranch, L., Mata, I.F., Díaz, M., Moris, G., et al. (2012). A search for SNCA 3' UTR variants identified SNP rs356165 as a determinant of disease risk and onset age in Parkinson's disease. J. Mol. Neurosci. MN *47*, 425–430.

Cardo, L.F., Coto, E., de Mena, L., Ribacoba, R., Mata, I.F., Menéndez, M., Moris, G., and Alvarez, V. (2014). Alpha-synuclein transcript isoforms in three different brain regions from Parkinson's disease and healthy subjects in relation to the SNCA rs356165/rs11931074 polymorphisms. Neurosci. Lett. *562*, 45–49.

Castello, A., Fischer, B., Eichelbaum, K., Horos, R., Beckmann, B.M., Strein, C., Davey, N.E., Humphreys, D.T., Preiss, T., Steinmetz, L.M., et al. (2012). Insights into RNA Biology from an Atlas of Mammalian mRNA-Binding Proteins. Cell *149*, 1393–1406.

Al-Chalabi, A., Dürr, A., Wood, N.W., Parkinson, M.H., Camuzat, A., Hulot, J.-S., Morrison, K.E., Renton, A., Sussmuth, S.D., Landwehrmeyer, B.G., et al. (2009). Genetic variants of the alpha-synuclein gene SNCA are associated with multiple system atrophy. PloS One *4*, e7114.

Chan, C.S., Guzman, J.N., Ilijic, E., Mercer, J.N., Rick, C., Tkatch, T., Meredith, G.E., and Surmeier, D.J. (2007). "Rejuvenation" protects neurons in mouse models of Parkinson's disease. Nature *447*, 1081–1086.

Chartier-Harlin, M.-C., Kachergus, J., Roumier, C., Mouroux, V., Douay, X., Lincoln, S., Levecque, C., Larvor, L., Andrieux, J., Hulihan, M., et al. (2004). Alpha-synuclein locus duplication as a cause of familial Parkinson's disease. Lancet Lond. Engl. *364*, 1167–1169.

Chartrand, P., Meng, X.H., Singer, R.H., and Long, R.M. (1999). Structural elements required for the localization of ASH1 mRNA and of a green fluorescent protein reporter particle in vivo. Curr. Biol. CB *9*, 333–336.

Chen, C.Y., and Shyu, A.B. (1995). AU-rich elements: characterization and importance in mRNA degradation. Trends Biochem. Sci. *20*, 465–470.

Cherny, D., Hoyer, W., Subramaniam, V., and Jovin, T.M. (2004). Double-stranded DNA stimulates the fibrillation of alpha-synuclein in vitro and is associated with the mature fibrils: an electron microscopy study. J. Mol. Biol. *344*, 929–938.

Chiba-Falek, O., and Nussbaum, R.L. (2001). Effect of allelic variation at the NACP-Rep1 repeat upstream of the alpha-synuclein gene (SNCA) on transcription in a cell culture luciferase reporter system. Hum. Mol. Genet. *10*, 3101–3109.

Choudhury, N.R., de Lima Alves, F., de Andrés-Aguayo, L., Graf, T., Cáceres, J.F., Rappsilber, J., and Michlewski, G. (2013). Tissue-specific control of brain-enriched miR-7 biogenesis. Genes Dev. *27*, 24–38.

Churchyard, A., Donnan, G.A., Hughes, A., Howells, D.W., Woodhouse, D., Wong, J.Y., Kalnins, R.M., Mendelsohn, F.A., and Paxinos, G. (1993). Dopa resistance in multiple-system atrophy: loss of postsynaptic D2 receptors. Ann. Neurol. *34*, 219–226.

Cirillo, D., Agostini, F., Klus, P., Marchese, D., Rodriguez, S., Bolognesi, B., and Tartaglia, G.G. (2013). Neurodegenerative diseases: Quantitative predictions of protein-RNA interactions. RNA N. Y. N *19*, 129–140.

Ciryam, P., Tartaglia, G.G., Morimoto, R.I., Dobson, C.M., and Vendruscolo, M. (2013). Widespread aggregation and

neurodegenerative diseases are associated with supersaturated proteins. Cell Rep. *5*, 781–790.

Clarke, G., Collins, R.A., Leavitt, B.R., Andrews, D.F., Hayden, M.R., Lumsden, C.J., and McInnes, R.R. (2000). A one-hit model of cell death in inherited neuronal degenerations. Nature *406*, 195–199.

Clayton, D.F., and George, J.M. (1998). The synucleins: a family of proteins involved in synaptic function, plasticity, neurodegeneration and disease. Trends Neurosci. *21*, 249–254.

Cléry, A., Blatter, M., and Allain, F.H.-T. (2008). RNA recognition motifs: boring? Not quite. Curr. Opin. Struct. Biol. *18*, 290–298.

Cok, S.J., Acton, S.J., and Morrison, A.R. (2003). The proximal region of the 3'-untranslated region of cyclooxygenase-2 is recognized by a multimeric protein complex containing HuR, TIA-1, TIAR, and the heterogeneous nuclear ribonucleoprotein U. J. Biol. Chem. *278*, 36157–36162.

Cok, S.J., Acton, S.J., Sexton, A.E., and Morrison, A.R. (2004). Identification of RNA-binding proteins in RAW 264.7 cells that recognize a lipopolysaccharide-responsive element in the 3-untranslated region of the murine cyclooxygenase-2 mRNA. J. Biol. Chem. *279*, 8196–8205.

Colgan, D.F., and Manley, J.L. (1997). Mechanism and regulation of mRNA polyadenylation. Genes Dev. *11*, 2755–2766.

Conway, K.A., Lee, S.J., Rochet, J.C., Ding, T.T., Williamson, R.E., and Lansbury, P.T. (2000a). Acceleration of oligomerization, not fibrillization, is a shared property of both alpha-synuclein mutations linked to early-onset Parkinson's disease: implications for pathogenesis and therapy. Proc. Natl. Acad. Sci. U. S. A. *97*, 571–576.

Conway, K.A., Harper, J.D., and Lansbury, P.T. (2000b). Fibrils formed in vitro from alpha-synuclein and two mutant forms linked to Parkinson's disease are typical amyloid. Biochemistry (Mosc.) *39*, 2552–2563.

Conway, K.A., Rochet, J.C., Bieganski, R.M., and Lansbury, P.T. (2001). Kinetic stabilization of the alpha-synuclein protofibril by a dopamine-alpha-synuclein adduct. Science *294*, 1346–1349.

Cox, S., Niskar, A.S., Narayan, K.M.V., and Marcus, M. (2007). Prevalence of self-reported diabetes and exposure to organochlorine pesticides among Mexican Americans: Hispanic health and nutrition examination survey, 1982-1984. Environ. Health Perspect. *115*, 1747–1752.

Cronin, K.D., Ge, D., Manninger, P., Linnertz, C., Rossoshek, A., Orrison, B.M., Bernard, D.J., El-Agnaf, O.M.A., Schlossmacher, M.G., Nussbaum, R.L., et al. (2009). Expansion of the Parkinson disease-associated SNCA-Rep1 allele upregulates human alpha-synuclein in transgenic mouse brain. Hum. Mol. Genet. *18*, 3274–3285.

Crowther, R.A., Jakes, R., Spillantini, M.G., and Goedert, M. (1998). Synthetic filaments assembled from C-terminally truncated alpha-synuclein. FEBS Lett. *436*, 309–312.

Curinha, A., Oliveira Braz, S., Pereira-Castro, I., Cruz, A., and Moreira, A. (2014). Implications of polyadenylation in health and disease. Nucl. Austin Tex *5*, 508–519.

Cykowski, M.D., Coon, E.A., Powell, S.Z., Jenkins, S.M., Benarroch, E.E., Low, P.A., Schmeichel, A.M., and Parisi, J.E. (2015). Expanding the spectrum of neuronal pathology in multiple system atrophy. Brain J. Neurol. *138*, 2293–2309.

Dabeva, M.D., Post-Beittenmiller, M.A., and Warner, J.R. (1986). Autogenous regulation of splicing of the transcript of a yeast ribosomal protein gene. Proc. Natl. Acad. Sci. U. S. A. *83*, 5854–5857.

Daher, J.P.L., Ying, M., Banerjee, R., McDonald, R.S., Hahn, M.D., Yang, L., Flint Beal, M., Thomas, B., Dawson, V.L., Dawson, T.M., et al. (2009). Conditional transgenic mice expressing C-terminally truncated human alpha-synuclein (alphaSyn119) exhibit reduced striatal dopamine without loss of nigrostriatal pathway dopaminergic neurons. Mol. Neurodegener. *4*, 34.

Dai, W., Zhang, G., and Makeyev, E.V. (2012). RNA-binding protein HuR autoregulates its expression by promoting alternative polyadenylation site usage. Nucleic Acids Res. *40*, 787–800.

Darnell, R.B. (2013). RNA protein interaction in neurons. Annu. Rev. Neurosci. *36*, 243–270.

Dassi, E., Malossini, A., Re, A., Mazza, T., Tebaldi, T., Caputi, L., and Quattrone, A. (2012). AURA: Atlas of UTR Regulatory Activity. Bioinforma. Oxf. Engl. *28*, 142–144.

Dassi, E., Zuccotti, P., Leo, S., Provenzani, A., Assfalg, M., D'Onofrio, M., Riva, P., and Quattrone, A. (2013). Hyper conserved elements in vertebrate mRNA 3'-UTRs reveal a translational network of RNA-binding proteins controlled by HuR. Nucleic Acids Res. *41*, 3201–3216.

Dauer, W., and Przedborski, S. (2003). Parkinson's disease: mechanisms and models. Neuron *39*, 889–909.

Davidson, W.S., Jonas, A., Clayton, D.F., and George, J.M. (1998). Stabilization of alpha-synuclein secondary structure upon binding to synthetic membranes. J. Biol. Chem. *273*, 9443–9449.

Davies, J.E., Berger, Z., and Rubinsztein, D.C. (2006). Oculopharyngeal muscular dystrophy: potential therapies for an aggregate-associated disorder. Int. J. Biochem. Cell Biol. *38*, 1457–1462.

Desplats, P., Lee, H.-J., Bae, E.-J., Patrick, C., Rockenstein, E., Crews, L., Spencer, B., Masliah, E., and Lee, S.-J. (2009). Inclusion formation and neuronal cell death through neuron-to-neuron transmission of alpha-synuclein. Proc. Natl. Acad. Sci. U. S. A. *106*, 13010–13015.

Dettmer, U., Newman, A.J., Soldner, F., Luth, E.S., Kim, N.C., von Saucken, V.E., Sanderson, J.B., Jaenisch, R., Bartels, T., and Selkoe, D. (2015). Parkinson-causing α-synuclein missense mutations shift native tetramers to monomers as a mechanism for disease initiation. Nat. Commun. *6*, 7314.

Didiot, M.-C., Tian, Z., Schaeffer, C., Subramanian, M., Mandel, J.-L., and Moine, H. (2008). The G-quartet containing FMRP binding site in FMR1 mRNA is a potent exonic splicing enhancer. Nucleic Acids Res. *36*, 4902–4912.

Dobson, C.M. (1999). Protein misfolding, evolution and disease. Trends Biochem. Sci. *24*, 329–332.

Doller, A., Huwiler, A., Müller, R., Radeke, H.H., Pfeilschifter, J., and Eberhardt, W. (2007). Protein kinase C alpha-dependent phosphorylation of the mRNA-stabilizing factor HuR: implications for posttranscriptional regulation of cyclooxygenase-2. Mol. Biol. Cell *18*, 2137–2148.

Doller, A., Pfeilschifter, J., and Eberhardt, W. (2008a). Signalling pathways regulating nucleo-cytoplasmic shuttling of the mRNA-binding protein HuR. Cell. Signal. *20*, 2165–2173.

Doller, A., Akool, E.-S., Huwiler, A., Müller, R., Radeke, H.H., Pfeilschifter, J., and Eberhardt, W. (2008b). Posttranslational modification of the AU-rich element binding protein HuR by protein kinase Cdelta elicits angiotensin II-induced stabilization and nuclear export of cyclooxygenase 2 mRNA. Mol. Cell. Biol. *28*, 2608–2625.

Doxakis, E. (2010). Post-transcriptional regulation of alpha-synuclein expression by mir-7 and mir-153. J. Biol. Chem. *285*, 12726–12734.

Dunham, J.H., and Hall, R.A. (2009). Enhancement of the surface expression of G protein-coupled receptors. Trends Biotechnol. *27*, 541–545.

Durie, D., Lewis, S.M., Liwak, U., Kisilewicz, M., Gorospe, M., and Holcik, M. (2011). RNA-binding protein HuR mediates cytoprotection through stimulation of XIAP translation. Oncogene *30*, 1460–1469.

Ehlers, M.D. (2003). Eppendorf 2003 prize-winning essay. Ubiquitin and the deconstruction of synapses. Science *302*, 800–801.

El-Agnaf, O.M.A., Salem, S.A., Paleologou, K.E., Cooper, L.J., Fullwood, N.J., Gibson, M.J., Curran, M.D., Court, J.A., Mann, D.M.A., Ikeda, S., et al. (2003). Alpha-synuclein implicated in Parkinson's disease is present in extracellular biological fluids, including human plasma. FASEB J. Off. Publ. Fed. Am. Soc. Exp. Biol. *17*, 1945–1947.

Elkon, R., Ugalde, A.P., and Agami, R. (2013). Alternative cleavage and polyadenylation: extent, regulation and function. Nat. Rev. Genet. *14*, 496–506.

Ellis, J.J., Broom, M., and Jones, S. (2007). Protein-RNA interactions: structural analysis and functional classes. Proteins *66*, 903–911.

Emmanouilidou, E., Melachroinou, K., Roumeliotis, T., Garbis, S.D., Ntzouni, M., Margaritis, L.H., Stefanis, L., and Vekrellis, K. (2010). Cell-produced alpha-synuclein is secreted in a calcium-dependent manner by exosomes and impacts neuronal survival. J. Neurosci. Off. J. Soc. Neurosci. *30*, 6838–6851.

Fan, X.C., and Steitz, J.A. (1998). HNS, a nuclear-cytoplasmic shuttling sequence in HuR. Proc. Natl. Acad. Sci. U. S. A. *95*, 15293–15298.

Fan, X., Messaed, C., Dion, P., Laganiere, J., Brais, B., Karpati, G., and Rouleau, G.A. (2003). HnRNP A1 and A/B interaction with PABPN1 in oculopharyngeal muscular dystrophy. Can. J. Neurol. Sci. J. Can. Sci. Neurol. *30*, 244–251.

Farrer, M., Maraganore, D.M., Lockhart, P., Singleton, A., Lesnick, T.G., de Andrade, M., West, A., de Silva, R., Hardy, J., and Hernandez, D. (2001). alpha-Synuclein gene haplotypes are associated with Parkinson's disease. Hum. Mol. Genet. *10*, 1847–1851.

Fechir, M., Linker, K., Pautz, A., Hubrich, T., and Kleinert, H. (2005). The RNA binding protein TIAR is involved in the regulation of human iNOS expression. Cell. Mol. Biol. Noisy--Gd. Fr. *51*, 299–305.

Fong, N., and Bentley, D.L. (2001). Capping, splicing, and 3' processing are independently stimulated by RNA polymerase II: different functions for different segments of the CTD. Genes Dev. *15*, 1783–1795.

Fujiwara, H., Hasegawa, M., Dohmae, N., Kawashima, A., Masliah, E., Goldberg, M.S., Shen, J., Takio, K., and Iwatsubo, T. (2002). alpha-Synuclein is phosphorylated in synucleinopathy lesions. Nat. Cell Biol. *4*, 160–164.

Gai, W.P., Power, J.H., Blumbergs, P.C., and Blessing, W.W. (1998). Multiple-system atrophy: a new alpha-synuclein disease? Lancet Lond. Engl. *352*, 547–548.

Galbán, S., Kuwano, Y., Pullmann, R., Martindale, J.L., Kim, H.H., Lal, A., Abdelmohsen, K., Yang, X., Dang, Y., Liu, J.O., et al. (2008). RNA-binding proteins HuR and PTB promote the translation of hypoxia-inducible factor 1alpha. Mol. Cell. Biol. *28*, 93–107.

Gallouzi, I.E., and Steitz, J.A. (2001). Delineation of mRNA export pathways by the use of cell-permeable peptides. Science *294*, 1895–1901.

Gao, N., Li, Y.-H., Li, X., Yu, S., Fu, G.-L., and Chen, B. (2007). Effect of alpha-synuclein on the promoter activity of tyrosine hydroxylase gene. Neurosci. Bull. *23*, 53–57.

George, J.M., Jin, H., Woods, W.S., and Clayton, D.F. (1995). Characterization of a novel protein regulated during the critical period for song learning in the zebra finch. Neuron *15*, 361–372.

Giasson, B.I., Murray, I.V., Trojanowski, J.Q., and Lee, V.M. (2001). A hydrophobic stretch of 12 amino acid residues in the middle of alpha-synuclein is essential for filament assembly. J. Biol. Chem. *276*, 2380–2386.

Gibb, W.R., and Lees, A.J. (1988). The relevance of the Lewy body to the pathogenesis of idiopathic Parkinson's disease. J. Neurol. Neurosurg. Psychiatry *51*, 745–752.

Gilks, N., Kedersha, N., Ayodele, M., Shen, L., Stoecklin, G., Dember, L.M., and Anderson, P. (2004). Stress Granule Assembly Is Mediated by Prion-like Aggregation of TIA-1. Mol. Biol. Cell *15*, 5383–5398.

Glisovic, T., Ben-David, Y., Lang, M.A., and Raffalli-Mathieu, F. (2003). Interplay between hnRNP A1 and a cis-acting element in the 3' UTR of CYP2A5 mRNA is central for high expression of the gene. FEBS Lett. *535*, 147–152.

Gloeckner, C.J., Kinkl, N., Schumacher, A., Braun, R.J., O'Neill, E., Meitinger, T., Kolch, W., Prokisch, H., and Ueffing, M. (2006). The Parkinson disease causing LRRK2 mutation I2020T is associated with increased kinase activity. Hum. Mol. Genet. *15*, 223–232.

Goers, J., Manning-Bog, A.B., McCormack, A.L., Millett, I.S., Doniach, S., Di Monte, D.A., Uversky, V.N., and Fink, A.L. (2003). Nuclear localization of alpha-synuclein and its interaction with histones. Biochemistry (Mosc.) *42*, 8465–8471.

Gousset, K., Schiff, E., Langevin, C., Marijanovic, Z., Caputo, A., Browman, D.T., Chenouard, N., de Chaumont, F., Martino, A., Enninga, J., et al. (2009). Prions hijack tunnelling nanotubes for intercellular spread. Nat. Cell Biol. *11*, 328–336.

Greenbaum, E.A., Graves, C.L., Mishizen-Eberz, A.J., Lupoli, M.A., Lynch, D.R., Englander, S.W., Axelsen, P.H., and Giasson, B.I. (2005). The E46K mutation in alpha-synuclein increases amyloid fibril formation. J. Biol. Chem. *280*, 7800–7807.

Gregersen, L.H., Schueler, M., Munschauer, M., Mastrobuoni, G., Chen, W., Kempa, S., Dieterich, C., and Landthaler, M. (2014). MOV10 Is a 5' to 3' RNA helicase contributing to UPF1 mRNA target degradation by translocation along 3' UTRs. Mol. Cell *54*, 573–585.

Grimson, A., Farh, K.K.-H., Johnston, W.K., Garrett-Engele, P., Lim, L.P., and Bartel, D.P. (2007). MicroRNA targeting specificity in mammals: determinants beyond seed pairing. Mol. Cell *27*, 91–105.

Gsponer, J., and Babu, M.M. (2012). Cellular strategies for regulating functional and nonfunctional protein aggregation. Cell Rep. *2*, 1425–1437.

Gunderson, S.I., Polycarpou-Schwarz, M., and Mattaj, I.W. (1998). U1 snRNP inhibits pre-mRNA polyadenylation through a direct interaction between U1 70K and poly(A) polymerase. Mol. Cell *1*, 255–264.

Güttinger, S., Mühlhäusser, P., Koller-Eichhorn, R., Brennecke, J., and Kutay, U. (2004). Transportin2 functions as importin and mediates nuclear import of HuR. Proc. Natl. Acad. Sci. U. S. A. *101*, 2918–2923.

Guzman, J.N., Sanchez-Padilla, J., Wokosin, D., Kondapalli, J., Ilijic, E., Schumacker, P.T., and Surmeier, D.J. (2010). Oxidant stress evoked by pacemaking in dopaminergic neurons is attenuated by DJ-1. Nature *468*, 696–700.

Hagerman, P.J., and Hagerman, R.J. (2004). The fragile-X premutation: a maturing perspective. Am. J. Hum. Genet. *74*, 805–816.

Halliday, G.M., Holton, J.L., Revesz, T., and Dickson, D.W. (2011). Neuropathology underlying clinical variability in patients with synucleinopathies. Acta Neuropathol. (Berl.) *122*, 187–204.

Han, T.W., Kato, M., Xie, S., Wu, L.C., Mirzaei, H., Pei, J., Chen, M., Xie, Y., Allen, J., Xiao, G., et al. (2012). Cell-free Formation of RNA Granules: Bound RNAs Identify Features and Components of Cellular Assemblies. Cell *149*, 768–779.

Hansen, C., Angot, E., Bergström, A.-L., Steiner, J.A., Pieri, L., Paul, G., Outeiro, T.F., Melki, R., Kallunki, P., Fog, K., et al. (2011). α-Synuclein propagates from mouse brain to grafted dopaminergic neurons and seeds aggregation in cultured human cells. J. Clin. Invest. *121*, 715–725.

Hardin, P.E., Hall, J.C., and Rosbash, M. (1990). Feedback of the Drosophila period gene product on circadian cycling of its messenger RNA levels. Nature *343*, 536–540.

Hartley, C.A., McKenna, M.C., Salman, R., Holmes, A., Casey, B.J., Phelps, E.A., and Glatt, C.E. (2012). Serotonin transporter polyadenylation polymorphism modulates the retention of fear extinction memory. Proc. Natl. Acad. Sci. U. S. A. *109*, 5493–5498.

Hasegawa, T., Konno, M., Baba, T., Sugeno, N., Kikuchi, A., Kobayashi, M., Miura, E., Tanaka, N., Tamai, K., Furukawa, K., et al. (2011). The AAA-ATPase VPS4 regulates extracellular secretion and lysosomal targeting of α-synuclein. PloS One *6*, e29460.

Hegde, M.L., and Rao, K.S.J. (2007). DNA induces folding in α-synuclein: Understanding the mechanism using chaperone property of osmolytes. Arch. Biochem. Biophys. *464*, 57–69.

Hisata J. (2002). Final supplemental environmental impact statement. Lake and stream rehabilitation: rotenone use and health risks.

Houlden H., C.V. (2016). Updates on potential therapeutic targets in MSA. ACNR 15:8-11.

Infante, J., Llorca, J., Berciano, J., and Combarros, O. (2005). Interleukin-8, intercellular adhesion molecule-1 and tumour necrosis factor-alpha gene polymorphisms and the risk for multiple system atrophy. J. Neurol. Sci. *228*, 11–13.

Iranzo, A., Tolosa, E., Gelpi, E., Molinuevo, J.L., Valldeoriola, F., Serradell, M., Sanchez-Valle, R., Vilaseca, I., Lomeña, F., Vilas, D., et al. (2013). Neurodegenerative disease status and post-mortem pathology in idiopathic rapid-eye-movement sleep behaviour disorder: an observational cohort study. Lancet Neurol. *12*, 443–453.

Ishizawa, K., Komori, T., Sasaki, S., Arai, N., Mizutani, T., and Hirose, T. (2004). Microglial activation parallels system degeneration in multiple system atrophy. J. Neuropathol. Exp. Neurol. *63*, 43–52.

Izquierdo, J.M. (2006). Control of the ATP synthase beta subunit expression by RNA-binding proteins TIA-1, TIAR, and HuR. Biochem. Biophys. Res. Commun. *348*, 703–711.

Jecmenica-Lukic, M., Poewe, W., Tolosa, E., and Wenning, G.K. (2012). Premotor signs and symptoms of multiple system atrophy. Lancet Neurol. *11*, 361–368.

Jenal, M., Elkon, R., Loayza-Puch, F., van Haaften, G., Kühn, U., Menzies, F.M., Oude Vrielink, J.A.F., Bos, A.J., Drost, J., Rooijers, K., et al. (2012). The poly(A)-binding protein nuclear 1 suppresses alternative cleavage and polyadenylation sites. Cell *149*, 538–553.

Jenner, P. (2003). Oxidative stress in Parkinson's disease. Ann. Neurol. *53 Suppl 3*, S26–S36; discussion S36–S38.

Ji, Z., and Tian, B. (2009). Reprogramming of 3' untranslated regions of mRNAs by alternative polyadenylation in generation of pluripotent stem cells from different cell types. PloS One *4*, e8419.

Ji, Z., Lee, J.Y., Pan, Z., Jiang, B., and Tian, B. (2009). Progressive lengthening of 3' untranslated regions of mRNAs by alternative polyadenylation during mouse embryonic development. Proc. Natl. Acad. Sci. U. S. A. *106*, 7028–7033.

Ji, Z., Luo, W., Li, W., Hoque, M., Pan, Z., Zhao, Y., and Tian, B. (2011). Transcriptional activity regulates alternative cleavage and polyadenylation. Mol. Syst. Biol. *7*, 534.

Jiang, C., and Schuman, E.M. (2002). Regulation and function of local protein synthesis in neuronal dendrites. Trends Biochem. Sci. *27*, 506–513.

Jonas, S., and Izaurralde, E. (2015). Towards a molecular understanding of microRNA-mediated gene silencing. Nat. Rev. Genet. *16*, 421–433.

Junn, E., Lee, K.-W., Jeong, B.S., Chan, T.W., Im, J.-Y., and Mouradian, M.M. (2009). Repression of alpha-synuclein expression and toxicity by microRNA-7. Proc. Natl. Acad. Sci. U. S. A. *106*, 13052–13057.

Kandala, D.T., Mohan, N., A, V., A P, S., G, R., and Laishram, R.S. (2016). CstF-64 and 3'-UTR cis-element determine Star-PAP specificity for target mRNA selection by excluding PAPα. Nucleic Acids Res. *44*, 811–823.

Katsanou, V., Papadaki, O., Milatos, S., Blackshear, P.J., Anderson, P., Kollias, G., and Kontoyiannis, D.L. (2005). HuR as a negative posttranscriptional modulator in inflammation. Mol. Cell *19*, 777–789.

Kedersha, N.L., Gupta, M., Li, W., Miller, I., and Anderson, P. (1999). RNA-binding proteins TIA-1 and TIAR link the phosphorylation of eIF-2 alpha to the assembly of mammalian stress granules. J. Cell Biol. *147*, 1431–1442.

Keene, J.D. (2007). RNA regulons: coordination of post-transcriptional events. Nat. Rev. Genet. *8*, 533–543.

Khalaf, O., Fauvet, B., Oueslati, A., Dikiy, I., Mahul-Mellier, A.-L., Ruggeri, F.S., Mbefo, M.K., Vercruysse, F., Dietler, G., Lee, S.-J., et al. (2014). The H50Q mutation enhances α-synuclein aggregation, secretion, and toxicity. J. Biol. Chem. *289*, 21856–21876.

Kiely, A.P., Ling, H., Asi, Y.T., Kara, E., Proukakis, C., Schapira, A.H., Morris, H.R., Roberts, H.C., Lubbe, S., Limousin, P., et al. (2015). Distinct clinical and neuropathological features of G51D SNCA mutation cases compared with SNCA duplication and H50Q mutation. Mol. Neurodegener. *10*, 41.

Kim, H.H., and Gorospe, M. (2008). Phosphorylated HuR shuttles in cycles. Cell Cycle Georget. Tex *7*, 3124–3126.

Kim, H.H., Abdelmohsen, K., Lal, A., Pullmann, R., Yang, X., Galban, S., Srikantan, S., Martindale, J.L., Blethrow, J., Shokat, K.M., et al. (2008a). Nuclear HuR accumulation through phosphorylation by Cdk1. Genes Dev. *22*, 1804–1815.

Kim, H.H., Yang, X., Kuwano, Y., and Gorospe, M. (2008b). Modification at HuR(S242) alters HuR localization and proliferative influence. Cell Cycle Georget. Tex *7*, 3371–3377.

Kim, H.S., Wilce, M.C.J., Yoga, Y.M.K., Pendini, N.R., Gunzburg, M.J., Cowieson, N.P., Wilson, G.M., Williams, B.R.G., Gorospe, M., and Wilce, J.A. (2011). Different modes of interaction by TIAR and HuR with target RNA and DNA. Nucleic Acids Res. *39*, 1117–1130.

Kim, T.D., Paik, S.R., and Yang, C.-H. (2002). Structural and functional implications of C-terminal regions of alpha-synuclein. Biochemistry (Mosc.) *41*, 13782–13790.

Kingsbury, A.E., Daniel, S.E., Sangha, H., Eisen, S., Lees, A.J., and Foster, O.J.F. (2004). Alteration in alpha-synuclein mRNA expression in Parkinson's disease. Mov. Disord. Off. J. Mov. Disord. Soc. *19*, 162–170.

Kishore, S., Jaskiewicz, L., Burger, L., Hausser, J., Khorshid, M., and Zavolan, M. (2011). A quantitative analysis of CLIP methods for identifying binding sites of RNA-binding proteins. Nat. Methods *8*, 559–564.

Ten Klooster, J.P., Leeuwen, I. v, Scheres, N., Anthony, E.C., and Hordijk, P.L. (2007). Rac1-induced cell migration requires membrane recruitment of the nuclear oncogene SET. EMBO J. *26*, 336–345.

Kong, J., and Lasko, P. (2012). Translational control in cellular and developmental processes. Nat. Rev. Genet. *13*, 383–394.

Kontopoulos, E., Parvin, J.D., and Feany, M.B. (2006). Alpha-synuclein acts in the nucleus to inhibit histone acetylation and promote neurotoxicity. Hum. Mol. Genet. *15*, 3012–3023.

Kordower, J.H., Chu, Y., Hauser, R.A., Freeman, T.B., and Olanow, C.W. (2008). Lewy body-like pathology in long-term embryonic nigral transplants in Parkinson's disease. Nat. Med. *14*, 504–506.

Korecka, J.A., van Kesteren, R.E., Blaas, E., Spitzer, S.O., Kamstra, J.H., Smit, A.B., Swaab, D.F., Verhaagen, J., and Bossers, K. (2013). Phenotypic characterization of retinoic acid differentiated SH-SY5Y cells by transcriptional profiling. PloS One *8*, e63862.

Kullmann, M., Göpfert, U., Siewe, B., and Hengst, L. (2002). ELAV/Hu proteins inhibit p27 translation via an IRES element in the p27 5'UTR. Genes Dev. *16*, 3087–3099.

Kyrpides, N.C., and Ouzounis, C.A. (1993). Mechanisms of specificity in mRNA degradation: autoregulation and cognate interactions. J. Theor. Biol. *163*, 373–392.

Lang, A.E., and Lozano, A.M. (1998). Parkinson's disease. First of two parts. N. Engl. J. Med. *339*, 1044–1053.

Langerveld, A.J., Mihalko, D., DeLong, C., Walburn, J., and Ide, C.F. (2007). Gene expression changes in postmortem tissue from the rostral pons of multiple system atrophy patients. Mov. Disord. Off. J. Mov. Disord. Soc. *22*, 766–777.

Langston, J.W., Ballard, P., Tetrud, J.W., and Irwin, I. (1983). Chronic Parkinsonism in humans due to a product of meperidine-analog synthesis. Science *219*, 979–980.

Lau, A.G., Irier, H.A., Gu, J., Tian, D., Ku, L., Liu, G., Xia, M., Fritsch, B., Zheng, J.Q., Dingledine, R., et al. (2010). Distinct 3'UTRs differentially regulate activity-dependent translation of brain-derived neurotrophic factor (BDNF). Proc. Natl. Acad. Sci. U. S. A. *107*, 15945–15950.

De Lau, L.M.L., and Breteler, M.M.B. (2006). Epidemiology of Parkinson's disease. Lancet Neurol. *5*, 525–535.

Lazowska, J., Jacq, C., and Slonimski, P.P. (1980). Sequence of introns and flanking exons in wild-type and box3 mutants of cytochrome b reveals an interlaced splicing protein coded by an intron. Cell *22*, 333–348.

Leandersson, K., Riesbeck, K., and Andersson, T. (2006). Wnt-5a mRNA translation is suppressed by the Elav-like protein HuR in human breast epithelial cells. Nucleic Acids Res. *34*, 3988–3999.

Lebedeva, S., Jens, M., Theil, K., Schwanhäusser, B., Selbach, M., Landthaler, M., and Rajewsky, N. (2011). Transcriptome-wide Analysis of Regulatory Interactions of the RNA-Binding Protein HuR. Mol. Cell *43*, 340–352.

Lee, F.J., Liu, F., Pristupa, Z.B., and Niznik, H.B. (2001). Direct binding and functional coupling of alpha-synuclein to the dopamine

transporters accelerate dopamine-induced apoptosis. FASEB J. Off. Publ. Fed. Am. Soc. Exp. Biol. *15*, 916–926.

Lefebvre, S., Bürglen, L., Reboullet, S., Clermont, O., Burlet, P., Viollet, L., Benichou, B., Cruaud, C., Millasseau, P., and Zeviani, M. (1995). Identification and characterization of a spinal muscular atrophy-determining gene. Cell *80*, 155–165.

Li, W.-W., Yang, R., Guo, J.-C., Ren, H.-M., Zha, X.-L., Cheng, J.-S., and Cai, D.-F. (2007). Localization of alpha-synuclein to mitochondria within midbrain of mice. Neuroreport *18*, 1543–1546.

Lianoglou, S., Garg, V., Yang, J.L., Leslie, C.S., and Mayr, C. (2013). Ubiquitously transcribed genes use alternative polyadenylation to achieve tissue-specific expression. Genes Dev. *27*, 2380–2396.

Liao, B., Hu, Y., and Brewer, G. (2007). Competitive binding of AUF1 and TIAR to MYC mRNA controls its translation. Nat. Struct. Mol. Biol. *14*, 511–518.

Linder, B., Fischer, U., and Gehring, N.H. (2015). mRNA metabolism and neuronal disease. FEBS Lett. *589*, 1598–1606.

Liu, B., and Hong, J.-S. (2003). Role of microglia in inflammation-mediated neurodegenerative diseases: mechanisms and strategies for therapeutic intervention. J. Pharmacol. Exp. Ther. *304*, 1–7.

Locascio, J.J., Eberly, S., Liao, Z., Liu, G., Hoesing, A.N., Duong, K., Trisini-Lipsanopoulos, A., Dhima, K., Hung, A.Y., Flaherty, A.W., et al. (2015). Association between α-synuclein blood transcripts and early, neuroimaging-supported Parkinson's disease. Brain *138*, 2659–2671.

Lotharius, J., Barg, S., Wiekop, P., Lundberg, C., Raymon, H.K., and Brundin, P. (2002). Effect of mutant alpha-synuclein on dopamine homeostasis in a new human mesencephalic cell line. J. Biol. Chem. *277*, 38884–38894.

Lu, Y.-C., Chang, S.-H., Hafner, M., Li, X., Tuschl, T., Elemento, O., and Hla, T. (2014). ELAVL1 modulates transcriptome-wide miRNA binding in murine macrophages. Cell Rep. *9*, 2330–2343.

Luk, K.C., Kehm, V., Carroll, J., Zhang, B., O'Brien, P., Trojanowski, J.Q., and Lee, V.M.-Y. (2012a). Pathological α-synuclein transmission initiates Parkinson-like neurodegeneration in nontransgenic mice. Science *338*, 949–953.

Luk, K.C., Kehm, V.M., Zhang, B., O'Brien, P., Trojanowski, J.Q., and Lee, V.M.Y. (2012b). Intracerebral inoculation of pathological α-synuclein initiates a rapidly progressive neurodegenerative α-synucleinopathy in mice. J. Exp. Med. *209*, 975–986.

Lukiw, W.J., and Bazan, N.G. (1997). Cyclooxygenase 2 RNA message abundance, stability, and hypervariability in sporadic Alzheimer neocortex. J. Neurosci. Res. *50*, 937–945.

Luoma, P., Melberg, A., Rinne, J.O., Kaukonen, J.A., Nupponen, N.N., Chalmers, R.M., Oldfors, A., Rautakorpi, I., Peltonen, L., Majamaa, K., et al. (2004). Parkinsonism, premature menopause, and mitochondrial DNA polymerase gamma mutations: clinical and molecular genetic study. Lancet Lond. Engl. *364*, 875–882.

Malygin, A.A., Parakhnevitch, N.M., Ivanov, A.V., Eperon, I.C., and Karpova, G.G. (2007). Human ribosomal protein S13 regulates expression of its own gene at the splicing step by a feedback mechanism. Nucleic Acids Res. *35*, 6414–6423.

Mandel, C.R., Bai, Y., and Tong, L. (2008). Protein factors in pre-mRNA 3'-end processing. Cell. Mol. Life Sci. CMLS *65*, 1099–1122.

Mansfield, K.D., and Keene, J.D. (2012). Neuron-specific ELAV/Hu proteins suppress HuR mRNA during neuronal differentiation by alternative polyadenylation. Nucleic Acids Res. *40*, 2734–2746.

Maraganore, D.M., de Andrade, M., Elbaz, A., Farrer, M.J., Ioannidis, J.P., Krüger, R., Rocca, W.A., Schneider, N.K., Lesnick, T.G., Lincoln, S.J., et al. (2006). Collaborative analysis of alpha-synuclein gene promoter variability and Parkinson disease. JAMA *296*, 661–670.

Martin, G., Gruber, A.R., Keller, W., and Zavolan, M. (2012). Genome-wide analysis of pre-mRNA 3' end processing reveals a

decisive role of human cleavage factor I in the regulation of 3' UTR length. Cell Rep. *1*, 753–763.

Martin, L.J., Pan, Y., Price, A.C., Sterling, W., Copeland, N.G., Jenkins, N.A., Price, D.L., and Lee, M.K. (2006). Parkinson's disease alpha-synuclein transgenic mice develop neuronal mitochondrial degeneration and cell death. J. Neurosci. Off. J. Soc. Neurosci. *26*, 41–50.

Masuda, A., Andersen, H.S., Doktor, T.K., Okamoto, T., Ito, M., Andresen, B.S., and Ohno, K. (2012). CUGBP1 and MBNL1 preferentially bind to 3' UTRs and facilitate mRNA decay. Sci. Rep. *2*, 209.

Masuda-Suzukake, M., Nonaka, T., Hosokawa, M., Oikawa, T., Arai, T., Akiyama, H., Mann, D.M.A., and Hasegawa, M. (2013). Prion-like spreading of pathological α-synuclein in brain. Brain J. Neurol. *136*, 1128–1138.

Matsuda, W., Furuta, T., Nakamura, K.C., Hioki, H., Fujiyama, F., Arai, R., and Kaneko, T. (2009). Single nigrostriatal dopaminergic neurons form widely spread and highly dense axonal arborizations in the neostriatum. J. Neurosci. Off. J. Soc. Neurosci. *29*, 444–453.

Mayford, M., Baranes, D., Podsypanina, K., and Kandel, E.R. (1996). The 3'-untranslated region of CaMKII alpha is a cis-acting signal for the localization and translation of mRNA in dendrites. Proc. Natl. Acad. Sci. U. S. A. *93*, 13250–13255.

Mayr, C., and Bartel, D.P. (2009a). Widespread shortening of 3'UTRs by alternative cleavage and polyadenylation activates oncogenes in cancer cells. Cell *138*, 673–684.

Mayr, C., and Bartel, D.P. (2009b). Widespread shortening of 3'UTRs by alternative cleavage and polyadenylation activates oncogenes in cancer cells. Cell *138*, 673–684.

Mazan-Mamczarz, K., Galbán, S., López de Silanes, I., Martindale, J.L., Atasoy, U., Keene, J.D., and Gorospe, M. (2003). RNA-binding protein HuR enhances p53 translation in response to ultraviolet light irradiation. Proc. Natl. Acad. Sci. U. S. A. *100*, 8354–8359.

Mazan-Mamczarz, K., Lal, A., Martindale, J.L., Kawai, T., and Gorospe, M. (2006). Translational repression by RNA-binding protein TIAR. Mol. Cell. Biol. *26*, 2716–2727.

McCarthy, J.J., Linnertz, C., Saucier, L., Burke, J.R., Hulette, C.M., Welsh-Bohmer, K.A., and Chiba-Falek, O. (2011). The effect of SNCA 3' region on the levels of SNCA-112 splicing variant. Neurogenetics *12*, 59–64.

McLean, J.R., Hallett, P.J., Cooper, O., Stanley, M., and Isacson, O. (2012). Transcript expression levels of full-length alpha-synuclein and its three alternatively spliced variants in Parkinson's disease brain regions and in a transgenic mouse model of alpha-synuclein overexpression. Mol. Cell. Neurosci. *49*, 230–239.

Melkonian, S., Argos, M., Pierce, B.L., Chen, Y., Islam, T., Ahmed, A., Syed, E.H., Parvez, F., Graziano, J., Rathouz, P.J., et al. (2011). A prospective study of the synergistic effects of arsenic exposure and smoking, sun exposure, fertilizer use, and pesticide use on risk of premalignant skin lesions in Bangladeshi men. Am. J. Epidemiol. *173*, 183–191.

Michlewski, G., and Cáceres, J.F. (2010). RNase-assisted RNA chromatography. RNA N. Y. N *16*, 1673–1678.

Miller, D.W., Hague, S.M., Clarimon, J., Baptista, M., Gwinn-Hardy, K., Cookson, M.R., and Singleton, A.B. (2004). Alpha-synuclein in blood and brain from familial Parkinson disease with SNCA locus triplication. Neurology *62*, 1835–1838.

Millevoi, S., and Vagner, S. (2010). Molecular mechanisms of eukaryotic pre-mRNA 3' end processing regulation. Nucleic Acids Res. *38*, 2757–2774.

Mills, J.D., Ward, M., Kim, W.S., Halliday, G.M., and Janitz, M. (2016). Strand-specific RNA-sequencing analysis of multiple system atrophy brain transcriptome. Neuroscience *322*, 234–250.

Miura, P., Shenker, S., Andreu-Agullo, C., Westholm, J.O., and Lai, E.C. (2013). Widespread and extensive lengthening of 3' UTRs in the mammalian brain. Genome Res. *23*, 812–825.

Mohr, S.E., Dillon, S.T., and Boswell, R.E. (2001). The RNA-binding protein Tsunagi interacts with Mago Nashi to establish polarity and localize oskar mRNA during Drosophila oogenesis. Genes Dev. *15*, 2886–2899.

De Moor, C.H., and Richter, J.D. (2001). Translational control in vertebrate development. Int. Rev. Cytol. *203*, 567–608.

Moore, M.J., and Proudfoot, N.J. (2009). Pre-mRNA processing reaches back to transcription and ahead to translation. Cell *136*, 688–700.

Mosner, J., Mummenbrauer, T., Bauer, C., Sczakiel, G., Grosse, F., and Deppert, W. (1995). Negative feedback regulation of wild-type p53 biosynthesis. EMBO J. *14*, 4442–4449.

Mukherjee, N., Corcoran, D.L., Nusbaum, J.D., Reid, D.W., Georgiev, S., Hafner, M., Ascano, M., Tuschl, T., Ohler, U., and Keene, J.D. (2011). Integrative regulatory mapping indicates that the RNA-binding protein HuR couples pre-mRNA processing and mRNA stability. Mol. Cell *43*, 327–339.

Murphy, D.D., Rueter, S.M., Trojanowski, J.Q., and Lee, V.M. (2000). Synucleins are developmentally expressed, and alpha-synuclein regulates the size of the presynaptic vesicular pool in primary hippocampal neurons. J. Neurosci. Off. J. Soc. Neurosci. *20*, 3214–3220.

Murray, I.V.J., Giasson, B.I., Quinn, S.M., Koppaka, V., Axelsen, P.H., Ischiropoulos, H., Trojanowski, J.Q., and Lee, V.M.-Y. (2003). Role of alpha-synuclein carboxy-terminus on fibril formation in vitro. Biochemistry (Mosc.) *42*, 8530–8540.

Neystat, M., Lynch, T., Przedborski, S., Kholodilov, N., Rzhetskaya, M., and Burke, R.E. (1999). Alpha-synuclein expression in substantia nigra and cortex in Parkinson's disease. Mov. Disord. Off. J. Mov. Disord. Soc. *14*, 417–422.

Nielsen, C.B., Shomron, N., Sandberg, R., Hornstein, E., Kitzman, J., and Burge, C.B. (2007). Determinants of targeting by endogenous and exogenous microRNAs and siRNAs. RNA N. Y. N *13*, 1894–1910.

Nielsen, M.S., Vorum, H., Lindersson, E., and Jensen, P.H. (2001). Ca2+ binding to alpha-synuclein regulates ligand binding and oligomerization. J. Biol. Chem. *276*, 22680–22684.

Nishimura, M., Kawakami, H., Komure, O., Maruyama, H., Morino, H., Izumi, Y., Nakamura, S., Kaji, R., and Kuno, S. (2002). Contribution of the interleukin-1beta gene polymorphism in multiple system atrophy. Mov. Disord. Off. J. Mov. Disord. Soc. *17*, 808–811.

Norris, E.H., Giasson, B.I., Hodara, R., Xu, S., Trojanowski, J.Q., Ischiropoulos, H., and Lee, V.M.-Y. (2005). Reversible inhibition of alpha-synuclein fibrillization by dopaminochrome-mediated conformational alterations. J. Biol. Chem. *280*, 21212–21219.

Onesto, C., Berra, E., Grépin, R., and Pagès, G. (2004). Poly(A)-binding protein-interacting protein 2, a strong regulator of vascular endothelial growth factor mRNA. J. Biol. Chem. *279*, 34217–34226.

Orth, M., and Schapira, A.H.V. (2002). Mitochondrial involvement in Parkinson's disease. Neurochem. Int. *40*, 533–541.

Palacino, J.J., Sagi, D., Goldberg, M.S., Krauss, S., Motz, C., Wacker, M., Klose, J., and Shen, J. (2004). Mitochondrial dysfunction and oxidative damage in parkin-deficient mice. J. Biol. Chem. *279*, 18614–18622.

Pappolla, M.A. (1986). Lewy bodies of Parkinson's disease. Immune electron microscopic demonstration of neurofilament antigens in constituent filaments. Arch. Pathol. Lab. Med. *110*, 1160–1163.

Peng, S.S., Chen, C.Y., Xu, N., and Shyu, A.B. (1998). RNA stabilization by the AU-rich element binding protein, HuR, an ELAV protein. EMBO J. *17*, 3461–3470.

Peng, X., Peng, X.M., Tehranian, R., Dietrich, P., Stefanis, L., and Perez, R.G. (2005). Alpha-synuclein activation of protein phosphatase 2A reduces tyrosine hydroxylase phosphorylation in dopaminergic cells. J. Cell Sci. *118*, 3523–3530.

Perrin, R.J., Woods, W.S., Clayton, D.F., and George, J.M. (2000). Interaction of human alpha-Synuclein and Parkinson's disease variants with phospholipids. Structural analysis using site-directed mutagenesis. J. Biol. Chem. *275*, 34393–34398.

Petrovic, I.N., Ling, H., Asi, Y., Ahmed, Z., Kukkle, P.L., Hazrati, L.-N., Lang, A.E., Revesz, T., Holton, J.L., and Lees, A.J. (2012). Multiple system atrophy-parkinsonism with slow progression and prolonged survival: a diagnostic catch. Mov. Disord. Off. J. Mov. Disord. Soc. *27*, 1186–1190.

Petrucelli, L., O'Farrell, C., Lockhart, P.J., Baptista, M., Kehoe, K., Vink, L., Choi, P., Wolozin, B., Farrer, M., Hardy, J., et al. (2002). Parkin protects against the toxicity associated with mutant alpha-synuclein: proteasome dysfunction selectively affects catecholaminergic neurons. Neuron *36*, 1007–1019.

Pinto, P.A.B., Henriques, T., Freitas, M.O., Martins, T., Domingues, R.G., Wyrzykowska, P.S., Coelho, P.A., Carmo, A.M., Sunkel, C.E., Proudfoot, N.J., et al. (2011). RNA polymerase II kinetics in polo polyadenylation signal selection. EMBO J. *30*, 2431–2444.

Podszywalow-Bartnicka, P., Wolczyk, M., Kusio-Kobialka, M., Wolanin, K., Skowronek, K., Nieborowska-Skorska, M., Dasgupta, Y., Skorski, T., and Piwocka, K. (2014). Downregulation of BRCA1 protein in BCR-ABL1 leukemia cells depends on stress-triggered TIAR-mediated suppression of translation. Cell Cycle Georget. Tex *13*, 3727–3741.

Poewe, W. (2009). Treatments for Parkinson disease--past achievements and current clinical needs. Neurology *72*, S65–S73.

Polymeropoulos, M.H., Lavedan, C., Leroy, E., Ide, S.E., Dehejia, A., Dutra, A., Pike, B., Root, H., Rubenstein, J., Boyer, R., et al. (1997). Mutation in the alpha-synuclein gene identified in families with Parkinson's disease. Science *276*, 2045–2047.

Porcari, R., Proukakis, C., Waudby, C.A., Bolognesi, B., Mangione, P.P., Paton, J.F., Mullin, S., Cabrita, L.D., Penco, A., Relini, A., et

al. (2015). The H50Q Mutation Induces a 10-fold Decrease in the Solubility of α-Synuclein. J. Biol. Chem. *290*, 2395–2404.

Proudfoot, N.J. (2011). Ending the message: poly(A) signals then and now. Genes Dev. *25*, 1770–1782.

Pullmann, R., Kim, H.H., Abdelmohsen, K., Lal, A., Martindale, J.L., Yang, X., and Gorospe, M. (2007). Analysis of turnover and translation regulatory RNA-binding protein expression through binding to cognate mRNAs. Mol. Cell. Biol. *27*, 6265–6278.

Van Raaij, M.E., van Gestel, J., Segers-Nolten, I.M.J., de Leeuw, S.W., and Subramaniam, V. (2008). Concentration dependence of alpha-synuclein fibril length assessed by quantitative atomic force microscopy and statistical-mechanical theory. Biophys. J. *95*, 4871–4878.

Rebane, A., Aab, A., and Steitz, J.A. (2004). Transportins 1 and 2 are redundant nuclear import factors for hnRNP A1 and HuR. RNA N. Y. N *10*, 590–599.

Reeve, A.K., Ludtmann, M.H.R., Angelova, P.R., Simcox, E.M., Horrocks, M.H., Klenerman, D., Gandhi, S., Turnbull, D.M., and Abramov, A.Y. (2015). Aggregated α-synuclein and complex I deficiency: exploration of their relationship in differentiated neurons. Cell Death Dis. *6*, e1820.

Rhinn, H., Qiang, L., Yamashita, T., Rhee, D., Zolin, A., Vanti, W., and Abeliovich, A. (2012). Alternative α-synuclein transcript usage as a convergent mechanism in Parkinson's disease pathology. Nat. Commun. *3*, 1084.

Ristimäki, A., Garfinkel, S., Wessendorf, J., Maciag, T., and Hla, T. (1994). Induction of cyclooxygenase-2 by interleukin-1 alpha. Evidence for post-transcriptional regulation. J. Biol. Chem. *269*, 11769–11775.

Ristimäki, A., Narko, K., and Hla, T. (1996). Down-regulation of cytokine-induced cyclo-oxygenase-2 transcript isoforms by dexamethasone: evidence for post-transcriptional regulation. Biochem. J. *318 (Pt 1)*, 325–331.

Rivers, R.C., Kumita, J.R., Tartaglia, G.G., Dedmon, M.M., Pawar, A., Vendruscolo, M., Dobson, C.M., and Christodoulou, J. (2008). Molecular determinants of the aggregation behavior of alpha- and beta-synuclein. Protein Sci. Publ. Protein Soc. *17*, 887–898.

Roberts, R.F., Wade-Martins, R., and Alegre-Abarrategui, J. (2015). Direct visualization of alpha-synuclein oligomers reveals previously undetected pathology in Parkinson's disease brain. Brain J. Neurol. *138*, 1642–1657.

Ross, C.A., and Poirier, M.A. (2005). Opinion: What is the role of protein aggregation in neurodegeneration? Nat. Rev. Mol. Cell Biol. *6*, 891–898.

Sachs, A. (1990). The role of poly(A) in the translation and stability of mRNA. Curr. Opin. Cell Biol. *2*, 1092–1098.

Satake, W., Nakabayashi, Y., Mizuta, I., Hirota, Y., Ito, C., Kubo, M., Kawaguchi, T., Tsunoda, T., Watanabe, M., Takeda, A., et al. (2009). Genome-wide association study identifies common variants at four loci as genetic risk factors for Parkinson's disease. Nat. Genet. *41*, 1303–1307.

Schaeffer, C., Bardoni, B., Mandel, J.-L., Ehresmann, B., Ehresmann, C., and Moine, H. (2001). The fragile X mental retardation protein binds specifically to its mRNA via a purine quartet motif. EMBO J *20*, 4803–4813.

Schaeffer, C., Beaulande, M., Ehresmann, C., Ehresmann, B., and Moine, H. (2003). The RNA binding protein FMRP: new connections and missing links. Biol. Cell Auspices Eur. Cell Biol. Organ. *95*, 221–228.

Schapira, A.H.V., and Tolosa, E. (2010). Molecular and clinical prodrome of Parkinson disease: implications for treatment. Nat. Rev. Neurol. *6*, 309–317.

Scheiba, R.M., de Opakua, A.I., Díaz-Quintana, A., Cruz-Gallardo, I., Martínez-Cruz, L.A., Martínez-Chantar, M.L., Blanco, F.J., and Díaz-Moreno, I. (2014). The C-terminal RNA binding motif of HuR is a multi-functional domain leading to HuR oligomerization and binding to U-rich RNA targets. RNA Biol. *11*, 1250–1261.

Scherrer, T., Mittal, N., Janga, S.C., and Gerber, A.P. (2010). A Screen for RNA-Binding Proteins in Yeast Indicates Dual Functions for Many Enzymes. PLoS ONE *5*, e15499.

Schiavi, S.C., Belasco, J.G., and Greenberg, M.E. (1992). Regulation of proto-oncogene mRNA stability. Biochim. Biophys. Acta *1114*, 95–106.

Schneider, C.A., Rasband, W.S., and Eliceiri, K.W. (2012). NIH Image to ImageJ: 25 years of image analysis. Nat. Methods *9*, 671–675.

Scholz, S.W., Houlden, H., Schulte, C., Sharma, M., Li, A., Berg, D., Melchers, A., Paudel, R., Gibbs, J.R., Simon-Sanchez, J., et al. (2009). SNCA variants are associated with increased risk for multiple system atrophy. Ann. Neurol. *65*, 610–614.

Shendelman, S., Jonason, A., Martinat, C., Leete, T., and Abeliovich, A. (2004). DJ-1 is a redox-dependent molecular chaperone that inhibits alpha-synuclein aggregate formation. PLoS Biol. *2*, e362.

Siddiqui, I.J., Pervaiz, N., and Abbasi, A.A. (2016). The Parkinson Disease gene SNCA: Evolutionary and structural insights with pathological implication. Sci. Rep. *6*, 24475.

Simón-Sánchez, J., Schulte, C., Bras, J.M., Sharma, M., Gibbs, J.R., Berg, D., Paisan-Ruiz, C., Lichtner, P., Scholz, S.W., Hernandez, D.G., et al. (2009). Genome-wide association study reveals genetic risk underlying Parkinson's disease. Nat. Genet. *41*, 1308–1312.

Singleton, A.B., Farrer, M., Johnson, J., Singleton, A., Hague, S., Kachergus, J., Hulihan, M., Peuralinna, T., Dutra, A., Nussbaum, R., et al. (2003). alpha-Synuclein locus triplication causes Parkinson's disease. Science *302*, 841.

Siprashvili, Z., Webster, D.E., Kretz, M., Johnston, D., Rinn, J.L., Chang, H.Y., and Khavari, P.A. (2012). Identification of proteins binding coding and non-coding human RNAs using protein microarrays. BMC Genomics *13*, 633.

Skliris, A., Papadaki, O., Kafasla, P., Karakasiliotis, I., Hazapis, O., Reczko, M., Grammenoudi, S., Bauer, J., and Kontoyiannis, D.L. (2015). Neuroprotection requires the functions of the RNA-binding protein HuR. Cell Death Differ. *22*, 703–718.

Sotiriou, S., Gibney, G., Baxevanis, A.D., and Nussbaum, R.L. (2009). A single nucleotide polymorphism in the 3'UTR of the SNCA gene encoding alpha-synuclein is a new potential susceptibility locus for Parkinson disease. Neurosci. Lett. *461*, 196–201.

Spies, N., Nielsen, C.B., Padgett, R.A., and Burge, C.B. (2009). Biased chromatin signatures around polyadenylation sites and exons. Mol. Cell *36*, 245–254.

Spillantini, M.G., Schmidt, M.L., Lee, V.M., Trojanowski, J.Q., Jakes, R., and Goedert, M. (1997). Alpha-synuclein in Lewy bodies. Nature *388*, 839–840.

Spillantini, M.G., Crowther, R.A., Jakes, R., Hasegawa, M., and Goedert, M. (1998). alpha-Synuclein in filamentous inclusions of Lewy bodies from Parkinson's disease and dementia with lewy bodies. Proc. Natl. Acad. Sci. U. S. A. *95*, 6469–6473.

Spira, P.J., Sharpe, D.M., Halliday, G., Cavanagh, J., and Nicholson, G.A. (2001). Clinical and pathological features of a Parkinsonian syndrome in a family with an Ala53Thr alpha-synuclein mutation. Ann. Neurol. *49*, 313–319.

Srikantan, S., Abdelmohsen, K., Lee, E.K., Tominaga, K., Subaran, S.S., Kuwano, Y., Kulshrestha, R., Panchakshari, R., Kim, H.H., Yang, X., et al. (2011). Translational control of TOP2A influences doxorubicin efficacy. Mol. Cell. Biol. *31*, 3790–3801.

Srikantan, S., Tominaga, K., and Gorospe, M. (2012). Functional interplay between RNA-binding protein HuR and microRNAs. Curr. Protein Pept. Sci. *13*, 372–379.

Stoecklin, G., Gross, B., Ming, X.-F., and Moroni, C. (2003). A novel mechanism of tumor suppression by destabilizing AU-rich growth factor mRNA. Oncogene *22*, 3554–3561.

Su, B., Wang, X., Zheng, L., Perry, G., Smith, M.A., and Zhu, X. (2010). Abnormal mitochondrial dynamics and neurodegenerative diseases. Biochim. Biophys. Acta *1802*, 135–142.

Subramaniam, K., Kandasamy, K., Joseph, K., Spicer, E.K., and Tholanikunnel, B.G. (2011). The 3'-untranslated region length and AU-rich RNA location modulate RNA-protein interaction and translational control of β2-adrenergic receptor mRNA. Mol. Cell. Biochem. *352*, 125–141.

Sulzer, D., and Surmeier, D.J. (2013). Neuronal vulnerability, pathogenesis, and Parkinson's disease. Mov. Disord. Off. J. Mov. Disord. Soc. *28*, 41–50.

Sureau, A., Gattoni, R., Dooghe, Y., Stévenin, J., and Soret, J. (2001). SC35 autoregulates its expression by promoting splicing events that destabilize its mRNAs. EMBO J. *20*, 1785–1796.

Surmeier, D.J., Guzman, J.N., Sanchez-Padilla, J., and Goldberg, J.A. (2011). The origins of oxidant stress in Parkinson's disease and therapeutic strategies. Antioxid. Redox Signal. *14*, 1289–1301.

Suswam, E.A., Nabors, L.B., Huang, Y., Yang, X., and King, P.H. (2005a). IL-1beta induces stabilization of IL-8 mRNA in malignant breast cancer cells via the 3' untranslated region: Involvement of divergent RNA-binding factors HuR, KSRP and TIAR. Int. J. Cancer *113*, 911–919.

Suswam, E.A., Li, Y.Y., Mahtani, H., and King, P.H. (2005b). Novel DNA-binding properties of the RNA-binding protein TIAR. Nucleic Acids Res. *33*, 4507–4518.

Tanner, C.M. (1992). Epidemiology of Parkinson's disease. Neurol. Clin. *10*, 317–329.

Tartaglia, G.G., Pechmann, S., Dobson, C.M., and Vendruscolo, M. (2007). Life on the edge: a link between gene expression levels and aggregation rates of human proteins. Trends Biochem. Sci. *32*, 204–206.

Tassone, F., De Rubeis, S., Carosi, C., La Fata, G., Serpa, G., Raske, C., Willemsen, R., Hagerman, P.J., and Bagni, C. (2011).

Differential usage of transcriptional start sites and polyadenylation sites in FMR1 premutation alleles. Nucleic Acids Res. *39*, 6172–6185.

Taylor, J.P., Hardy, J., and Fischbeck, K.H. (2002). Toxic proteins in neurodegenerative disease. Science *296*, 1991–1995.

Tessier, C.R., Doyle, G.A., Clark, B.A., Pitot, H.C., and Ross, J. (2004). Mammary tumor induction in transgenic mice expressing an RNA-binding protein. Cancer Res. *64*, 209–214.

Toba, G., and White, K. (2008). The third RNA recognition motif of Drosophila ELAV protein has a role in multimerization. Nucleic Acids Res. *36*, 1390–1399.

Toniolo, D., and Rizzolio, F. (2007). X chromosome and ovarian failure. Semin. Reprod. Med. *25*, 264–271.

Le Tonquèze, O., Gschloessl, B., Legagneux, V., Paillard, L., and Audic, Y. (2016). Identification of CELF1 RNA targets by CLIP-seq in human HeLa cells. Genomics Data *8*, 97–103.

Touchman, J.W., Dehejia, A., Chiba-Falek, O., Cabin, D.E., Schwartz, J.R., Orrison, B.M., Polymeropoulos, M.H., and Nussbaum, R.L. (2001). Human and mouse alpha-synuclein genes: comparative genomic sequence analysis and identification of a novel gene regulatory element. Genome Res. *11*, 78–86.

Uéda, K., Fukushima, H., Masliah, E., Xia, Y., Iwai, A., Yoshimoto, M., Otero, D.A., Kondo, J., Ihara, Y., and Saitoh, T. (1993). Molecular cloning of cDNA encoding an unrecognized component of amyloid in Alzheimer disease. Proc. Natl. Acad. Sci. U. S. A. *90*, 11282–11286.

Ulitsky, I., Shkumatava, A., Jan, C.H., Subtelny, A.O., Koppstein, D., Bell, G.W., Sive, H., and Bartel, D.P. (2012). Extensive alternative polyadenylation during zebrafish development. Genome Res. *22*, 2054–2066.

Valente, E.M., Abou-Sleiman, P.M., Caputo, V., Muqit, M.M.K., Harvey, K., Gispert, S., Ali, Z., Del Turco, D., Bentivoglio, A.R.,

Healy, D.G., et al. (2004). Hereditary early-onset Parkinson's disease caused by mutations in PINK1. Science *304*, 1158–1160.

Vandesompele, J., De Preter, K., Pattyn, F., Poppe, B., Van Roy, N., De Paepe, A., and Speleman, F. (2002). Accurate normalization of real-time quantitative RT-PCR data by geometric averaging of multiple internal control genes. Genome Biol. *3*, RESEARCH0034.

Venda, L.L., Cragg, S.J., Buchman, V.L., and Wade-Martins, R. (2010). α-Synuclein and dopamine at the crossroads of Parkinson's disease. Trends Neurosci. *33*, 559–568.

Wang, W., Fan, J., Yang, X., Fürer-Galban, S., Lopez de Silanes, I., von Kobbe, C., Guo, J., Georas, S.N., Foufelle, F., Hardie, D.G., et al. (2002). AMP-activated kinase regulates cytoplasmic HuR. Mol. Cell. Biol. *22*, 3425–3436.

Wang, Z., Kayikci, M., Briese, M., Zarnack, K., Luscombe, N.M., Rot, G., Zupan, B., Curk, T., and Ule, J. (2010). iCLIP predicts the dual splicing effects of TIA-RNA interactions. PLoS Biol. *8*, e1000530.

Weinreb, P.H., Zhen, W., Poon, A.W., Conway, K.A., and Lansbury, P.T. (1996). NACP, a protein implicated in Alzheimer's disease and learning, is natively unfolded. Biochemistry (Mosc.) *35*, 13709–13715.

Wenning, G.K., Ben Shlomo, Y., Magalhães, M., Daniel, S.E., and Quinn, N.P. (1994). Clinical features and natural history of multiple system atrophy. An analysis of 100 cases. Brain J. Neurol. *117 (Pt 4)*, 835–845.

Wersinger, C., and Sidhu, A. (2003). Attenuation of dopamine transporter activity by alpha-synuclein. Neurosci. Lett. *340*, 189–192.

West, A.B., Moore, D.J., Biskup, S., Bugayenko, A., Smith, W.W., Ross, C.A., Dawson, V.L., and Dawson, T.M. (2005). Parkinson's disease-associated mutations in leucine-rich repeat kinase 2 augment kinase activity. Proc. Natl. Acad. Sci. U. S. A. *102*, 16842–16847.

Wigington, C.P., Jung, J., Rye, E.A., Belauret, S.L., Philpot, A.M., Feng, Y., Santangelo, P.J., and Corbett, A.H. (2015). Post-transcriptional regulation of programmed cell death 4 (PDCD4) mRNA by the RNA-binding proteins human antigen R (HuR) and T-cell intracellular antigen 1 (TIA1). J. Biol. Chem. *290*, 3468–3487.

Wolters, E.C. (2009). Non-motor extranigral signs and symptoms in Parkinson's disease. Parkinsonism Relat. Disord. *15 Suppl 3*, S6–S12.

Workman, E., Veith, A., and Battle, D.J. (2014). U1A regulates 3' processing of the survival motor neuron mRNA. J. Biol. Chem. *289*, 3703–3712.

Xia, Y., Rohan de Silva, H.A., Rosi, B.L., Yamaoka, L.H., Rimmler, J.B., Pericak-Vance, M.A., Roses, A.D., Chen, X., Masliah, E., DeTeresa, R., et al. (1996). Genetic studies in Alzheimer's disease with an NACP/alpha-synuclein polymorphism. Ann. Neurol. *40*, 207–215.

Xu, M., and Hecht, N.B. (2007). Polypyrimidine tract binding protein 2 stabilizes phosphoglycerate kinase 2 mRNA in murine male germ cells by binding to its 3'UTR. Biol. Reprod. *76*, 1025–1033.

Xu, F., Zhang, X., Lei, Y., Liu, X., Liu, Z., Tong, T., and Wang, W. (2010). Loss of repression of HuR translation by miR-16 may be responsible for the elevation of HuR in human breast carcinoma. J. Cell. Biochem. *111*, 727–734.

Yang, Q., Coseno, M., Gilmartin, G.M., and Doublié, S. (2011). Crystal structure of a human cleavage factor CFI(m)25/CFI(m)68/RNA complex provides an insight into poly(A) site recognition and RNA looping. Struct. Lond. Engl. 1993 *19*, 368–377.

Yao, C., Biesinger, J., Wan, J., Weng, L., Xing, Y., Xie, X., and Shi, Y. (2012). Transcriptome-wide analyses of CstF64-RNA interactions in global regulation of mRNA alternative polyadenylation. Proc. Natl. Acad. Sci. U. S. A. *109*, 18773–18778.

Yokota, T., Sugawara, K., Ito, K., Takahashi, R., Ariga, H., and Mizusawa, H. (2003). Down regulation of DJ-1 enhances cell death by oxidative stress, ER stress, and proteasome inhibition. Biochem. Biophys. Res. Commun. *312*, 1342–1348.

Yoon, Y., McKenna, M.C., Rollins, D.A., Song, M., Nuriel, T., Gross, S.S., Xu, G., and Glatt, C.E. (2013). Anxiety-associated alternative polyadenylation of the serotonin transporter mRNA confers translational regulation by hnRNPK. Proc. Natl. Acad. Sci. U. S. A. *110*, 11624–11629.

Yost, H.J., Petersen, R.B., and Lindquist, S. (1990). RNA metabolism: strategies for regulation in the heat shock response. Trends Genet. TIG *6*, 223–227.

Yu, S., Zuo, X., Li, Y., Zhang, C., Zhou, M., Zhang, Y.A., Uéda, K., and Chan, P. (2004). Inhibition of tyrosine hydroxylase expression in alpha-synuclein-transfected dopaminergic neuronal cells. Neurosci. Lett. *367*, 34–39.

Zhang, H., Lee, J.Y., and Tian, B. (2005a). Biased alternative polyadenylation in human tissues. Genome Biol. *6*, R100.

Zhang, N.-Y., Tang, Z., and Liu, C.-W. (2008). alpha-Synuclein protofibrils inhibit 26 S proteasome-mediated protein degradation: understanding the cytotoxicity of protein protofibrils in neurodegenerative disease pathogenesis. J. Biol. Chem. *283*, 20288–20298.

Zhang, T., Delestienne, N., Huez, G., Kruys, V., and Gueydan, C. (2005b). Identification of the sequence determinants mediating the nucleo-cytoplasmic shuttling of TIAR and TIA-1 RNA-binding proteins. J. Cell Sci. *118*, 5453–5463.

Zheng Dinghai, T.B. (2014). RNA-binding proteins in Regulation of Alternative Cleavage and Polyadenylation. In System Biology of RNA Binding Proteins,.

Zhu, M., and Fink, A.L. (2003). Lipid binding inhibits alpha-synuclein fibril formation. J. Biol. Chem. *278*, 16873–16877.

Zhu, H., Zhou, H.-L., Hasman, R.A., and Lou, H. (2007). Hu proteins regulate polyadenylation by blocking sites containing U-rich sequences. J. Biol. Chem. *282*, 2203–2210.